

NOVEMBER 2015

M.Sc. in Food Engineering

AYŞE SELCEN SEMERCİÖZ

**UNIVERSITY OF GAZİANTEP
GRADUATE SCHOOL OF
NATURAL & APPLIED SCIENCES**

**DEVELOPMENT OF NEW CARBONACEOUS
MATERIAL FROM GRAPEFRUIT PEEL FOR THE
ADSORPTION OF Cu^{+2} IONS**

**M.Sc. THESIS
IN
FOOD ENGINEERING**

**BY
AYŞE SELCEN SEMERCİÖZ
NOVEMBER 2015**

Development of New Carbonaceous Material from
Grapefruit Peel for the Adsorption of Cu⁺² Ions

M.Sc. Thesis
in
Food Engineering
University of Gaziantep

Supervisor
Prof. Dr. Hüseyin BOZKURT
Co-supervisor
Prof. Dr. Fahrettin GÖĞÜŞ

By
Ayşe Selcen SEMERCİÖZ

November 2015

© 2015 [Ayşe Selcen SEMERCİÖZ]

REPUBLIC OF TURKEY
UNIVERSITY OF GAZİANTEP
GRADUATE SCHOOL OF NATURAL & APPLIED SCIENCES
FOOD ENGINEERING DEPARTMENT

Name of the thesis: Development of New Carbonaceous Material from Grapefruit Peel for the Adsorption of Cu⁺² ions

Name of student: Ayşe Selcen SEMERCİÖZ

Exam date: 25.11.2015

Approval of the Graduate School of Natural and Applied Sciences


Prof. Dr. Metin BEDİR


Director

I certify that this thesis satisfies all the requirements as a thesis for the degree of Master of Science.

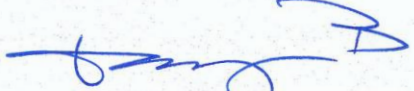

Prof. Dr. Ali Rıza TEKİN

Head of Department

This is to certify that we have read this thesis and that in our consensus opinion it is fully adequate, in scope and quality, as a thesis for the degree of Master of Science.


Prof. Dr. Fahrettin Göğüş

Co-supervisor

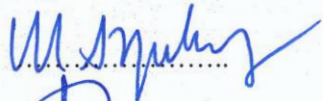

Prof. Dr. Hüseyin BOZKURT

Supervisor

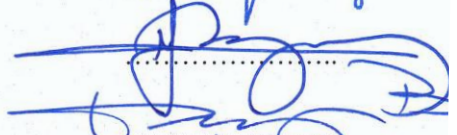
Examining Committee Members

Signature

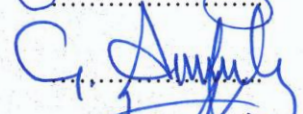
Asst. Prof. Dr. Metin AÇIKYILDIZ (Chairman)



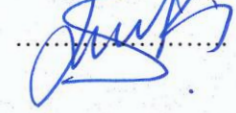
Prof. Dr. Mustafa BAYRAM



Prof. Dr. Hüseyin BOZKURT



Assoc. Prof. Dr. Abuzer ÇELEKLİ



Asst. Prof. Dr. Derya KOÇAK YANIK



I hereby declare that all information in this document has been obtained and presented in accordance with academic rules and ethical conduct. I also declare that, as required by these rules and conduct, I have fully cited and referenced all material and results that are not original to this work.

Ayşe Selcen SEMERCİÖZ

ABSTRACT

DEVELOPMENT OF NEW CARBONACEOUS MATERIAL FROM GRAPEFRUIT PEEL FOR THE ADSORPTION OF Cu^{+2} IONS

SEMERCİÖZ, Selcen Ayşe

M.Sc. in Food Engineering

Supervisor(s): Prof. Dr. Hüseyin BOZKURT

Prof. Dr. Fahrettin GÖĞÜŞ

November 2015, 90 pages

In this study, new kind of adsorbent was produced from grapefruit peel by *low temperature-microwave assisted hydrothermal carbonization* technique. Adsorption mechanism of this new material and its Cu^{+2} ion adsorption capacity were investigated. The obtained material was characterized by FTIR-ATR spectroscopy and SEM analyses and new developed slits, dependently increment in surface area and changes in surface functional groups of material were observed after carbonization. Effects of different conditions on the adsorption capacity (q_e , mg/g) were studied. Activation process improved the adsorption capacity of adsorbent as almost twice. Increasing pH, temperature and initial Cu^{+2} ion concentration caused the increment in adsorption capacity. Kinetic behavior was described by Pseudo second order, Logistic and Elovich models while Langmuir, Freundlich and Dubinin-Radushkevich models were carried out to define isothermal behavior of adsorption. According to both R^2 and SSE values, Logistic and Freundlich models were found as the best models to describe the kinetic behavior and equilibrium isotherm, respectively. Maximum adsorption capacity was observed as 48.22 mg/g at 318 K and 60 mg/L Cu^{+2} concentration. Thermodynamic studies showed that adsorption process was spontaneous and endothermic and mainly controlled by physico-chemical mechanism. As a result, adsorbent produced by economic, fast and eco-friendly HTC technique had a good potential as adsorbent in the adsorption of Cu^{+2} ion and this material could be improved for other heavy metal adsorption processes.

Keywords: Grapefruit peel, Adsorption kinetic, Isotherm, Thermodynamic

ÖZET

Cu⁺² İYONLARININ ADSORPSİYONU İÇİN GREYFURT KABUĞUNDAN KARBON İÇERİKLİ YENİ MALZEME GELİŞTİRİLMESİ

SEMERCİÖZ, Selcen Ayşe

Yüksek Lisans, Gıda Mühendisliği Bölümü

Tez Yöneticisi(leri): Prof. Dr. Hüseyin BOZKURT

Prof. Dr. Fahrettin GÖĞÜŞ

Kasım 2015, 90 sayfa

Bu çalışmada, greyfurt kabuğundan *düşük sıcaklıkta-mikrodalga ile hidrotermal karbonizasyon* yöntemiyle yeni bir tür adsorbent üretilmiştir. Bu yeni malzemenin adsorpsiyon mekanizması ve Cu⁺² iyonunu adsorpsiyon kapasitesi incelenmiştir. Elde edilen malzeme FTIR-ATR spektroskopu ve SEM cihazı ile karakterize edilmiş ve yüzeyde yarıkların oluştuğu, dolayısıyla; aktif yüzey alanının arttığı ve karbonizasyon işlemi sonrasında malzemenin fonksiyonel yüzey gruplarının değiştiği görülmüştür. Farklı koşulların adsorpsiyon kapasitesi (q_t, mg/g) üzerine etkileri incelenmiştir. Aktivasyon işlemi ile adsorpsiyon kapasitesi yaklaşık iki katına çıkmıştır. Artan pH, sıcaklık ve başlangıç Cu⁺² iyon konsantrasyonu adsorpsiyon kapasitesini de arttırmıştır. Adsorpsiyonun kinetik davranış yalancı ikinci derece, Logistik ve Elovich modelleri ile; izotermal davranış ise Langmuir, Freundlich ve Dubinin-Radushkevich modelleri ile tanımlanmaya çalışılmıştır. Hem R² hem de SSE değerlerine göre; kinetik verileri tanımlayan en iyi modelin Logistik; denge verilerini tanımlayan en iyi modelin ise Freundlich olduğu görülmüştür. Maksimum adsorpsiyon kapasitesi 318 K ve 60 mg/L Cu⁺² konsantrasyonunda 48.22 mg/g olarak elde edilmiştir. Termodinamik hesaplamalar adsorpsiyon işleminin spontan ve endotermik olduğunu ve fiziko-kimyasal bir mekanizma ile kontrol edildiğini göstermektedir. Sonuç olarak; ekonomik, hızlı ve çevre dostu bir üretim tekniğiyle geliştirilen malzemenin Cu⁺² iyonu adsorpsiyonunda kullanım potansiyeli olduğu görülmüştür ve bu malzeme diğer ağır metallerin adsorpsiyonu için de geliştirilebilir niteliktedir.

Anahtar kelimeler: Greyfurt kabuğu, Adsorpsiyon kinetiği, İzoterm, Termodinamik

To My Parents...

ACKNOWLEDGEMENTS

I would like to express my deepest gratitude to my supervisors, Prof. Dr. Hüseyin Bozkurt and Prof. Dr. Fahrettin Göğüş for their guidance, patience, and supports throughout this research. Additionally, I am so grateful to them for their invaluable advice and encouragement not only about this research but also my life.

I would also like to extend my gratitude to Assoc.Prof.Dr. Abuzer Çelekli for his support, insight and time he dedicated to my thesis.

My sincere thanks also go to Assis. Prof. Dr. Derya Koçak Yanık and Res. Assist. Hasene Keskin Çavdar for their advices and guidance and being an inspiration for me.

Besides, I would like to thank all my friends to their emotional support and motivation, most especially Doğuş Çimen.

I would like to acknowledge to Food Engineering Department, University of Gaziantep for the technical and administrative support and special thanks to Ekrem Erikçi.

Finally, very special thanks to my sweet family; my father for his insightful comments, my mom for her suggestions and motivation and my brother and sister for their moral support and encouraging opinions.

CONTENTS

ABSTRACT.....	vi
ÖZET	vii
ACKNOWLEDGEMENTS	viii
CONTENTS.....	ixx
LIST OF FIGURES	xii
LIST OF TABLES.....	xiv
LIST OF SYMBOLS / ABBREVIATIONS	xvi
CHAPTER 1	1
INTRODUCTION	1
1.1. Water Pollution	2
1.2. Heavy Metal Pollution	3
1.3. Heavy Metal Purification Techniques from Wastewater	5
1.3.1. Ion exchange	6
1.3.2. Chemical precipitation	6
1.3.3. Coagulation and flocculation	6
1.3.4. Sedimentation	7
1.3.5. Membrane filtration	7
1.3.6. Flotation	7
1.3.7. Electrochemical methods	8
1.3.8. Adsorption.....	8
1.4. Activated Hydrochar as an Adsorbent	9
1.4.1. Principle of adsorption by activated char.....	10
1.4.2. Production of activated char	11
1.4.3. Microwave application in hydrothermal carbonization process	13
1.4.4. Valorization of grapefruit peel as activated hydrochar	14
1.5. Modeling	16
1.5.1. Adsorption kinetics	16
1.5.2. Adsorption equilibrium isotherms	18
1.5.2.1. Langmuir isotherm.....	18
1.5.2.2. Freundlich isotherm	20

1.5.2.3. Dubinin-Radushkevich isotherm.....	20
1.5.3. Adsorption thermodynamic.....	21
1.6. Aim of Study.....	23
CHAPTER II.....	25
MATERIALS AND METHODS.....	25
2.1. Preparation of Adsorbate.....	25
2.2. Preparation of Material.....	25
2.2.1. Determination of moisture content.....	25
2.2.2. Pretreatment of peel.....	25
2.2.3. Preparation of hydrochar.....	27
2.2.4. Activation of hydrochar.....	27
2.3. Precipitation Test of Cu ⁺² Ions.....	27
2.4. Hydrochar Characterization.....	28
2.4.1. SEM analysis.....	28
2.4.2. FTIR analysis.....	28
2.4.3. Determination of pH zero point charge of adsorbent.....	28
2.4.4. The effectiveness of activation process.....	28
2.5. Batch Adsorption Studies.....	29
2.5.1. Effect of adsorbent dose.....	29
2.5.2. Effect of initial pH.....	29
2.5.3. Effect of initial copper concentration and process temperature.....	29
2.6. Adsorption Kinetics.....	30
2.7. Equilibrium Models.....	30
2.8. Thermodynamic Studies.....	32
2.9. Statistical Analysis.....	32
2.10. Validation of Models.....	32
CHAPTER 3.....	33
RESULTS AND DISCUSSION.....	33
3.1. Adsorbent Characterization.....	34
3.1.1. FTIR-ATR analyses.....	34
3.1.2. SEM analysis.....	41
3.1.3. Activation of hydrochar with KOH.....	42
3.2. Batch Adsorption Studies.....	42
3.2.1. Effect of initial solution pH and pH _{zpc}	43
3.2.2. Effect of adsorbent dose.....	44
3.2.3. Effect of temperature and initial Cu ⁺² ion concentration.....	46

3.3. Adsorption Kinetics	48
3.3.1. Nonlinear Pseudo second-order kinetic model	49
3.3.2. Logistic kinetic model.....	52
3.3.3. Elovich kinetic model	55
3.4. Adsorption Equilibrium Isotherms.....	57
3.4.1. Langmuir isotherm.....	58
3.4.2. Freundlich isotherm	59
3.4.3. Dubinin-Radushkevich isotherm.....	61
3.5. Thermodynamic Studies	62
CHAPTER IV	65
CONCLUSION.....	65
REFERENCES	67
APPENDIX.....	75

LIST OF FIGURES

	Page
Figure 2.1 Schematic diagram of experimental design.....	26
Figure 3.1 Comparison of (a) dried peel, (b) activated hydrochar, (c) inactive hydrochar.....	36
Figure 3.2 Cu ⁺² ion sorption by activated hydrochar: (a) before sorption, (b) after sorption	40
Figure 3.3 (a) SEM image of dried grapefruit peel, (b ₁) activated hydrochar at x2000, (b ₂) activated hydrochar at x 10000.....	41
Figure 3.4 Cu ⁺² ion precipitation at different pH regime	43
Figure 3.5 Initial pH effect on Cu ⁺² ion sorption.....	44
Figure 3.6 Adsorbent dose effect on equilibrium sorption capacity and % Cu (II) removal	45
Figure 3.7 Effect of initial Cu ⁺² ion concentration at three different temperatures	46
Figure 3.8 Effect of temperature for five different concentrations	47
Figure 3.9 Nonlinear Pseudo second order kinetic model for Cu ⁺² ion adsorption onto activated hydrochar at 298 K	50
Figure 3.10 Nonlinear Pseudo second order kinetic model for Cu ⁺² ion adsorption onto activated hydrochar at 308 K	50
Figure 3.11 Nonlinear Pseudo second order kinetic model for Cu ⁺² ion sorption onto activated hydrochar at 318 K	51
Figure 3.12 Logistic kinetic model for Cu ⁺² ion adsorption onto activated hydrochar at 298 K	53
Figure 3.13 Logistic kinetic model for Cu ⁺² ion adsorption onto activated hydrochar at 308 K	53

Figure 3.14 Logistic kinetic model for Cu^{+2} ion adsorption onto activated hydrochar at 318 K	54
Figure 3.15 Elovich kinetic model for Cu^{+2} ion adsorption onto activated hydrochar at 298 K	55
Figure 3.16 Elovich kinetic model for Cu^{+2} ion adsorption onto activated hydrochar at 308 K	56
Figure 3.17 Elovich kinetic model for Cu^{+2} ion adsorption onto activated hydrochar at 318 K	56
Figure 3.18 Langmuir Isotherm for adsorption of Cu^{+2} on activated hydrochar at different temperature	59
Figure 3.19 Freundlich Isotherm for adsorption of Cu^{+2} on activated hydrochar at different temperature	60
Figure A.1 pH_{zpc} of activated hydrochar	85

LIST OF TABLES

	Page
Table 1.1 Some of heavy metal limitations in drinking (WHO, 2011)	4
Table 1.2 Comparison of physisorption and chemisorption	9
Table 2.1 Equations of used kinetic models	31
Table 2.2 Equations of used equilibrium models	31
Table 3.1 FTIR-ATR spectrum frequencies (1/cm) of sorbents before adsorption	35
Table 3.2 FTIR-ATR spectrum frequencies (1/cm) of activated hydrochar before and after adsorption.....	39
Table 3.3 R^2 and SSE values and parameters of three kinetic models.....	49
Table 3.4 R^2 , and SSE values and parameters of three isotherms	58
Table 3.5 Gibbs free energy, enthalpy and entropy change values of adsorption process	63
Table A.1 q_t values of experiments at 298 K.....	75
Table A.2 q_t values of experiments at 308 K.....	75
Table A.3 q_t values of experiments at 318 K	76
Table A.4 ANOVA results of q_t values of experiments	76
Table A.5 ANOVA results of q_t values of experiments for each initial Cu^{+2} concentration at 308K	77
Table A.6 ANOVA results of q_t values of experiments for each initial Cu^{+2} concentration at 308K	78
Table A.7 ANOVA results of q_t - initial Cu^{+2} concentration relationship for each time at 298 K	79

Table A.8 ANOVA results of q_t - initial Cu^{+2} concentration relationship for each time at 308 K	81
Table A.9 ANOVA results of q_t - initial Cu^{+2} concentration relationship for each time at 318 K	83
Table A.10 ANOVA results of q_t - initial Cu^{+2} concentration relationship for each time at 318 K	85

LIST OF SYMBOLS / ABBREVIATIONS

A	Maximum sorption values from Logistic model (mg/g)
AAS	Atomic Absorption Spectrophotometer
AOAC	Association of Official Agricultural Chemists
C_e	Equilibrium concentration of the solute in the liquid
D-R	Dubinin and Radushkevich
E	Free energy (kJ/mol) from Dubinin–Radushkevich isotherm
E_a	Activation energy
FTIR-ATR	Fourier Transform Infrared – Attenuated Total Reflectance
HMF	Hydroxymethylfurfural
HTC	Hydrothermal carbonization
IUPAC	International Union of Pure and Applied Chemistry
k_2	Pseudo second-order rate constant (g/mg.min)
K_f	Freundlich constant as adsorption capacity [(mg/g) (L/g) ^{1/n}]
K_L	Langmuir constant (L/mg)
n	Favorability of adsorption for Freundlich Model
pH _{zpc}	pH of zero point charge
q_{exp}	Experimental adsorbed adsorbate amount (mg/g) at equilibrium
q_e	Equilibrium concentration of a solute on the surface of an adsorbent (mg/g)
q_{pred}	Predicted adsorbed adsorbate amount (mg/g) at time t (min)
q_L	Monolayer sorption capacity (mg/g) from Langmuir isotherm
q_m	Maximum sorption capacity (mg/g) from Freundlich isotherm

R_L	Dimensionless constant referred to as separation factor or equilibrium parameter
R^2	Correlation coefficient
SSE	Sum of square of error
SEM	Scanning electron microscopy
SPSS	Statistical package for social sciences
USDA	United States Department of Agriculture
WHO	World Health Organization
ε^2	Dubinin–Radushkevich isotherm constant
β	Constant related to the sorption energy (mol^2/kJ^2) for Dubinin- Radushkevich Model
μ	Adsorption rate constant from logistic kinetic model
ΔG^0	The Gibb’s free energy change (kJ/mol)
ΔH^0	Enthalpy change (kJ/mol)
ΔS^0	Entropy change (J/mol.K)
α	Initial adsorbate sorption rate (mmol/(g.min))
β	Desorption constant (g/mmol) for Elovich Model

CHAPTER 1

INTRODUCTION

Industrialization and production numbers have been increasing; in parallel with population growth, demands and consumption increment. While this increment contributes economy positively; on the other side, it brings along the pollution that could threaten the ecological balance if no precaution is taken. Waste material formation is unavoidable in a process line and elimination of this waste material is manufacture's responsibility. This issue is at least as important as quality of product and needs the attention and inspection.

Water resources, one of the cornerstones of lifecycle, have been polluted by industrial wastes leaved unrestrainedly to the nature and pollutants which can bio-accumulate on the living organisms; transfer among them, finally; causes detriments with increased effect. In case of using this contaminated water for irrigation and agricultural activities, livestock rising or direct consumption; it can cause severe damages on living organisms.

The importance of "Industrial Pollution" is not understood completely. This topic needs to be divided into subheadings because pollutants include different chemical substances with different effects. One of these subheadings is 'Heavy Metal Pollution' and it is the most common type. Besides; in contrast to organic pollutants, heavy metals do not decompose naturally so this title is at more important situation.

Discharging of the heavy metals into the surface and ground water can cause cumulating of them on the earth, plants and living bodies. They can cause increasing in ROS (reactive oxygen species) and hold the vital compounds in the living cells and cause the lysis of them, loss of enzymatic activity or incorrect operation of enzyme. Consequently, while it was a controllable problem at the beginning; it turns the problem which can cause permanent damage and even death of organism.

Increasing wastes; leaving these wastes to nature without control; as a result of that; increasing health problem and extinction of some species cause the focusing of scientists on this subject. Formation of waste material is unavoidable but it is not impossible to prevent the pollution of nature. In the light of this view; available treatment techniques and recycling technologies have been improved day by day. For becoming widespread of using these techniques and technologies; it is needed to cheaper setup and sustainability cost and adopted by investors. In addition to this; waste management system of factories must be controlled, sanctions should be applied if necessary or should be rewarded.

1.1. Water Pollution

Water covers almost three-quarters of the earth's surface, but there is limited amount of usable fresh water. Less than one percentage of total water can be used for daily water supply needs (Inglezakis and Pouloupoulos, 2006). Potable water requirement for human population, usable water requirement for animals and agricultural activities will never end. Due to the increasing industrialization, waste material has been threatening this critical water amount because of weak adequacy in wastewater management.

According to recent studies with drinking water; more than 800 specific organic and inorganic chemical compounds have been identified within. Industrial and municipal discharge, urban and rural runoff, natural decomposition of vegetable and animal matter, and water/wastewater chlorination are sources of these organic and inorganic chemical compounds. Many of these chemicals are carcinogenic and cause many other ailments with varying intensity and character (Bansal and Goyal, 2005).

Waste material resulting from production process is inevitable. Management of this waste material is crucial. Especially for treatment of wastewater, there are several methods to remove harmful contaminations (heavy metal, dye, microbial organism, etc.). Ion exchange, coagulation, reverse osmosis, oxidation, sedimentation, and adsorption etc. are the most common used techniques.

Due to the presence of wide range and amount of organic and inorganic materials in contaminated water, common techniques can be insufficient, expensive and can cause further increment in the pollution because of the their chemical wastes.

Accordingly; alternative proper and cheaper eco-friendly techniques or modification on current techniques have been needed.

1.2.Heavy Metal Pollution

According to scientific definitions; 'heavy metal' as a term refers to any metallic element which has relatively high density and toxic or poisonous even at low concentration. This definition includes; the group of metals and metalloids that have density higher than 4 g/cm^3 , in other words; almost five times higher than density of water (Hawkes, 1997).

'Heavy metal' expression is not only about having high density, but also it is deal with the chemical features. Lead (Pb), cadmium (Cd), zinc (Zn), mercury (Hg), arsenic (As), silver (Ag), chromium (Cr), copper (Cu), iron (Fe), and the platinum group elements are named as heavy metal.

Heavy metals can present as component of the earth crust and they can enter the body system by means of food web, water and air, besides; they can bio-accumulate in trophic states of food pyramide in progress of time. Bio-accumulation takes time but during that time detrimental effect of heavy metal also increases exponentially. Studies in recent years show that; metals can be transferred through the food web. If agricultural soils are contaminated by irrigation water consist of heavy metals, these heavy metals can be taken up by plants and accumulate in their tissues. Over and above this; when contaminated plants are grazed or water is drunk by animals or this polluted water mix in habitat of marine species; heavy metals will hold and accumulate on their tissues, and milk (Duruibe et al., 2007). Terminally; when these contaminated plants and animals or water sources are consumed by human, these metals cannot be metabolized or eliminated entirely and this situation causes various illness. For instance, cadmium accumulates primarily in the kidneys and considered as probably carcinogenic to humans, similarly; toxic effects of mercury are seen mainly in the kidney in both humans and laboratory animals and oral poisoning causes primarily in haemorrhagic gastritis and colitis; the ultimate damage to the kidney. Exposure to lead is associated with a wide range of effects, including various neurodevelopmental effects, mortality (mainly due to cardiovascular diseases), impaired renal function, hypertension, impaired fertility and adverse pregnancy outcomes. For silver, the only obvious sign is argyria, a condition in

which skin and hair are heavily discolored by silver in the tissues (WHO, 2011). In conclusion; pollutants can be transferred through the food web without being noticed and with increased adverse effect (Duruibe et al., 2007). For these reasons, World Health Organization (WHO) announced the maximum acceptable limits of heavy metals (Table 1.1).

Table 1.1 Some of heavy metal limitations in drinking water (WHO, 2011)

Heavy metal type	Maximum acceptable concentrations
Copper	2 ppm
Arsenic	10 ppb
Cadmium	3 ppb
Lead	10 ppb
Mercury	6 ppb
Silver	Has not determined yet
Nickel	70 ppb

To understand adverse effects of these metals; it should be known that the most toxic forms of these metals when they are at the most stable oxidation states. Studies show that heavy metals have poisoning effect because of their interaction with biomolecules that belong to normal body biochemistry in the normal metabolic processes. It has been observed in these studies that; when heavy metals taken, they are converted to their stable oxidation states because of the acidic medium of the stomach. At that state they can combine with body's biomolecules to make stable chemical bonds, thereby; mutilating their structures and hindering them from the bioreactions of their functions (Bansal and Goyal, 2005; Duruibe et al., 2007).

Heavy metals are part of the nature normally, they are found in soil and stone and they can be transferred to water naturally. On the other hand; soil can prevent the contamination of water from heavy metal. Heavy metals carry positive charge. Soil particles and loose dust have also charge. Organic matters in the soil tend to have a several charged sites on their surfaces. The negative charged matters show a tendency to bind the metal cations. This makes them insoluble in water and prevents the carrying of them through to lifecycle. However, there is something to be added; pH has important effect on situation described above. If pH is low it means there H^+

ions and they are cation. These cations are attracted to negative charges of soil. Thereby; there is not enough side to attract with the heavy metals which means that more metals remain in the soluble stage and can contaminate the water sources easily. Besides; there are additional heavy metal pollution sources like ‘Human Activities’. Hence; natural ways cannot be enough the overcoming to this pollution (NVSWCD Newsletter, 2015).

Copper is a metal that has been used in a wide range of application and technologies. Besides; it is one of the toxic metals which can cause health problem, for instance; excessive intake results in accumulation in the liver and produces gastrointestinal problems. It is known that; this metal is released into environment by both natural and anthropogenic sources, especially mining and industrial activities, and automobile exhausts. As with all heavy metals; copper can leach into underground waters, move along water pathways and finally depositing in the aquifer or translocate through surface waters and subsequently soil (Bansal and Goyal, 2005).

However, copper is important essential mineral for human, Bansal and Goyal (2005) mentioned that the biotoxic effects in human biochemistry are of great concern. It was emphasized that understanding the conditions of metals (such as the concentrations and oxidation states which make them harmful and understanding how biotoxicity take place) is important point. Also, there are other important effective points such as their sources, leaching processes, chemical conversions etc. In the light of this information; it can be recommended that potable waters should be processed with suitable and effective treatment to remove copper and other heavy metals before domestic supply.

1.3. Heavy Metal Purification Techniques from Wastewater

Natural or anthropogenic pollution of water by copper and other heavy metals is unavoidable so recovering of this kind of water must be considered. Contaminated water can be treated and regained with several techniques. These techniques include ion exchange (Al-Enezi et al., 2004), chemical precipitation (González-Muñoz et al., 2006), membrane filtration (reverse osmosis, nano-filtration, ultra-filtration, and electro-dialysis etc.) (Cséfalvay, 2007) coagulation-flocculation (El Samrani et al., 2008), flotation (Rubbio and Tessele, 1997), electrochemical methods (Heidmann and Calmano, 2008), and adsorption (Fu and Wang, 2011).

1.3.1. Ion exchange

In this technique there is an insoluble matrix. This matrix is resin or ion-exchange polymer normally in the form of small (0.5-1 mm diameter) beads. Resin (either synthetic or natural solid resin), has the specific ability to exchange its cations with the metals in the wastewater. In purification of wastewater, ion-exchange resins are used to remove heavy metal (e.g. copper, lead or cadmium) ions from solution, replacing them with more innocuous ions, such as sodium and potassium. However, there are some disadvantages of this technique such as; calcium sulphate and iron fouling, organic, bacterial and chlorine contamination to treated water (Alchin, 2008).

1.3.2. Chemical precipitation

With this technique, heavy metal ions are precipitated by reaction with some specific chemicals. Residual precipitates can be separated from the water by sedimentation or filtration. Then, treated water can be appropriately discharged or reused. Conventionally, chemical precipitation processes include hydroxide precipitation and sulfide precipitation. On the other hand, chemical precipitation is suitable to treat wastewater containing high concentration heavy metal ions and it is ineffective when metal ion concentration is low (Fu and Wang, 2011). It needs to be combined with supplier techniques.

1.3.3. Coagulation and flocculation

As another heavy metal removing way from wastewater is a set of coagulation and flocculation followed by sedimentation and filtration techniques. Principle of coagulation is the destabilization of colloids by neutralizing the forces which keep them apart. Aluminum, ferrous sulfate and ferric chloride are the examples as widely used coagulants in the conventional wastewater treatment processes (Fu and Wang, 2011). The main disadvantage of coagulation is being suitable only for the hydrophobic colloids and suspended particles. In order to overcome this problem, new kinds of coagulants have been improved (Chang and Wang, 2007). Flocculation is a technique which includes using of polymers to form bridges between the flocs. By this means, particles are bonded as large agglomerates or clumps. Once suspended particles are flocculated into larger particles and they can be removed by filtration or flotation (Fu and Wang, 2011). The main disadvantages of this method

are operational cost and in some cases, considerable quantities of coagulant and flocculant needing to achieve the required level of flocculation.

1.3.4. Sedimentation

As a physical water treatment process, gravimetric forces are used to remove suspended solids from water in sedimentation technique (Omelia, 1998). By the means of turbulence of moving water, solid particles can be entrained and removed naturally. Sedimentation ponds are used for the purpose of removing entrained solids by sedimentation (Goldman et al., 1986). In order to provide continuous removal of solids being deposited by sedimentation; clarifier tanks with mechanical equipment are used (Hammer, 1975). Using this method without any coagulant, it can take too much time and may be toxic if used improperly.

1.3.5. Membrane filtration

With different types of membranes, membrane filtration technologies have good potential for heavy metal removal. Having high efficiency, easy operation and space saving properties make this technique common. The membrane processes used to remove metals from the wastewater are ultra-filtration, reverse osmosis, nano-filtration and electro-dialysis (Fu and Wang, 2011). Except electro-dialysis, for other membrane filtration techniques, high operational pressure is needed. In electro-dialysis technique, as its name suggest, electrical potential difference is driving force for separation. It should be added that, for membrane separation techniques there are some disincentive situations as having high cost, complex process, membrane slugging and low permeate flux (Fu and Wang, 2011).

1.3.6. Flotation

Flotation has been used to separate heavy metal from a liquid phase using bubble attachment, originated in mineral processing. Dissolved air, ion and precipitation flotation techniques are the main flotation processes for the removal of metal ions from solution (Fu and Wang, 2011). This technique has several advantages, such as high metal selectivity, high removal efficiency, high overflow rates, low detention periods, low operating cost and production of more concentrated sludge (Rubio et al., 2002). On the other hand, its disadvantages are having high initial capital cost, high maintenance and labor costs.

1.3.7. Electrochemical methods

Principle of electrochemical method is the plating-out of metal ions on a cathode surface and recovering of metals in the elemental metal state. This technique needs relatively large capital investment and the expensive electricity supply, so they haven't been widely applied (Fu and Wang, 2011).

1.3.8. Adsorption

The adsorption process is a favoured technique because of its flexibility in design and operation and ability of providing high-quality treated effluent. Additionally, adsorbents can be regenerated by suitable desorption process because of being reversible in some cases (Fu and Wang, 2011).

As a term “adsorption” is a surface phenomenon which is defined as the increment in concentration of a particular component at the surface or interface between two phases (Faust and Aly, 1998). To make it clear, it can be said that; unsaturated and unbalanced molecular forces, present on every solid surface, is the reason of adsorption. Thereby, when a solid surface is come into contact with a liquid or gas, an interaction occurs between the fields of forces of the surface and that of the liquid or the gas. The solid surface tends to satisfy these residual forces by attracting and retaining the molecules, atoms, or ions of the gas or liquid on its surface. Process is that surface exposure is called adsorption (Bansal and Goyal, 2005).

There are two types forces that play role in adsorption; physical forces with weak interactions (dipole moments, polarization forces, dispersive forces, or short-range repulsive interactions) and chemical forces with strong bonds that are valance forces arising out of the redistribution of electrons between the solid surface and the adsorbed atoms. On the basis of type of forces involved, the adsorption is divided into two types: physisorption and chemisorptions. In previous studies, it is mentioned that; the adsorbate is bound to the surface by relatively weak Van der Waals forces in physical adsorption. On the other hand, chemisorption involves exchange or sharing of electrons between the adsorbate molecules and the surface of the adsorbent resulting in a chemical reaction. In the light of all the facts mentioned above it can be said that; chemisorption is stronger than physisorption (Bansal and Goyal, 2005). Differences between two types of adsorption are summarized at Table 1.2.

Table 1.2 Comparison of physisorption and chemisorption

Comparison Criteria	Physisorption	Chemisorption
Effective forces	Weak van der Waals forces	Chemical bond forces
Activation energy dependency	It does not require any activation energy	It requires activation energy
Temperature dependency	Decreases with increase of temperature	Increases with increase of temperature
Occurrence dependency	It is not specific in nature	It is specific in nature and occurs only when there is some possibility of compound formation between the adsorbed and adsorbent
Adsorption layer	Single layer or multilayer	Only single layer

Nature of the adsorbate and adsorbent; the reactivity of the surface; the surface area of the adsorbate; temperature and pressure of adsorption have an effect upon the type of adsorption that takes place in a given adsorbate-adsorbent system (Bansal and Goyal, 2005).

Lately, agricultural wastes have recently become popular as adsorbent because of being effective, eco-friendly and having low cost. Peanut husk (Han et al., 2008), fiber from palm tree trunk (Hameed and El-Khaiary, 2008), rice bran (Wang and Qin, 2005), and pistachio shell (Turan et al., 2011) are examples for these kinds of adsorbents. In recent years, activated char or carbon as adsorbent, especially obtained from agricultural wastes, is getting more popular for adsorption treatment.

1.4. Activated Hydrochar as an Adsorbent

Activated char or carbon is an adsorbent material which has inner surface area and pore volume and developed from substances that have rich carbon content. Their expanded surface area, micro-pore structure, high adsorption capacity and surface reactivity make them excellent adsorbents. There is no exact chemical formula that describes their structure.

Manufacturing process of these materials involves the following steps: raw material preparation, carbonization, and activation (Yang, 2003). Carbonization step can be processed by thermal or hydrothermal ways.

Organic based activated carbon or char contains carbon dominantly and the remaining hydrogen, oxygen, sulphur and nitrogen. On the other hand, it can include other types of elements with respect to raw material and added chemicals during the process. In spite of activated carbon is an effective adsorbent and has wide range application in industry, it still needs the improvement about cheaper and shorter preparation techniques.

Active carbon has advantages over the other adsorbents;

- It does not need the drying process before industrial separation and purification process.
- By means of expanded, accessible and penetrable inner surface area; it can adsorb nonpolar or weakly polar molecules (Yang, 2003).

1.4.1. Principle of adsorption by activated char

The uniqueness of carbonized material is summarized as; its porous structure determines its adsorption capacity, its chemical structure influences its interaction with polar and nonpolar adsorbates, its active sites determine its chemical reactions with other atoms. Thereby, it can be clearly seen that the adsorptive character of an activated char does not only depend on total surface area and pore size distribution but also it depends on surface properties. This situation is interpreted properly for adsorption of metal cations from the aqueous solutions by Bansal and Goyal (2005). They laid emphasis on, adsorption capacity depends on the physico-chemical characteristics of the carbon surface, which include surface area, pore size distribution, electro-kinetic properties, the chemistry of the carbon surface, and the nature of the metal ions in the solution.

In order to clearly understand the effectiveness of activated char's surface character on metal adsorption capacity, it should be known that there are acidic and basic carbon-oxygen surface groups on it. Carboxyl, lactone, and phenol groups are known as acidic groups and they make the surface polar and hydrophilic. Pyrone and chromene structures are known as basic groups. Accordingly, pH of the solution is also effective, because; these two parameters determine the nature and concentration

of the ionic and molecular species in the solution. Herein, zero point charge (pH zpc) is an important term to explain relationship between pH and surface chemistry of char. It describes the pH condition when the electrical charge density on a surface is zero. Below this pH point; surface has a positive charge which refers the presence of basic surface groups, above this pH point; surface has a negative charge due to the ionization of acidic carbon-oxygen surface groups (Bansal and Goyal, 2005).

1.4.2. Production of activated char

As well as activated char or carbon is color, taste and odor remover, it can also be used for removing of organic or inorganic materials. In literature; some organic materials like apricot seed (Önal et al., 2010), tea waste (Ozmaç, 2010), oil stone (Bohli et al., 2011), apple peel (Hesas et al., 2013), and switchgrass (Regmi et al., 2012) etc. have been used for preparation carbonaceous material. At these studies, carbonaceous materials were obtained by variable ways. Some of them used dry pyrolysis technique and others used wet pyrolysis, also known as hydrothermal carbonization (HTC).

As a term dry pyrolysis is defined as thermal destruction of organic macromolecules in the absence of oxygen into smaller molecules. These destructed parts comprise a high energy content and significant organic content (Prakash and Karunanithi, 2008). If this decomposition is carried out in the presence of subcritical, liquid water, it is often called hydrous pyrolysis or hydrothermal carbonization. Both techniques have same aim which is carbonizing of the material; making products with higher carbon contents (Libra et al., 2011).

Difference in products obtained from these techniques was summarized by Libra et al. (2011) like that; while eco-friendly conversion processes and applications for biomass had been searching, this was resulted in a variety of terms to describe the solid product from dry or wet pyrolysis. Chemical description of this solid is a *char—a solid decomposition product of a natural or synthetic organic material* (Fitzer et al., 1995; IUPAC, 1997). Traditionally, such solids are called “charcoal” if obtained from wood, peat, coal or some related natural organic materials and usually used for cooking purposes. In the fields of soil and agricultural sciences, the term ‘biochar’ has been propagated to mean charred organic matter, which is applied to soil with the intent of improve soil properties (Lehmann et al., 2009). The solid product from wet

pyrolysis process is called ‘hydrochar’ (Libra et al., 2011). If this carbonaceous material is activated by chemically or physically to improve sorption capacity, surface chemistry and porosity; it can be called as “activated hydrochar”.

In HTC technique, raw material is surrounded by water during the reaction. Water phase is kept in a liquid state by high pressure in reactors. This water phase is known as “subcritical water phase”. The pressure may be equal to the vapor pressure of water at a given temperature or higher. Therefore, necessary pressure range is at least 16 bars at 200°C. At that point, very little gas (1–5%) is generated, and most organics remain as or are transformed into solids (Behrendt et al., 2008). As in dry pyrolysis, reaction temperature (and pressure) determines the product distribution (Libra et al., 2011).

When examining the dry pyrolysis technique; the temperature is between 200 and 500°C in a largely inert atmosphere. These conditions lead to the thermal degradation of biomacromolecules with no oxidation except by the oxygen contained in the biomass feed. In this technique, more heat is required for decomposition, for instance; hemicelluloses mainly decompose between 200 and 400°C, while cellulose decomposes at higher temperatures (300–400°C). By contrast, lignin is the most stable component, gradually decomposing between 180 and 600°C (Groenli et al., 2002). In comparison, during hydrothermal carbonization (HTC) the material is heated in subcritical water to between 150 and 250°C at autogenic pressures (Libra et al., 2011). HTC technique needs lower energy for carbonization. The underlying cause of this situation is starting of that mechanism with hydrolysis of biomass which exhibits lower activation energy than most of the pyrolytic decomposition reactions in HTC technique (Mok et al., 1992). Thereby, the principle biomass components are less stable under hydrothermal conditions, which lead to lower decomposition temperatures. Hemicellulose can be decomposed between 180 and 200°C, most of the lignin between 180 and 220°C, and cellulose above approximately 220°C by this technique (Bobleter, 1994).

Briefly, HTC technique's advantages are;

- energy requirement and working conditions are milder,
- because of react in water phase, there is no requirement for poisonous solvent,
- utilization of biomass, which is a renewable and sustainable material, as a source of carbon,
- low operational cost,
- without needing of pretreatment (single stage operation),
- modification possibility to meet the needs or usage possibility with other materials,
- without needing of purification operation for obtained carbonaceous material,
- suitability for scaling and improvement, and
- without needing of added cooling system during the process (Aydıncak, 2012).

As summary, HTC technique can convert wet input material into carbonaceous solids at relatively high yields without the need for an energy-intensive drying before or during the process (Libra et al., 2011).

1.4.3. Microwave application in hydrothermal carbonization process

Up to the present, conventional heating is used to produce char commonly. This method includes three mechanisms for heat transferring to the samples; conduction, convection and radiation mechanisms (Xie et al., 1999; Thakur et al., 2007). The surface of the particles is heated before their interiors, including a thermal gradient between the surface and core of each particle (Thostenson and Chou, 1999; Yadoji et al., 2003). Because of this thermal gradient, there would be heterogeneous microstructure at high heating rates (Oghbaei and Mirzaee, 2010).

In despite of conventional ovens, processed material interacts with electromagnetic radiation at microwave oven. Because of the heat being generated by the material itself in its bulk, the heat can reach the entire volume much faster and selectively. In depth, the principle of microwave heating is the dielectric heating in which energy is absorbed by ions or molecules that are either induced or permanent dipoles. Unlike conventional heating, the energy conversion occurs by two mechanisms: ion conduction and dipole rotation inside particles (Gupta et al., in press). This

opportunity results in a homogeneous material, with faster production, while providing a significant reduction in energy losses (Clarck and Sutton, 1996).

On the further side of these advantages, it is an economic way. Use of microwaves in a process is classified as clean technology, following the global trend towards the use of alternative environmentally friendly methods (Guiotoku et al., 2011).

Nowadays, microwave heating has been used for the preparation of carbonaceous materials for instance; from tobacco stem, cotton stalks, rice husk, pine apple peel, mangosteen peel, orange peel precursors (Li et al., 2008; Deng et al., 2009; Foo and Hameed, 2011; Foo and Hameed, 2012a; Foo and Hameed, 2012b; Foo and Hameed, 2012c). It is said that; in carbonization process within the microwave, the efficiency is very close to %100. In other words; almost all the carbon from material is converted into carbonized material, without generating CO and CO₂ (Guiotoku et al., 2011).

Improved method which includes the combination of hydrothermal carbonization and microwave heating is one of the most advanced technologies to convert bio-waste with high moisture levels, because it eliminates the drying step (Guiotoku et al., 2011). Additionally, this heating method offers advantages about process time and last product homogeneity since; the reaction time was decreased compared to conventional hydrothermal carbonization and application of homogeneous heating with selective power to the product. These factors improve the properties of the final products and enable the synthesis of new materials that could not be obtained by conventional methods (Guiotoku et al., 2011).

In the light of this information, it can be said that there are different methods to produce char and each method's parameters can be changed according to the used raw material so last material's properties would be varied.

1.4.4. Valorization of grapefruit peel as activated hydrochar

The grapefruit (*Citrus paradisi*), is a citrus fruit related to the orange, lemon and pomelo. It is hybrid originating in Barbados as an accidental cross between two introduced species, sweet orange (*Citrus sinensis*) and pomelo or shaddock (*C. grandis*), both of which were introduced from Asia in the seventeenth century

(Carrington et al., 2003). It was named as "grapefruit" in 1814 in Jamaica, which reflects the way it's arranged when it grows and hanging in clusters just like grapes.

Grapefruit has been produced and consumed in wide area. According to the USDA data; 6,086,000 tones grapefruit had been produced worldwide at 2013-2014. China is on the first place with 3,717,000 tones in production; United States follows it with 950,000 tones production. Turkey has the sixth rank (235,000 tones) (USDA, 2013-2014).

Juice of citrus fruit has highly consumed throughout the world. When looking the numbers at 2013-2014 years; 897,000 tones of grapefruits were processed industrially (USDA 2013-2014). During production, fruit pulp and peel are formed as waste material. These parts have high carbon content and valuable substances. When examining with detailed; for a standard citrus fruit, peel is almost %50 of whole fruit (Marin et al., 2007) and %20-25 of peel is dry matter. This solid phase contains sugars, cellulose, hemicellulose, pectin, and d-limonene (Bampidis et al., 2006). Thereby, grapefruit peel, as a waste, has potential to be evaluated for the production of activated char.

Carbonization of these kinds of bio-wastes takes quite long time in nature. With the improved techniques like as hydrothermal carbonization, HTC, this process has been shortened and final materials can be used in many purposes with positive contribution to nature. During the carbonization of grapefruit peel; hydrolysis is the first step. At that step, water reacts with extractives, hemicellulose, or cellulose and breaks ester and ether bonds, resulting in a wide range of products, including soluble oligomers like (oligo-) saccharides from cellulose and hemicelluloses (Sevilla and Fuertes, 2009; Funke and Ziegler, 2010). A very small portion of lignin reacts at higher HTC temperature and releases phenol and phenolic derivatives (Zhang et al., 2008; Yan et al., 2009). After hydrolysis, dehydration and decarboxylation of hydrolyzed products most likely take place immediately and simultaneously (Reza et al., 2014a). At hydrothermal conditions, intermediate materials occur like 5-Hydroxymethylfurfural (HMF), erythrose, and aldehydes, which further dehydrate and decarboxylate into CO₂ and H₂O (Sevilla and Fuertes, 2009a; Kruse et al., 2015). Most of these intermediates undergo condensation, polymerization, and aromatization. In literature, the products of these simultaneous condensation;

polymerization and aromatization are called as bio-crude. The liquid bio-crude, after successive polymerization and aromatization, converts into solid product with or without auto-nucleation. This solid product is a part of the desired hydrochar (Reza et al., 2014b).

Whole reactions that take place under hydrothermal conditions need heat energy. When heating is applied by microwave energy, HTC method is getting more advantageous.

1.5. Modeling

1.5.1. Adsorption kinetics

Kinetic evaluations are important to examine the mechanism, efficiency and rate limiting step of sorption process. Kinetic modeling provides the estimation of sorption rate and gives opinion about characteristic of possible reaction mechanisms (Robati, 2013). This information is used in the modeling and design of the process.

Both adsorption capacity and adsorption kinetic depend on the characteristic of carbon and experimental conditions. Some of the common types of kinetic models used in sorption process are; Pseudo-first order, Pseudo-second order, Elovich and logistic equations. While describing the kinetic equations differential rate law and integral rate law terms are used. Differential form is used for representing the law in molecular level; integral form is used for determining the reaction order and the value of the rate constant from experimental measurements.

When a reaction progresses at a rate depends linearly on only one reactant concentration, this reaction is considered as first-order reaction. In second order reactions, rate is proportional to the product of two reactant concentrations; the sum of the exponents in the rate law is equal to two. Many important biological reactions and systems containing various kinds of sorbates (heavy metals in cationic and anionic forms, organic dyes, phenols, etc.) and sorbents (inorganic minerals, activated carbons, raw biomass, etc.) can be described using second order kinetics (Plazinski et al., 2013).

In order to describe the kinetics of heavy metal removal by natural zeolites, mathematical form of the Pseudo-second order equation was used by Blanchard et al. (1984). Nowadays, it is one of the most common mathematical expression applied to

the kinetic data observed from solid/solution sorption systems (Plazinski et al., 2013) and used to predict the relationship between q_{exp} and q_{pred} . (Plazinski et al., 2009). This kinetic model is represented as;

$$\frac{t}{q_t} = \frac{1}{k_2 \cdot q_e^2} + \frac{t}{q_e} \quad (1.1)$$

Where, q_e and q_t show the adsorbed adsorbate amount (mg/g) at equilibrium and at time t (min), respectively. k_2 (g/mg.min) is the Pseudo second-order rate constant.

Elovich equation is another common kinetic model in sorption processes which describes adsorption with kinetic principle that adsorption site increase exponentially with adsorption (Hammud et al., 2011). Recently, this model has been used to describe the adsorption process of pollutants from aqueous solutions, such as cadmium removal from effluents using bone char (Cheung et al., 2001), and Cr^{+6} and Cu^{+2} adsorption by chitin, chitosan, and *Rhizopus arrhizus* (Sağ and Aktay, 2002).

$$q_t = \frac{1}{\beta} \cdot (\ln(1 + (\alpha \cdot \beta \cdot t))) \quad (1.2)$$

The constants α and β were obtained from the slope and intercept of the linear plot of q_t versus $\ln(t)$. α is the initial adsorbate sorption rate (mmol/(g*min)), β is the desorption constant (g/mmol).

Logistic model is a sigmoidal model and it has been used to define growth of microorganisms, biomass, and biovolume productions by microorganisms during the cultivation (Zwietering et al., 1990). In recent studies, Logistic model has been used to describe the whole adsorption process (Çelekli et al., 2009; Çelekli et al., 2012).

This model is expressed as:

$$q_t = \frac{A}{1 + \left(\frac{t}{b}\right)^c} \quad (1.3)$$

Where q_t is the amount of adsorbed adsorbate (mg/g) at time t (min) and A is the maximum sorption at equilibrium (mg/g), t is time (min), and b and c are the Logistic constants.

1.5.2. Adsorption equilibrium isotherms

In an adsorbent-adsorbate system, if they are contacted enough, equilibrium is reached between them. The equilibrium relationship is described by adsorption isotherms. It is a curve that relating the equilibrium concentration of a solute on the surface of an adsorbent, q_e , to the concentration of the solute in the liquid, C_e , with which it is in contact at a given temperature.

By means of isotherms, some useful information can be predicted. It is mentioned in Bansal and Goyal (2005) study that an isotherm helps in the determination of the surface area of the adsorbent, the volume of the pores, and their size distribution. Besides, isotherm provides important information on the subject of the magnitude of the enthalpy of adsorption. Also, the parameter of sorbent regeneration method, for example; temperature or pressure swing and the magnitude of the required swing, the length of the unusable (or unused) bed and the product purities can be predicted by the means of isotherms (Yang, 2003). Freundlich (Freundlich 1906); Langmuir (Langmuir 1916; Langmuir 1918); BET-theory (Brunauer et al. 1938); Temkin (Temkin, 1940); Dubinin- Radushkevich (D-R) (Dubinin and Radushkevich 1947); HacsKaylo and LeVan (HacsKaylo and LeVan 1985); are the models of sorption isotherm. According to the previous studies, it can be said that; for wastewater treatment with activated char or carbon, most commonly used isotherms are Freundlich, Langmuir and Dubinin-Radushkevich (D-R) isotherms. Basic differences between Langmuir, Freundlich and Dubinin-Radushkevich isotherms are; Langmuir isotherm is a theoretical constructed, Freundlich isotherm has empirical origin and Dubinin-Radushkevich has semi-empirical origin.

1.5.2.1. Langmuir isotherm

Langmuir isotherm is the first theoretically developed model to describe the gas adsorption onto solid surface at a fixed temperature by Langmuir (1916). It was created by assuming an adsorbate behaves as an ideal gas at isothermal conditions. Langmuir model can be also called as localized model because of its principle. Its definition is given at literature as follows; isotherm model which describes quantitatively the formation of a monolayer adsorbate on the outer surface of the adsorbent, and after that no further adsorption takes place (Vermeulan et al., 1966). In other words, this isotherm is valid for monolayer adsorption onto a surface

containing a finite number of identical sites and assumes that there are uniform energies of adsorption onto the surface; the surface is excellently smooth and homogenous; so that the lateral interactions between the adsorbed entities are negligible (Bansal and Goyal, 2005; Dada et al., 2012).

Langmuir isotherm is expressed in Eq. (1.4):

$$\frac{C_e}{q_e} = \frac{1}{q_L \cdot K_L} + \frac{C_e}{q_L} \quad (1.4)$$

Where q_e is the equilibrium adsorbate concentration on adsorbent (mg/g), C_e is the equilibrium adsorbate concentration in solution (mg/L), q_L is the monolayer sorption capacity (mg/g), and K_L is the Langmuir constant (L/mg) related to the energy of sorption.

The essential features of the Langmuir isotherm may be expressed in terms of equilibrium parameter R_L , which is a dimensionless constant referred to as separation factor or equilibrium parameter (Webber and Chakravarti, 1974). Value of R_L indicates that sorption process is irreversible ($R_L = 0$); favorable ($0 < R_L < 1$); linear ($R_L = 1$); and unfavorable ($R_L > 1$). This value can be calculated by use of Langmuir constant, K_L , in Eq. 1.5:

$$R_L = \frac{1}{1 + (K_L \cdot C_0)} \quad (1.5)$$

On the other hand, there are some limitations of this isotherm. At first, Langmuir model is valid under low pressure conditions. Because according to hypothesis, the adsorbed gas has to behave ideally in the vapor phase and this condition is approachable at low pressure conditions only. Second limitation is mentioned above as assuming homogeneous surface. This is well known that solid surface has heterogeneous structure. Thirdly, it was assumed that there is no interaction between adsorbed molecules but in the presence of weak force attraction, this is impossible although, experimental results have been fitted by based on this Equation, or by developed equations from Langmuir concept. Thus, the Langmuir equilibrium model still retains an important position in physisorption as well as chemisorption theories (Bansal and Goyal, 2005).

1.5.2.2. Freundlich isotherm

This adsorption isotherm which is the oldest nonlinear isotherm describes empirical relationship between the solute concentration on the surface of adsorbent and the concentration of the solute in the liquid which it is in contact (Freundlich, 1906).

The Freundlich isotherm is a limiting form of the Langmuir isotherm, and is applicable only in the middle ranges of vapor pressures (Bansal and Goyal, 2005). In other words, it was used to describe adsorption variety with pressure change until saturation pressure is reached. This is a limitation for that model. On the other side, in contrast to Langmuir, this model is commonly used to describe the adsorption characteristics for the heterogeneous surface (Hutson and Yang, 2000).

Freundlich isotherm is expressed in Eq. (1.6);

$$\log q_e = \log K_f + \frac{1}{n} \cdot \log C_e \quad (1.6)$$

The Freundlich constant K_f [(mg/g) (L/g)^{1/n}] is an approximate indicator of adsorption capacity, while n indicates the favorability of adsorption. If $n < 1$ it refers poor, $1 < n < 2$ it refers moderately difficult, or refers good in ranging from 2 to 10 (Chen et al., 2011)

1.5.2.3. Dubinin-Radushkevich isotherm

Dubinin–Radushkevich isotherm describes an adsorption mechanism with a Gaussian energy distribution onto a heterogeneous surface (Dabrowski, 2001; Gunay et al., 2007). One of the unique features of the Dubinin-Radushkevich (D-R) isotherm is being temperature-dependent. When adsorption data at different temperatures are plotted as a function of logarithm of adsorbed material amount $\ln(q_e)$ versus Dubinin–Radushkevich isotherm constant, ε^2 , all suitable data will lie on the same curve, named as the characteristic curve (Foo and Hameed, 2010). Dubinin et al. (1966) had researched on the effect of surface character on the absorbability of different gases and adsorption of different solutes from solutions on activated carbons. They acquired that the characteristic curves of different vapors on the same adsorbent were related to each other. Based on this phenomenon, it was observed that if the Dubinin–Radushkevich isotherm constant, ε , corresponding to a

certain volume of adsorption space, W , on the characteristic curve for one vapor was multiplied by a constant, the adsorption potential corresponding to the same value of W on the characteristic curve of another vapor could be found (Bansal and Goyal, 2005).

In recent years, studies have used the Dubinin–Radushkevich (DR) equilibrium isotherm for description of adsorption in microporous materials, especially those of a carbonaceous origin (Nguyen and Do, 2001).

D–R isotherm is described as:

$$\ln q_e = \ln q_m - \beta \varepsilon^2 \quad (1.7)$$

$$\varepsilon = R \cdot T \cdot \ln\left(1 + \frac{1}{C_e}\right) \quad (1.8)$$

where q_m is the maximum sorption capacity (mg/g), β is a constant related to the sorption energy (mol^2/kJ^2), ε is the Dubinin–Radushkevich isotherm constant, R is the gas constant (8.314 J/mol.K), and T is absolute temperature (K).

It has been applied to differentiate distinguish the physical and chemical adsorption of metal ions by evaluation of mean of its free energy E (kJ/mol) from β values (Zheng, 2008);

$$E = \frac{1}{\sqrt{-2 \cdot \beta}} \quad (1.9)$$

If value of E is between 8 kJ/mol and 16 kJ/mol , it can be said that sorption process is chemical in nature, while lower than 8 kJ/mol indicates that the sorption is physical in nature (Zheng, 2008).

1.5.3. Adsorption thermodynamic

Thermodynamics gives an idea about the characteristic behavior of material as a function of state variables (P , T , chemical composition etc.). In the case of thermodynamics of an adsorption process; determination of value of the thermodynamic quantities (activation energy, activation parameters, Gibb’s free energy change, enthalpy and entropy of adsorption values) are required to estimate and optimize the performance and predict the mechanism of an adsorption separation

process and design of process (Saha and Chowdhury, 2011). These functions have been evaluated by adsorption isotherms and are compared with theoretical considerations (Bansal and Goyal, 2005).

In adsorption separation, activation energy is defined as the energy that must be overcome by the adsorbate to interact with the functional groups on the surface of the adsorbent (Saha and Chowdhury, 2011). It is usually denoted by E_a , and given in units of kJ/mol. The activation energy, E_a , for the adsorption can be determined by use of adsorption rate constant at different temperatures from the Arrhenius equation. Generally, rate constant value from Pseudo-second order kinetic model is used for E_a calculation but in the present study this value was obtained by adsorption rate constant from Logistic kinetic model, μ , and Arrhenius equation was modified as follows:

$$\ln \mu = \ln A - \frac{E_a}{R.T} \quad (1.10)$$

where μ is the adsorption rate constant from Logistic kinetic model (1/min), A is the frequency factor, E_a is the activation energy (kJ/mol), R is the gas constant (8.314 J/mol*K) and T is the absolute temperature (K). E_a and A values can be obtained by slope and the intercept of graph of $\ln(\mu)$ versus $1/T$.

As it mentioned before, there are two main adsorption processes; chemical and physical. Both need energy to take place. At that point, the magnitude of activation energy can give an idea about the type of adsorption whether chemisorption or physisorption. In literature, it is mentioned that; the activation energy for in physical sorption energy is required, ranging from 5 to 40 kJ/ mol. On the other hand, chemical sorption involves stronger forces than the physical sorption and thus high activation energy is required (40–800 kJ/ mol) (Çelekli et al., 2012).

Besides determination of type of adsorption, thermodynamic considerations can give idea about whether process is spontaneous or not. The Gibb's free energy change, ΔG^0 , indicates the spontaneity of a chemical reaction (Eqn 1.11). If ΔG^0 (kJ/mol) has a negative value it means that interaction occurs spontaneously at a given temperature. Both enthalpy, ΔH^0 (kJ/mol) and entropy, ΔS^0 (J/mol*K) factors can be calculated from Gibb's free energy of the process (Eqn 1.12).

$$\Delta G = -R. T. \ln(K_L) \quad (1.11)$$

$$\Delta G = \Delta H - \Delta S. T \quad (1.12)$$

where R is the universal gas constant (8.314 J/mol.K), T is the temperature (K), and K_L is Langmuir constant (L/mol) obtained the plot of C_e/q_e versus C_e .

As a well-known information; negative value of ΔH^0 indicates that the adsorption phenomenon is exothermic while a positive value implies that the adsorption process is endothermic. This phenomenon arises from behavior of phases of adsorption system; in endothermic process the adsorbate species has to displace more than one water molecule for their adsorption; this results in the endothermal tendency of the adsorption process. Therefore ΔH^0 will be positive. In an exothermic process, the total energy absorbed for breaking of bond is less than the total energy released from bond occurrence between adsorbate and adsorbent and this results in the release of extra energy in the form of heat. Therefore ΔH^0 will be negative (Saha and Chowdhury, 2011).

Value of entropy change, ΔS^0 , gives idea about measure of disorder; positive value of ΔS^0 indicates increment of randomness at the solid/solution interface with some structural changes in the adsorbate and the adsorbent, additionally; the affinity of the adsorbent towards the adsorbate species. On the other hand, a negative value of entropy change, ΔS^0 , indicates a decreased disorder at the solid/liquid interface during the adsorption process (Saha and Chowdhury, 2011).

1.6.Aim of Study

Aims of present study was to develop an effective and low cost adsorbent from grapefruit peel as an agricultural waste, which has also elimination problem, to remove heavy metals, specifically Cu^{+2} ions from aqueous solutions. While this valorization is processed, making material in better quality with energy and time saving is considered by using microwave-assisted hydrothermal carbonization technique. In this way, grapefruit peel which is produced as waste material but actually very valuable material because of its chemical and porous structure is evaluated as adsorbent and heavy metal contaminated wastewater is regained.

Aims of this study were;

- removing heavy metals, specifically Cu^{+2} , from aqueous solution by adsorption,
- valorization of waste grapefruit peel, which has also elimination difficulty at industry, as an adsorbent,
- using of eco-friendly, energy and time saving method to make adsorbent; microwave assisted-HTC, and
- porosity improvement of adsorbent to make it more favorable.

CHAPTER II

MATERIALS AND METHODS

2.1. Preparation of Adsorbate

Stock Cu^{+2} solution (1000 mg/L) was prepared by dissolving copper fine powder in the %2 HNO_3 solution and stored at 4 °C. The working samples (5, 10, 20, 40 and 60 mg/L Cu^{+2}) were diluted from this stock solution. All the chemicals (e.g. %65 HNO_3 (CAS: 7697-37-2, Merck), copper fine powder (CAS: 7440-50-8, Merck), %99.8 ethanol (CAS: 64-17-5, Sigma-Aldrich) and pure KOH pellet (CAS: 1310-58-3, Sigma-Aldrich)) were used as analytical grade. All solutions were prepared with ultra pure water.

Experimental design is given at Figure 2.1.

2.2. Preparation of Material

2.2.1. Determination of moisture content

Grapefruits were supplied from a farm of Hatay, Turkey. Peels separated from the fruit were ground into small pieces with Waring blender (Stamford, USA). Moisture content of ground grapefruit peel (1 g) was analyzed by drying until reaching to the constant weight in a forced air oven at 105 °C (AOAC, 1999). Values were expressed for the moisture content. All measurements were done in triplicate. The initial moisture content of grapefruit peel was measured as 79% wet basis.

2.2.2. Pretreatment of peel

About 4 g of ground peel was weighted and put into 35 ml vial. CO_2 free-ultra pure water was added onto peel but amount of that water was determined according to the initial moisture content of peel. Because of having vial with limited volume and requiring head space to be able to controlling inner pressure; amount of total water with moisture of peels was determined as 4 times of peel in the vial. A magnetic

stirrer bar was put into vial to get homogeneous mixing. Peel:water (1:4 (w/v)) mixture was sealed with special cap of vial and put into microwave batch reactor (Cem, Discover-Sp W/Activent, USA). Constant microwave energy (150 W; 37.5 W/g) was applied for 15 min. In this stage, extraction of water-soluble materials into water phase was aimed. While extracting of these materials; the porous structure was maintained by means of microwave heating. Following this; water phase was decanted and solid part was collected for further charring process.

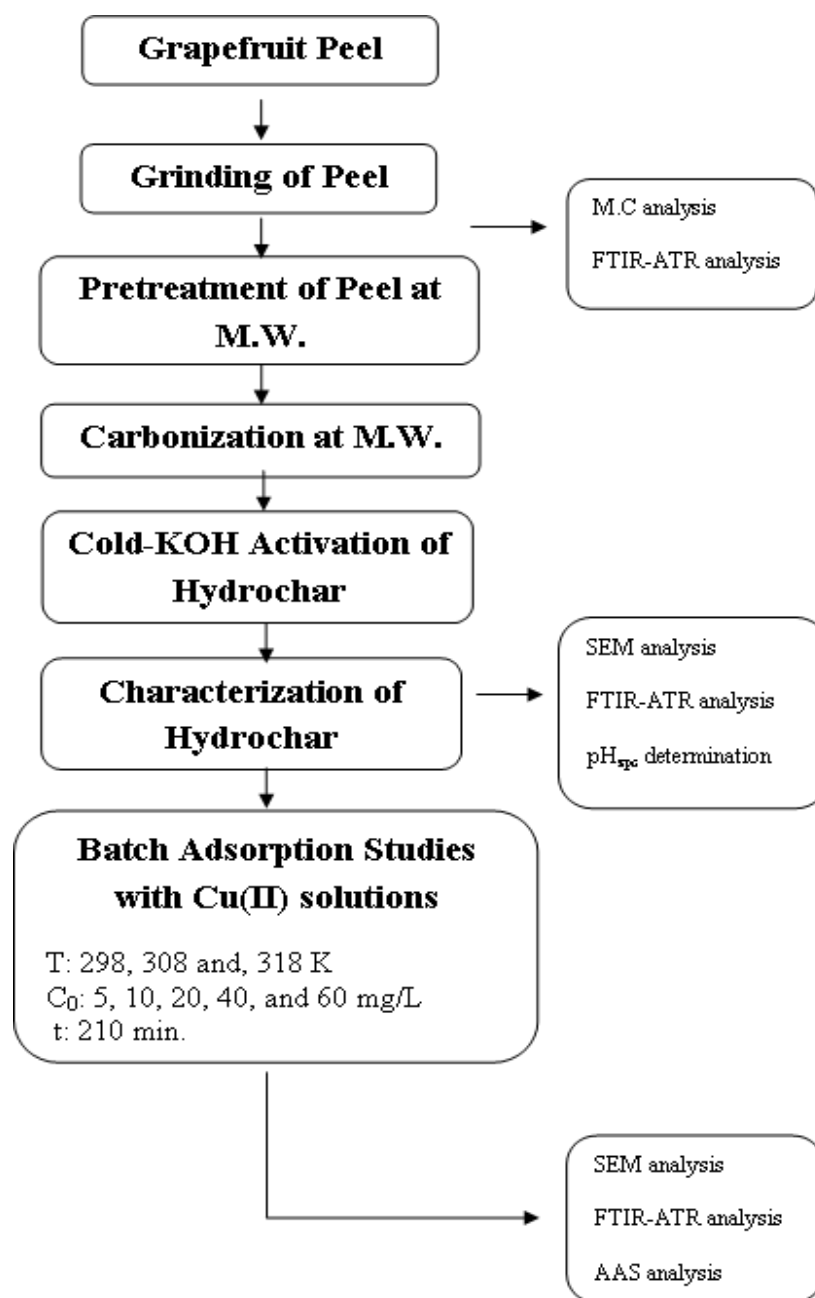


Figure 2.1 Schematic diagram of experimental design

2.2.3. Preparation of hydrochar

Hydrothermal carbonization (HTC) method recommended by Balu et al. (2012) was modified to meet need of the present study. At low-temperature, microwave-assisted hydrothermal process was implemented to hydrochar preparation with microwave energy of 250 W for 20 min. Three times of CO₂ free-ultra pure water was added onto the collected solid residue. Solid residue: water mixture (1:3 (w/v)) was exposed to 210-215 °C and carbonized by microwave. During charring process, pressure in the closed vial which exposed to microwave heating reached a maximum value of 20.4 atm. Hydrochar obtained from HTC process was filtered with filter cloth and washed with ethanol and following distilled water to remove residual condensed components.

2.2.4. Activation of hydrochar

In order to get higher porosity, hydrochar was treated with 1 M KOH solution (at ratio of 1:200 w/v) for 2 h. After then, hydrochar was washed with ultra pure water and neutralized with 0.1 M HNO₃, because; the pH of the activated hydrochar might affect the metal adsorption (Regmi et al., 2012). The hydrochar was dried in oven at 105 °C, weighed repeatedly until reaching its constant weight. Dried and activated hydrochar was ground with ceramic mortar and sieved. Particle size between 250 and 355 µm of activated hydrochar was selected for the sorption process.

2.3. Precipitation Test of Cu⁺² Ions

Metal ion precipitation occurs at high pH values, which is generally a concern in differentiation the metal removal by adsorption technique. Therefore, effect of pH values on Cu⁺² ion precipitation without adsorbent was affirmed. About 100 ml of 10 mg/L initial concentration Cu⁺² ion solutions in 250 ml Erlenmeyer at pH between 2.5 and 7.5 were agitated by using shaker (INNOVA 40R, Germany) at 150 rpm and ambient temperature during 24 h. After centrifugation process, Cu⁺² ion concentrations in supernatant were analyzed by Atomic Absorption Spectrometer (AAS) (Perkin Elmer, AAnalyst 800, USA) at the 324.75 nm which was recommended value by the AAS. According to relationship between initial and final Cu⁺² concentrations, precipitation pH was determined.

2.4. Hydrochar Characterization

2.4.1. SEM analysis

Adsorbent samples were prepared diversely to evaluate difference on adsorbent's surface morphology. For that purpose, dried peel and activated hydrochars were treated with 100 ml pure water without Cu^{+2} ions in 250 ml erlenmayer at pH 6.3 and 45 °C and stirred in the shaker (INNOVA 40R, Germany). Samples were held onto an adhesive carbon band on an aluminum stub followed by sputter coating with gold. Surface morphology of these samples was studied using a scanning electron microscopy (SEM) (JEOL-6390LV, USA).

2.4.2. FTIR analysis

To determine the effect of carbonization process on surface chemistry and functional groups responsible for the adsorption, Fourier transform infrared (FTIR-ATR) spectrometer (PerkinElmer Spectrum 100 FTIR-ATR Spectrometer, USA) was used. At pH 6.3 and 45 °C; dried peel, inactive and activated hydrochars were treated with ultra pure water, and activated hydrochar was treated with solution of 40 mg/L Cu^{+2} ions as samples.

2.4.3. Determination of pH zero point charge of adsorbent

The pH zero point charge (pH_{zpc}) of hydrochar was determined by use of powder addition method (Kumar et al., 2007). About 0.5 g adsorbent and 50 ml solution of 0.1 M NaCl were mixed in 100 ml erlenmayer flask. Batch experiments were performed at various initial pH (pH_i) values (ranging from pH 2 to 9), adjusted with 0.1 M HNO_3 and 1.0 M NaOH solutions. Sample sets were agitated on the shaker at 150 rpm and room temperature 24 h. The final pH (pH_f) was measured at equilibrium. The value of pH_{zpc} was determined from the plot of pH_f versus pH_i .

2.4.4. The effectiveness of activation process

In order to determination of effectiveness of activation step, small scale batch sorption study was done. At pH 6.3 and 25°C (298 K), 1 g/L of inactive and activated adsorbents were treated with 100 ml solution of 20 mg/L initial Cu^{+2} ions in 250 ml Erlenmayer flask during 24 h. After then, withdrawn samples from sets by pipette were centrifuged. After that, remaining Cu^{+2} ion in the supernatant was analyzed with Atomic Absorption Spectrophotometer (AAS) at 324.75 nm.

2.5. Batch Adsorption Studies

Adsorption studies were handled with activated hydrochar by batch process. Whole experiment sets were carried out by agitating in the shaker at 150 rpm and certain temperature.

2.5.1. Effect of adsorbent dose

It was tested by the addition of activated hydrochar to the solution of Cu^{+2} . Adsorbent doses ranging from 0.5 to 4 g/L were treated with 20 mg/L Cu^{+2} solution at 25 °C (298 K) during 210 min. Then, the samples with exact volume were taken from each set by pipette and centrifuged at 6000 rpm for 15 min to precipitate the suspended adsorbent. After then, residual concentration of Cu^{+2} ions in the supernatant was diluted and analyzed by using Flame-AAS at the wavelength of 324.75 nm.

2.5.2 Effect of initial pH

Adsorbent (1g/L) was treated with 100 mL solution of 20 mg/L Cu^{+2} ions at pH 4, 5 and 6 in 250 mL erlenmeyers. These sets were stirred by using the shaker at 150 rpm and 25 °C (298 K) during 210 min. Then, samples with exact volume were taken from each set by pipette and after then centrifuged at 6000 rpm for 15 min to precipitate the suspended adsorbent. Subsequently, remaining Cu^{+2} ions in the supernatant liquid was diluted and analyzed by using flame AAS at the wavelength of 324.75 nm.

2.5.3. Effect of initial copper concentration and process temperature

About 0.5 g/L activated hydrochar samples were added into 250 ml erlenmayer flasks containing 100 ml solutions of Cu^{+2} ions ranging from 5 to 60 mg/L at optimum pH value. The pH of each solution was adjusted to the desired value with diluted or concentrated HNO_3 and/or NaOH solutions. The flasks were agitated by using orbital shaker at 150 rpm during 210 min.

Samples were taken from each set at 0, 5, 10, 15, 30, 45, 60, 90, 120, 150, 180 and 210 min. They were centrifuged at 6000 rpm for 15 min to precipitate the suspended adsorbent. Then, the supernatant liquid was diluted and after then analyzed for the determination residual Cu^{+2} concentration by use of AAS at 324.75 nm. Three different temperatures (298, 308 and 318 K) were used to evaluate the effect of

temperature values on the adsorption process. All experiments were performed triplicate and average values were given in the present study. At this stage; the effects of initial Cu^{+2} concentration and process temperature were examined at the same time. Adsorbed Cu^{+2} ions on adsorbent at equilibrium, q_e (mg/g), and at time t , q_t , were calculated by using equations 2.1 and 2.2, respectively:

$$q_e = \frac{(C_0 - C_e) \cdot V}{m} \quad (2.1)$$

$$q_t = \frac{(C_0 - C_t) \cdot V}{m} \quad (2.2)$$

C_0 and C_e (mg/L) are the initial and equilibrium concentrations of Cu^{+2} ions, respectively. V (L) is the volume of the solution, and m (g) is the mass of adsorbent.

2.6. Adsorption Kinetics

In a solid/liquid system, determination of removal rate of a solute from solution is an important step for the suitable sorption system design (Plazinski et al., 2009). Sorption mechanism and time dependency character of this sorption system can be predicted by several kinetic equations. In order to investigate the sorption kinetics of Cu^{+2} ions on the hydrochar, the most commonly used kinetic models; Pseudo second-order kinetic model (Eq.1.1), Elovich model (1.2) and Logistic model (Eq.1.3) were applied to experimental data. Equations of kinetic models are given on Table 2.1.

In order to obtain the q_t values, samples were taken from experiment sets with time interval at part 2.5.3 and their Cu^{+2} concentrations were analyzed with AAS according to recommended procedure. Data from AAS was used to calculate q_t values by Eq. 2.2.

2.7. Equilibrium Models

Langmuir (Eq.1.4), Freundlich (Eq.1.6) and Dubinin-Radushkevich (Eq.1.7) isotherms were applied to describe relationship between adsorbed Cu^{+2} ions per unit mass of hydrochar (q_{eq} ; mg/g) and equilibrium metal ion concentration (C_{eq} ; mg/L). The equations of isotherm models are given on Table 2.2.

Table 2.1 Equations of used kinetic models

Kinetic Model	Equations	Reference
Pseudo-second order	$\frac{t}{q_t} = \frac{1}{k_2 \cdot q_e^2} + \frac{t}{q_e}$	Ho and McKay (1999)
Elovich	$q_t = \frac{1}{\beta} \cdot (\ln(1 + (\alpha \cdot \beta \cdot t)))$	Plazinski et al. (2009)
Logistic	$q_t = \frac{A}{1 + \left(\frac{t}{b}\right)^c}$	Çelekli et al. (2009)

q_t : adsorbed adsorbate amount at time t , q_e : adsorbed adsorbate amount at equilibrium, k_2 : Pseudo second-order rate constant, β : desorption constant, α : initial adsorbate sorption rate, A : maximum sorption at equilibrium, b and c : Logistic constants

Table 2.2 Equations of used isotherm models

Equilibrium Model	Equation	Reference
Freundlich	$\log q_e = \log K_f + \frac{1}{n} \cdot \log C_e$	Freundlich (1906)
Langmuir	$\frac{C_e}{q_e} = \frac{1}{q_L \cdot K_L} + \frac{C_e}{q_L}$ $R_L = \frac{1}{1 + (K_L \cdot C_0)}$	Langmuir (1918)
Dubinin-Radushkevich	$\ln q_e = \ln q_m - \beta \varepsilon^2$ $\varepsilon = R \cdot T \cdot \ln\left(1 + \frac{1}{C_e}\right)$	Dubinin-Radushkevich (1947)

K_f : Freundlich constant as adsorption capacity, n : favorability of adsorption, C_e : equilibrium adsorbate concentration in solution q_L : monolayer sorption capacity, R_L : Dimensionless constant referred to as separation factor (equilibrium parameter), K_L : Langmuir constant related to the energy of sorption, C_0 : initial solute concentration, q_m : D-R isotherm maximum sorption capacity, β : constant related to the sorption energy, ε : D-R isotherm constant, R : gas constant, and T : absolute temperature

2.8. Thermodynamic Studies

Thermodynamic studies were performed at three different temperatures (298, 308, and 318 K). From Eq.1.11, Gibbs free energy change values (ΔG°) were calculated by using of K_L constant from Langmuir model. Other variables, entropy (ΔS°) and enthalpy changes (ΔH°) were calculated from ΔG° versus T (K) plot by using Eq.1.12.

2.9. Statistical Analysis

The analysis of variance (ANOVA) is used to determine whether there are any significant differences between the means of independent groups. One-way ANOVA was carried out for the contact time and initial Cu^{+2} concentrations to determine the significant differences at $\alpha=0.05$. Also, three-way ANOVA was performed to find the significant difference in the time-temperature -initial Cu^{+2} concentrations by using the SPSS version 16.0 (SPSS Inc., Chicago, IL, USA). Duncan's multiple range test was applied to determine any significant differences in among groups.

2.10. Validation of Models

Fitting of experimental data to isotherm and kinetic models was SigmaPlot software version 11 (Systat Software, Inc., California, USA) via the Marquardt–Levenberg algorithm. On the other hand, with this algorithm, q_{pred} values and constants of kinetic equations and equilibrium isotherm constants were obtained by using SigmaPlot software version 11 (Systat Software, Inc., California, USA) via the Marquardt–Levenberg algorithm.

In order to evaluate the goodness of fitting; correlation coefficients (R^2) and the sums of squared error (SSE) were carried out between experimental and predicted data and calculated by use of Eq. 2.3.

$$SSE = \sqrt{\frac{\sum(q_{\text{exp}} - q_{\text{predict}})^2}{N}} \quad (2.3)$$

CHAPTER 3

RESULTS AND DISCUSSION

In the present study, hydrochar obtained from grapefruit peel was performed as an adsorbent to remove Cu^{+2} ion from aqueous solution. Microwave assisted-hydrothermal carbonization technique was used to prepare that char from grapefruit. To understand its chemical structure, sorption performance, capacity and dependencies of these properties; some laboratory scale experiment sets were prepared and instrumental analyses were done.

The underlying reasons for choosing grapefruit peel as raw material were possession acidic character which can change the pH of earth, therefore; having annihilation problem as an industrial waste, on the other side; containment of evaluable precious chemicals in its structure. When citrus genus is examined, there are 20% dry matter (sugars, cellulose, hemicellulose, pectin, and d-limonene) and 80% water (Bampidis et al., 2006). Mentioned dry matter composition makes that peel favorable as raw material for carbonization.

Water is one of the most practicable green solvent because of its non-toxicity, non-flammability properties, and wide availability. With that opinion; low temperature hydrothermal carbonization technique was chosen to prepare “greener” sorbent with a large solid fraction without considerable liquefied or gasified carbon fractions. Despite, hydrochars have not got porous structure very well, their oxygen functionalities and surface active sides make them utilizable as metal ion sorbent (Titirici, 2012).

3.1. Adsorbent Characterization

3.1.1. FTIR-ATR analyses

In order to investigate functional groups on hydrochar and responsible ones for adsorption process, FTIR-ATR was performed for four samples; dried peel without Cu^{+2} , inactive hydrochar without Cu^{+2} ; activated hydrochar without Cu^{+2} and activated hydrochar with 40 mg/L Cu^{+2} . The results of analyses are given on Tables 3.1 and 3.2 and on Figure 3.1.

Differences between dried peel and carbonized peel were observed in results of FTIR-ATR. Shifting of some peaks, losing of peaks or occurrence of new peaks was observed. Aliphatic hydroxyl bond for water (O-H stretching) at 3329 $1/\text{cm}$ for dried peel shifted to 3333 $1/\text{cm}$ and aliphatic hydrocarbon (C-H) bond shifted from 2889 $1/\text{cm}$ to 2900 $1/\text{cm}$ in carbonized peel (Reza et al., 2014c). Peak at 1728 $1/\text{cm}$ represented the presence of carboxylic acid groups of hemicellulose (C=O) in dry peel sorbent. After carbonization, this peak disappeared because of starting of hemicellulose decomposition at temperature near the 215 °C. Same result was reported by earlier studies of low temperature HTC process of biomass (Grénman et al., 2011; Reza et al., 2013; Reza et al., 2014a). On the other hand, new peak around 1700 $1/\text{cm}$ which indicate C=O stretching in ketone, aldehyde, quinone, ester, and carboxylic acid functional groups (Koch et al., 1998; Pradhan and Sandle 1998), was formed during carbonization process. 1608 $1/\text{cm}$ peak of aromatic carbon skeletons (C=C) of lignin in dry peel sorbent was preserved with a little increased intensity in hydrochar which could be due to an increase in aromatization (Roman et al., 2013). On the other hand, presence of this bond in hydrochars could refer that some lignin fragments and intermediate structures remained in the resulting hydrochars. As a new peak, 1515 $1/\text{cm}$ represented aromatic carbon skeletons. In literature, same band was seen in hydrochar obtained from corn stover and it was interpreted as C–H or N–H bending (Fuertes et al., 2010). In another study, this peak was interpreted as C=C bond and presence of it with 1620 $1/\text{cm}$ band after HTC was interpreted as indicator of aromatization of saccharide samples (Sevilla and Fuertes, 2009b). At near the 1430 and 1318 $1/\text{cm}$, there were peaks in dry peel but with negligible intensity.

Table 3.1 FTIR-ATR spectrum frequencies (1/cm) of sorbents before adsorption

Type of vibration	Compound type	Dried peel (1/cm)	Inactive hydrochar (1/cm)	Activated hydrochar (1/cm)
O-H stretching	Acid, methanol and water	3329	3333	3335
C-H stretching	Alkyl, aliphatic and aromatic	2889 -	2902 -	2913 2850
C=O stretching	Esters, ketones, amides, carboxylic acids	1728	1700	1700
C=C stretching	Aromatic carbon skelatons	1608 -	1609 1515	1604 -
C-H bending	Aromatic acids of hemicellulose	1426 (very small)	1432	1428
		-	1365	1365
		1318 (very small)	1315	1315
C-O-C stretching	Glycosidic bonds of cellulose	1240 -	1242 1158	1242 1157
	Esters (aromatic)	-	1104	1103
	Ethers (aromatic, olefinic or aliphatic)	-	1026	1026
	Aromatic bonds of hemicellulose	-	892	900

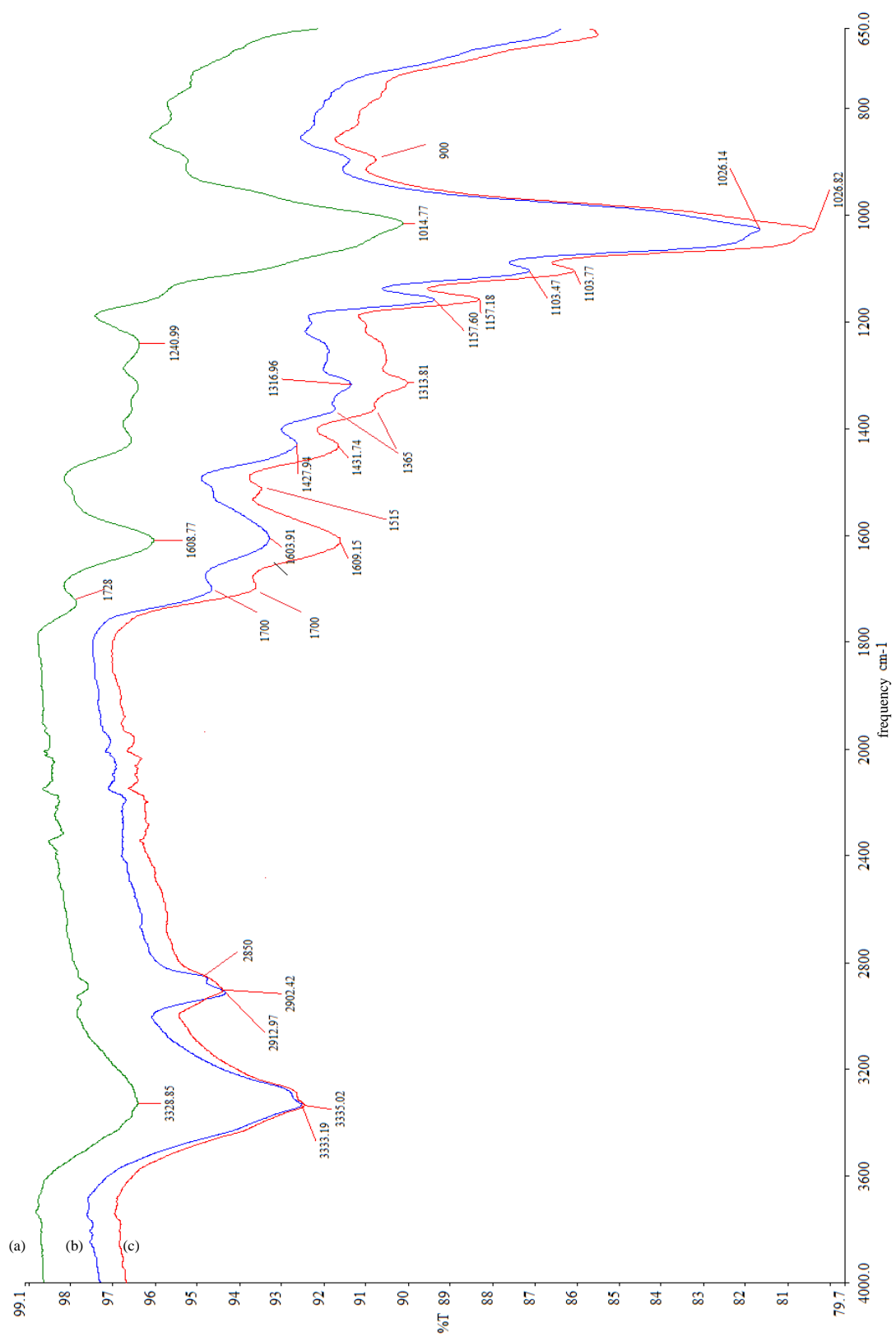


Figure 3.1 Comparison of (a) dried peel, (b) activated hydrochar, (c) inactive hydrochar

Aforementioned peaks were observed in hydrochars at 1432 and 1315 $1/\text{cm}$ with increased intensity. They were known as carboxylic acid peaks and indicated that hemicellulose had degraded. Reza et al. (2014a) found same peak at 1430 $1/\text{cm}$ in their study. They studied loblolly pine HTC and it was observed that hydrochar stayed as acidic during HTC process and this peak increased with the temperature increment, therefore; they interpreted this situation as an evidence of increased carboxylic acid production with increased HTC temperature. As another new peak after HTC, 1365 $1/\text{cm}$ was observed. This peak referred as aromatic acids of hemicelluloses (C-H) and this information confirmed again the breakdown of hemicelluloses in peel at temperature near the 215°C . Peaks, which presented at the range of 1242-1026 $1/\text{cm}$, were sign of C-O-C stretching. Each band could be interpreted differently. Peaks at 1240 $1/\text{cm}$ and near 1160 $1/\text{cm}$ referred the glycosidic bonds of cellulose. In literature it is mentioned that liquid water at 200°C breaks the glycosidic bonds of hemicellulose (Grénman et al., 2011) but in the case of cellulose it is harder than. So that it could be concluded that some of cellulose in dry peel was degraded but much of it in the hydrochar samples remained unreacted at temperature near the 215°C . Last peaks in this vibration type were 1104 and 1026 $1/\text{cm}$ and they referred the aromatic esters and ethers. They might have been result of aromatization of carboxylic acids and degradation of carbonhydrates. Occurrence of 900–892 $1/\text{cm}$ aromatic carbon hydrogen bonds of hemicellulose (C-H) could be thought as result of hemicellulose degradation.

Although some of bands in dry peel were also seen at hydrochar, most of aromatic carbon rich bonds were observed in only hydrochar or observed increased intensity in hydrochar. This was probably due to degradation of hemicellulose and partially degradation of lignin and cellulose at experiment temperature in the present study.

With regard to activation process, there were also some differences in terms of peak occurrence, losing and intensity. Peak at 2850 $1/\text{cm}$ (C-H) was a new peak after the activation process. This process might affect the occurrence of some aliphatics and aromatics. In literature, hydrochar obtained from grape pomace have double peaks at 2920 and 2850 $1/\text{cm}$ and these peaks were interpreted as C-H stretching vibration and deforming vibration, respectively. Therefore, the presence of aliphatic and hydroaromatic structures was deduced (Pala et al., 2014). Beside, peak at 1515 $1/\text{cm}$

disappeared with the effect of KOH. C=C bond might have broken by activation and turned into different type of bond such as C=O.

After adsorption event, new peaks; shifting of present peaks and/or losing of some of peaks were observed in activated hydrochar (Figure 3.2). Peak of C-H stretching at 2913 1/cm shifted to 2906 1/cm with decreased intensity. This decrement caused the thinking of resulting of Cu^{+2} ion sorption, because; Cu^{+2} ion cannot be identified by FTIR-ATR analysis. So that, losing of some peaks or decreasing of transmittance could be thought as presence interaction between of Cu^{+2} ions and functional groups at that band. As same, peak of C-H stretching at 2850 1/cm could not be seen after the adsorption. At that point, it could be thought that; some of aromatics in hydrochar might have played a role in sorption process. Carboxylic acid peak (C=O) at 1700 1/cm disappeared because of same probable reason. Aromatic carbon skeletons (C=C) at 1604 1/cm lost its intensity after adsorption. C-H bending at 1428 1/cm, which occurred because of hemicellulose degradation, performed in sorption of Cu^{+2} ion and disappeared, same as peaks at 1365 and 1317 1/cm. New peak at 1343 1/cm might have related with these disappeared peaks as a resulted of Cu^{+2} ion sorption. As it can be seen from Table 3.2, there was no considerable differences at C-O-C stretching band region so it could be concluded that sides at this region might not have played effective role in Cu^{+2} ion adsorption but it should be added, peaks at 1103 and 1026 1/cm were observed with decreased intensity after sorption. They could be taken part in sorption process. 825 1/cm band (C-H) was observed after Cu^{+2} ion adsorption which could be thought as this band might have taken part in adsorption.

FTIR-ATR analyses confirmed that some of surface groups, which include C-H, C=O and C-O-C bonds, could play significant role on adsorption of Cu^{+2} ions by the activated hydrochar.

Table 3.2 FTIR-ATR spectrum frequencies (1/cm) of activated hydrochar before and after adsorption

Type of vibration	Compound type	Before Sorption (1/cm)	After Sorption (1/cm)
O-H stretching	Acid, methanol and water	3335	3334
C-H stretching	Alkyl, aliphatic and aromatic	2913 2850	2906 -
C=O stretching	Esters, ketones, amides, carboxylic acids	1700	-
C=C stretching	Aromatic carbon skelatons	1604	1603
C-H bending	Aromatic acids of hemicellulose	1428 1365 1317	- - 1343
C-O-C stretching	Pyranose ring of lignin Aromatic esters Ethers (aromatic, olefinic or aliphatic)	1157 1103 1026	1157 1104 1027
C-H bending	Aromatic bonds of hemicellulose	900 -	900 825

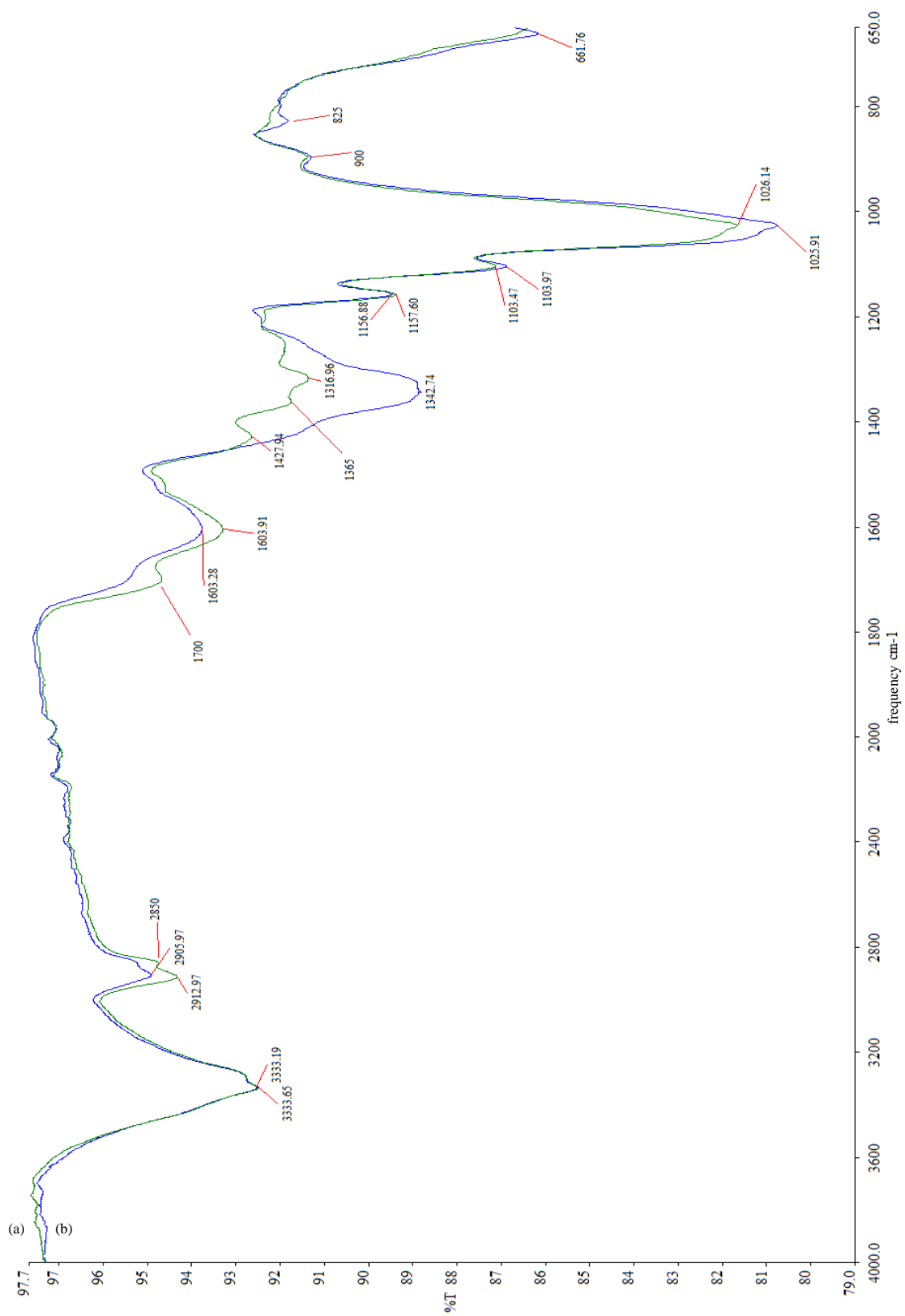
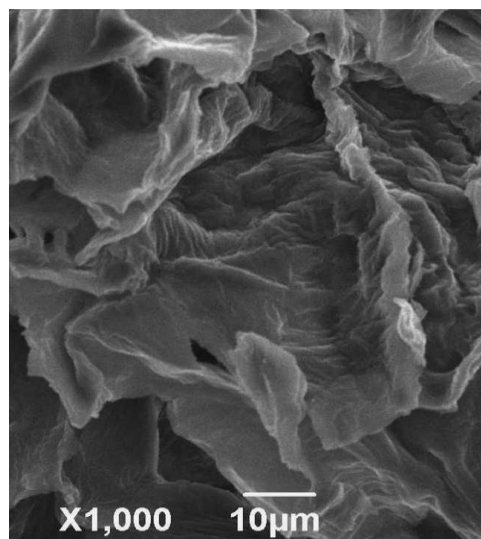


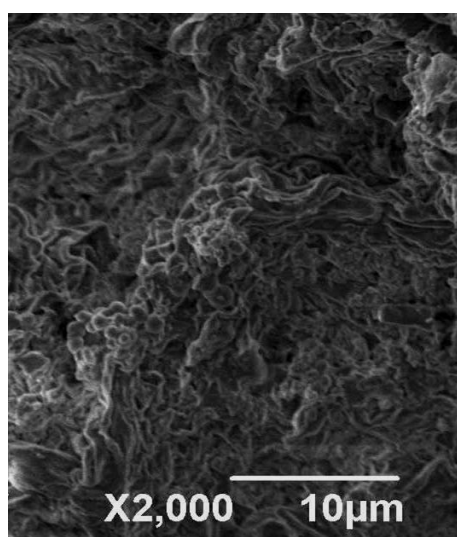
Figure 3.2 Cu⁺² ion sorption by activated hydrochar: (a) before sorption, (b) after sorption

3.1.2. SEM analysis

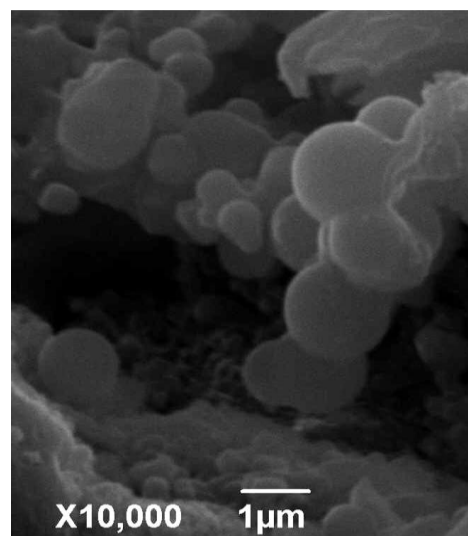
Surface structures of dried peel, activated hydrochar at x2000 and activated hydrochar at 10000 by use of SEM are given on Fig. 3a, b₁, and b₂, respectively. Differences between surface topologies of materials were obviously observed on the SEM graphs. The surface of dried peel was smooth and unbroken as plate (Figure 3a). On the contrary, surface of activated hydrochar had spaces and opened slits. Spherical shape surface causes higher surface area. These slits and increased total surface area could be effective on Cu⁺² ion sorption capacity.



(a)



(b₁)



(b₂)

Figure 3.3 (a) SEM image of dried grapefruit peel, (b₁) activated hydrochar at x2000, (b₂) activated hydrochar at x 10000

In literature, similar images were obtained from hydrochars which evolved from raw cellulose, glucose (Sevilla et al., 2009a; Sevilla et al., 2009b), and cassava flour (Gustan, 2014). By means of microwave application instead of conventional method, final porous carbonaceous material was obtained in shorter time (20 min) and at lower temperature (215 °C).

3.1.3. Activation of hydrochar with KOH

In order to enhance sorption capacity with porosity increment and cleaning up filled or blocked pores of hydrochar, cold activation process with KOH was implemented. To understand effect of that step on the adsorption capacity, batch adsorption process was carried out with two adsorbents inactive and activated hydrochars (1g/L) were treated with 100 ml solution of 20 mg/L Cu^{+2} in 250 ml flask at pH 6.4 and 298 K. As a result, it was observed that adsorption capacity of activated hydrochar was almost two times more than inactive hydrochar. Therefore, activated hydrochar was selected for further experiments.

3.2. Batch Adsorption Studies

In order to distinguish the metal removal phenomena because of adsorption, precipitation test was done at different pH values in the absence of any adsorbent. Cu^{+2} ion precipitation for the adsorbent free solutions was plotted against pH values (Figure 3.4). Results clearly showed that precipitation of Cu^{+2} ion was starting at pH 6.6. In literature, same value was observed for Cu^{+2} ion (Regmi et al., 2012). To observe exact adsorption performance of sorbent, pH value of whole experiment solutions was maintained as 6.35 ± 0.5 .

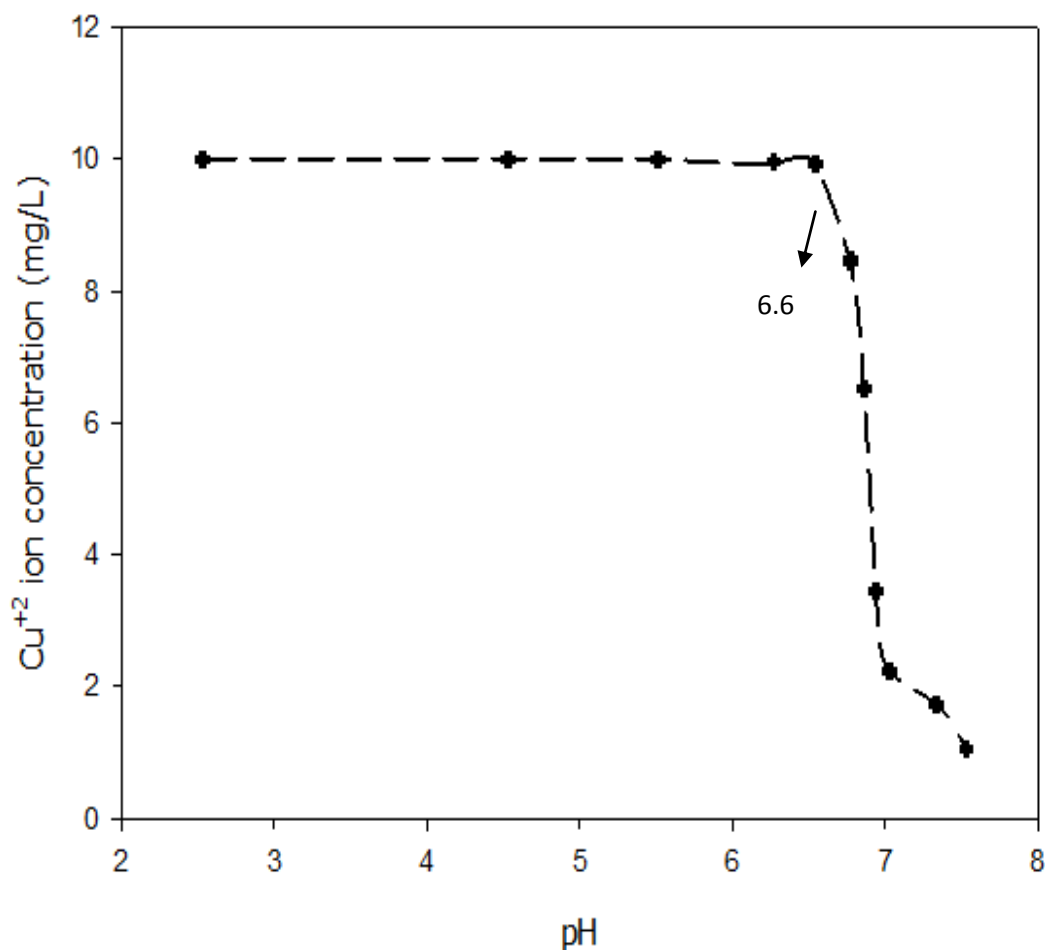


Figure 3.4 Cu²⁺ ion precipitation at different pH regime

3.2.1. Effect of initial solution pH and pH_{zpc}

The pH_{zpc} of activated hydrochar was found as pH 6.8, where electrostatic repulsion between adsorbent molecules is at minimum. When pH of the solution is lower than that of pH_{zpc} value, the adsorbent gets positively charged and at higher pH values than that point, adsorbent gets negatively charged. This behavior affects the environment pH effect on adsorption and correspondingly, adsorption capacity.

In the case of adsorption phenomena, solution pH (process environment) is one of the most important factor affecting the sorption process. Effect of initial pH regime values on the adsorption of Cu²⁺ on the activated hydrochar is given on Fig. 3.5. It was observed that sorption capacity of activated hydrochar was getting better with increased pH value of solution. This behavior is related with the changing of surface properties of adsorbent as increasing pH. It could be said that increment in pH of solution caused the movement of H⁺ ion to the solution instead of sorbent surface, through; more Cu²⁺ ions could be caught by the sorbent. In other words, at low pH,

adsorption capacity was also low because of the linkage of H^+ ions with oxygen containing functional groups on hydrochar that hindered access for the metal ions. From the Figure 3.5, it can be seen that amount of adsorbed metal at pH 4 was lower than at pH 6 because the surface of the adsorbent get more positively charged at the lower pH. Therefore, adsorption capacity of hydrochar reduced with decreasing the pH of the solution. In this case, maximum pH value was chosen as 6 because of precipitation of Cu^{+2} ion about pH 6.6.

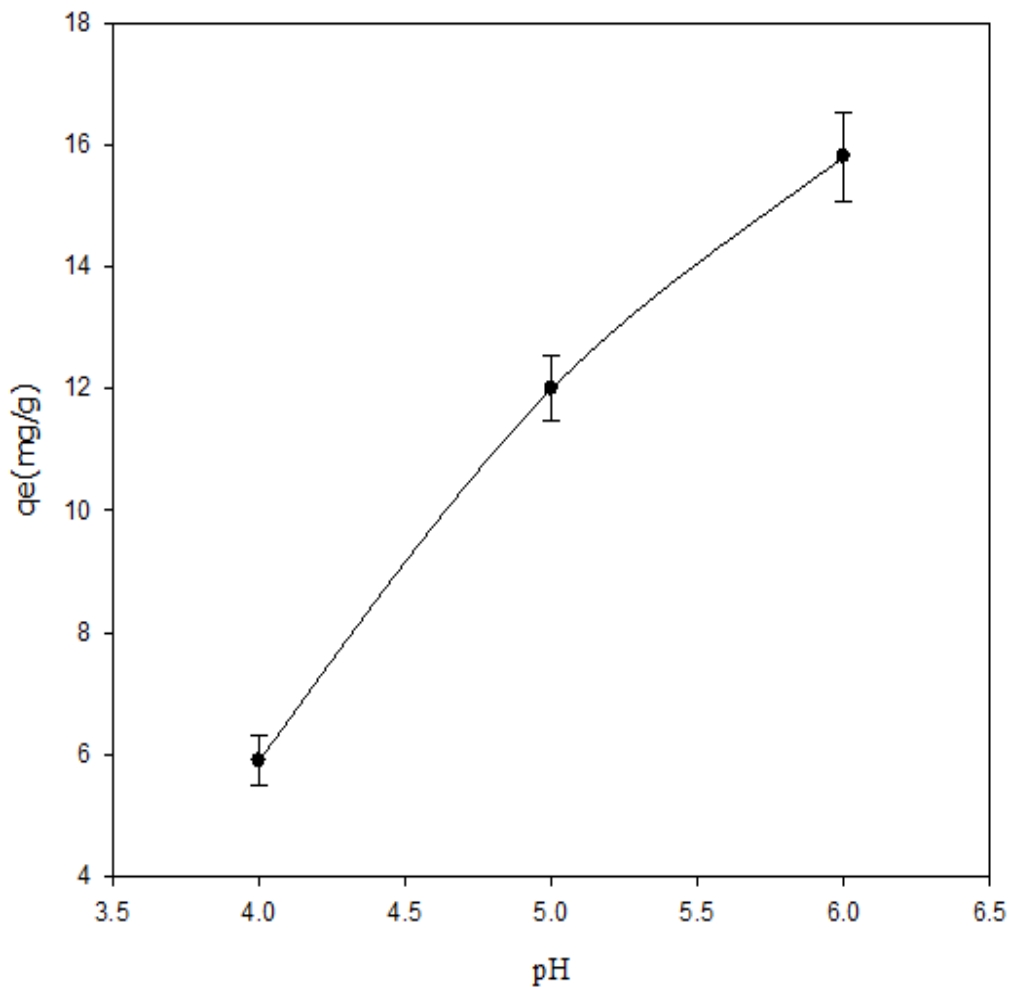


Figure 3.5 Initial pH effect on Cu^{+2} ion sorption ($C_0 = 20$ mg/L, 1g/L adsorbent dose)

3.2.2. Effect of adsorbent dose

In order to investigate adsorbent dose effect on the adsorption capacity, experiments were carried out at various activated sorbent doses (0.5, 1.0, 2.0, and 4.0 mg/L) and initial concentration of Cu^{+2} was fixed as 20 mg/L at the temperature of 298 K and pH 6.3. After 210 min, samples were taken from adsorbate solutions, diluted and

examined by AAS. According to the results from there, q_e values were calculated by Eq. 2.1 and plotted (Figure 3.6).

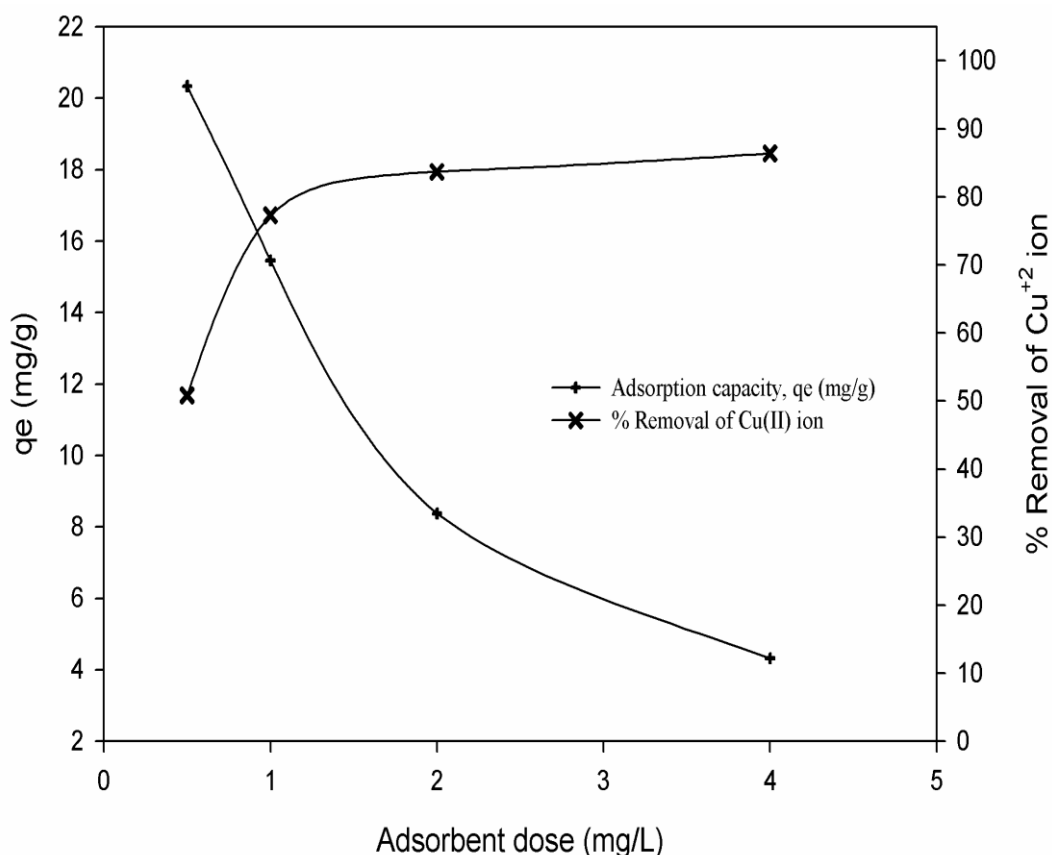


Figure 3.6 Adsorbent dose effect on equilibrium sorption capacity and % Cu (II) removal ($C_0 = 20$ mg/L)

At same initial Cu^{+2} concentration, increment in adsorbent dose caused the decrement in adsorption capacity at equilibrium. This could be due to aggregation of adsorbent at high adsorbent dose, which prevent interaction between adsorbent and metal ions. Additionally, this result can be interpreted with sorption capacity of sorbent, q_e . It refers the milligram sorbate on gram sorbent. In the light of that description, it could be concluded that; at same initial Cu^{+2} concentration, the numerator (adsorbed Cu^{+2}) was almost same because 0.5 g/L dose as minimum dose would be enough for adsorption of 20 mg/L Cu^{+2} solution, but; denominator (sorbent concentration) was increased so that, total value decreased. Because of this result, all experiments were done with 0.5 g/L adsorbent dose. Similar behavior was found by Rao et al. (2010) in the study of Cd^{+2} removing with teak leaves powder.

3.2.3. Effect of temperature and initial Cu^{+2} ion concentration

In order to investigate effects of temperature and initial Cu^{+2} concentration on the sorption process, experiments were carried out at 100 ml, different initial Cu^{+2} concentration (5, 10, 20, 40, and 60 mg/L) and temperature (298, 308, and 318 K) for 210 min with 0.5 g/L activated hydrochar dose and at 6.3 pH. Samples were taken from adsorption solutions in exact volume with certain time interval in order to find contact time effect determination and kinetic studies later. Results of initial Cu^{+2} concentration and temperature effect on the adsorption capacity are given on Figure 3.7, and Figure 3.8 respectively.

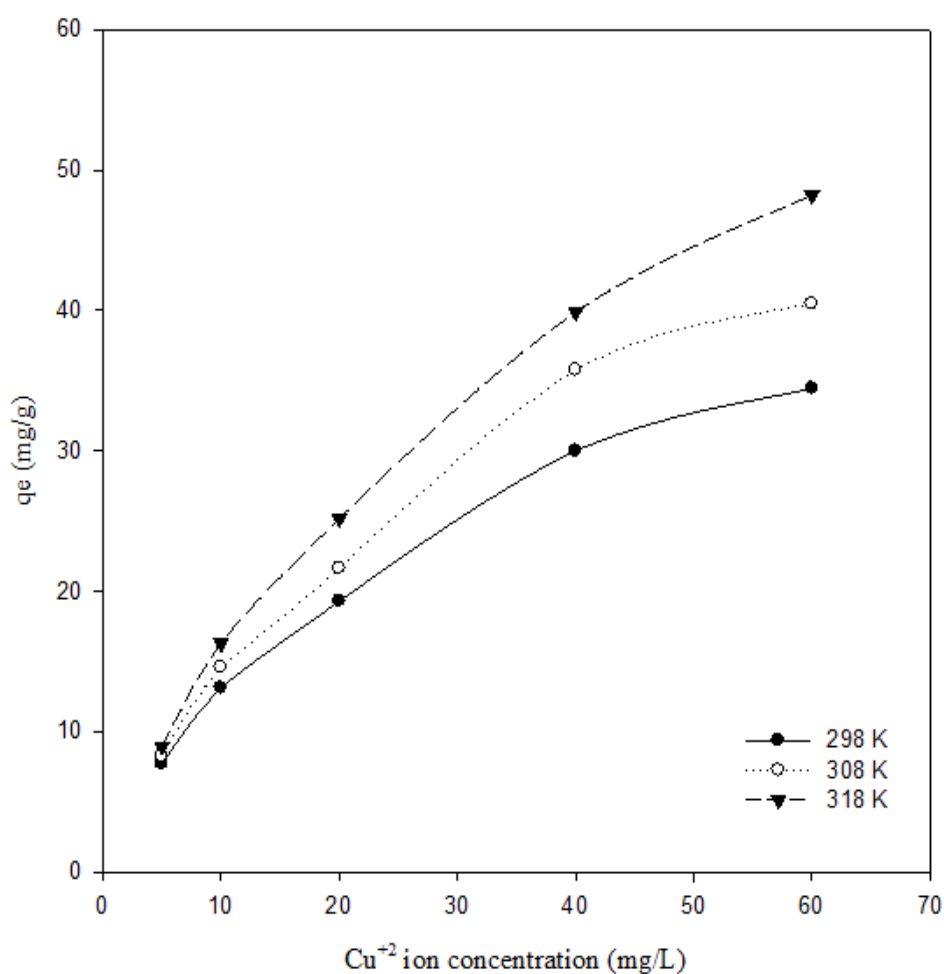


Figure 3.7 Effect of initial Cu^{+2} ion concentration at three different temperatures

As it is seen from Figure 3.7, there was a directly proportional relationship between the initial Cu^{+2} concentrations (mg/L) and equilibrium sorption value after 210 min. This behavior would be result of increased driving force for mass transfer with

increased Cu^{+2} ion concentration. Additionally, high metal concentration may have caused increasing interaction probability of Cu^{+2} with adsorbent surface. The highest adsorption capacity, q_e , was observed at 318 K for 60 mg/L Cu^{+2} concentration.

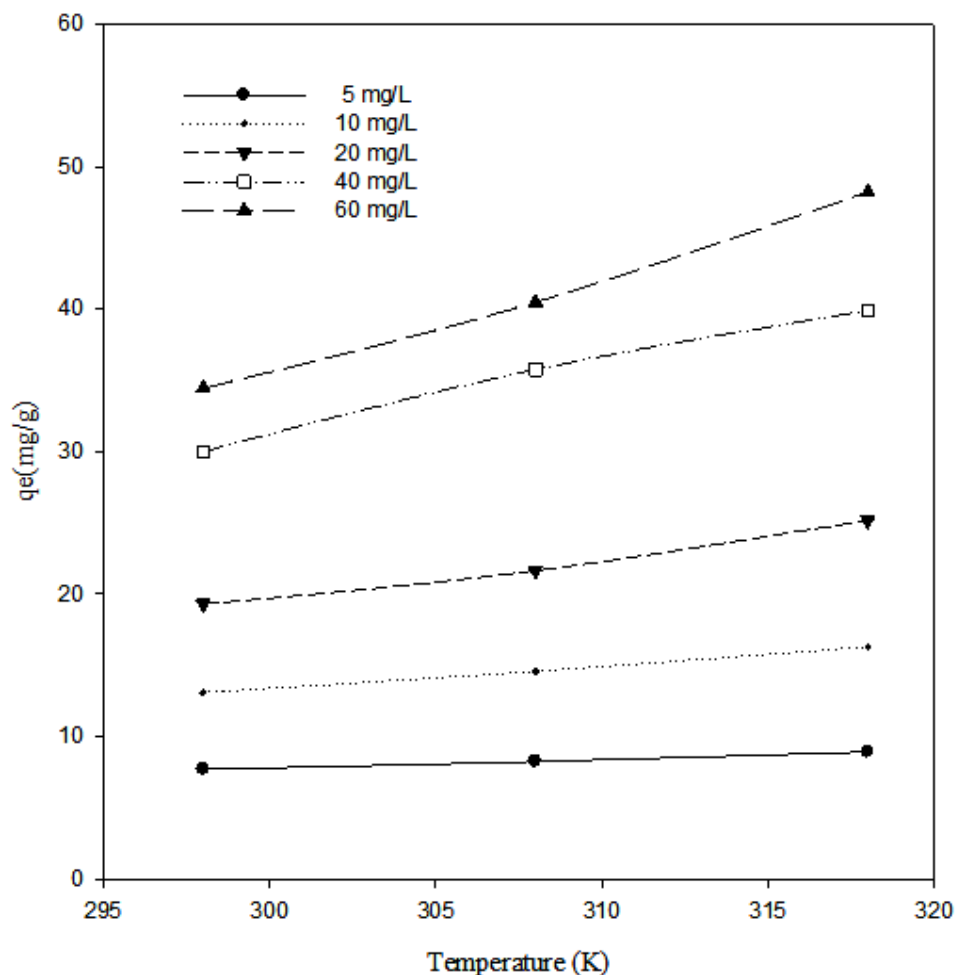


Figure 3.8 Effect of temperature for five different concentrations

Effect of temperature on the adsorption capacity is given on Fig.3.8. There was no significant effect ($p>0.05$) of temperature on adsorption capacity at lower concentration. At higher initial Cu^{+2} concentrations, temperature effect was more recognizable. Also, from graph, it would be predicted that there were still capacity to adsorb more Cu^{+2} ions at these conditions, therefore; higher than 60 mg/L Cu^{+2} ion concentration could be experimented for that adsorbent dose to understand the limitation about that. In study of Cu^{+2} ion adsorption by biomass, similar temperature effect was seen for 100 mg/L initial Cu^{+2} concentration (Bayram, 2014).

3.3. Adsorption Kinetics

Before the mathematical expressions, q_{exp} data are subjected to statistical analyses with ANOVA. One way ANOVA analyses were carried out to determine the significance level as function of contact time and initial Cu^{+2} concentration for each temperature values. Three way ANOVA analysis was done as function of temperature, time and initial concentration at same time. According to the results, for each initial Cu^{+2} concentration, there were significant differences between q_{exp} values at 298 K, 308 K and 318 K. Also, q_{exp} values at 2.5, 5, 10, 15, 30, 45, 60, 90, 120, 150, 180 and 210 min at 298, 308 and 318 K for each initial Cu^{+2} concentration gave significant relationship between each other. Moreover, in three way ANOVA analysis, there was a significant relationship with regard to temperature-time-concentration parameters (Table A.13, A.19).

Adsorption kinetic experiments of activated hydrochar (0.5 g/L) were carried out at five different Cu^{+2} concentrations with pH at 6.3 and three different temperatures (298, 308, and 318 K). Nonlinear Pseudo second-order kinetic model (Eq. 1.1), Logistic model (Eq. 1.3) and Elovich model (Eq. 1.2) were applied to experimental data. Their correlation coefficients, R^2 , and sum of square values, SSE (Eq. 2.3.) are given at Table 3.3.

Table 3.3 R² and SSE values and parameters of three kinetic models

Temp. (K)	C ₀ (mg/L)	Pseudo-second order			Logistic				Elovich		
		R ²	SSE	k ₂ *	R ²	SSE	A**	μ***	R ²	SSE	β****
298	5	0.961	0.384	0.074	0.987	0.223	7.700	5.044	0.999	0.042	1.498
	10	0.980	0.479	0.040	0.993	0.282	13.000	7.662	0.997	0.154	0.868
	20	0.980	0.717	0.025	0.999	0.087	22.438	10.866	0.997	0.262	0.567
	40	0.977	1.153	0.021	0.999	0.160	36.427	19.401	0.998	0.310	0.411
	60	0.974	1.452	0.012	0.999	0.185	42.488	18.409	0.998	0.367	0.292
308	5	0.960	0.417	0.066	0.986	0.245	8.250	5.334	0.999	0.044	1.367
	10	0.978	0.549	0.040	0.993	0.299	14.600	9.069	0.998	0.140	0.817
	20	0.978	0.824	0.0240	0.999	0.084	25.701	12.640	0.998	0.244	0.518
	40	0.946	1.423	0.019	0.999	0.195	46.363	24.715	0.999	0.283	0.364
	60	0.977	1.587	0.011	0.999	0.227	47.989	22.448	0.997	0.538	0.262
318	5	0.958	0.467	0.060	0.985	0.278	8.930	5.760	0.999	0.060	1.253
	10	0.976	0.647	0.031	0.992	0.376	16.300	9.550	0.998	0.177	0.681
	20	0.977	0.966	0.023	0.999	0.105	30.598	15.848	0.998	0.244	0.475
	40	0.974	1.643	0.018	0.999	0.221	54.631	28.167	0.999	0.276	0.330
	60	0.977	1.900	0.011	0.999	0.255	58.624	29.716	0.998	0.524	0.240

* : Pseudo second-order rate constant (g/mg.min)

** : Maximum sorption values from Logistic model (mg/g)

*** : Adsorption rate constant from logistic kinetic model (1/min)

**** : Desorption constant (g/mmol) for Elovich Model

3.3.1. Nonlinear Pseudo second-order kinetic model

This model is very common in interpretation of adsorption kinetic. It predicts the behavior over the whole range of adsorption. Adsorbed adsorbate amount at any given time, q_t , can be found by using of Pseudo second-order rate constant, k_2 , and adsorbed adsorbate amount at equilibrium, q_e (Eq.1.1.).

To understand effect of contact time on adsorption process, q_t vs. time relationship at three different temperatures and five different initial Cu⁺² concentrations were plotted. These results were compared with Pseudo second order kinetic model calculated q_t values (Figures 3.9, 3.11). R² and SSE values (Eq. 2.2.) of fitting of this model to experimental data and rate constant values, k , are given at Table 3.3.

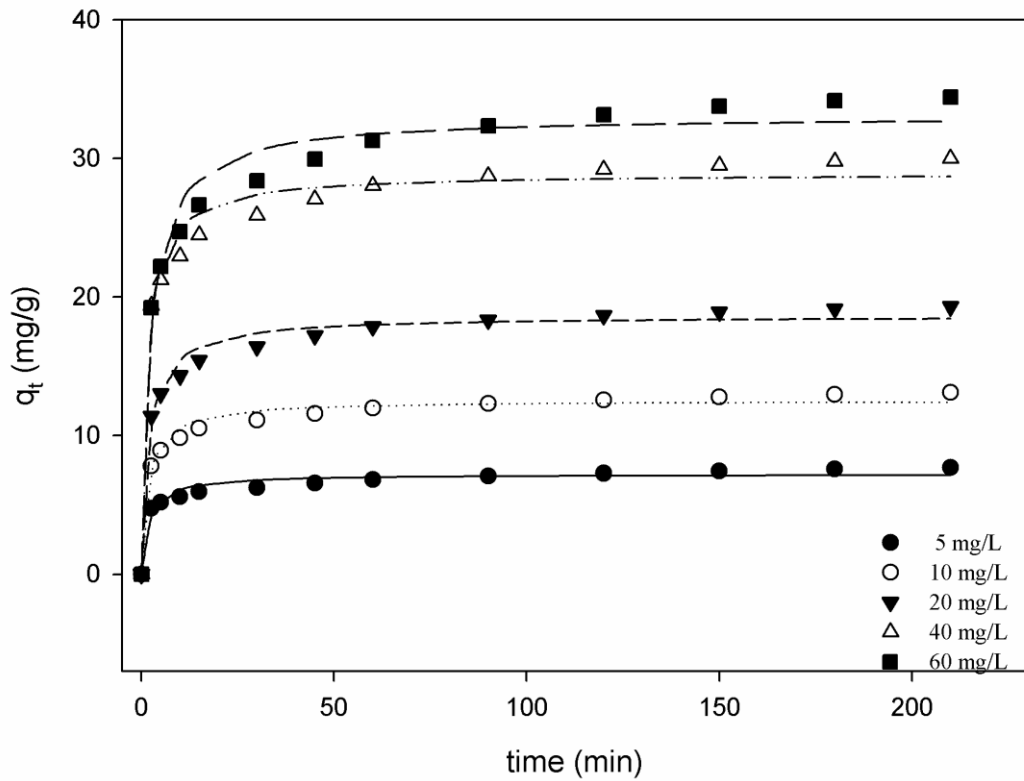


Figure 3.9 Nonlinear Pseudo second order kinetic model for Cu^{+2} ion sorption onto activated hydrochar at 298 K: symbols indicate experimental and lines indicate predicted values

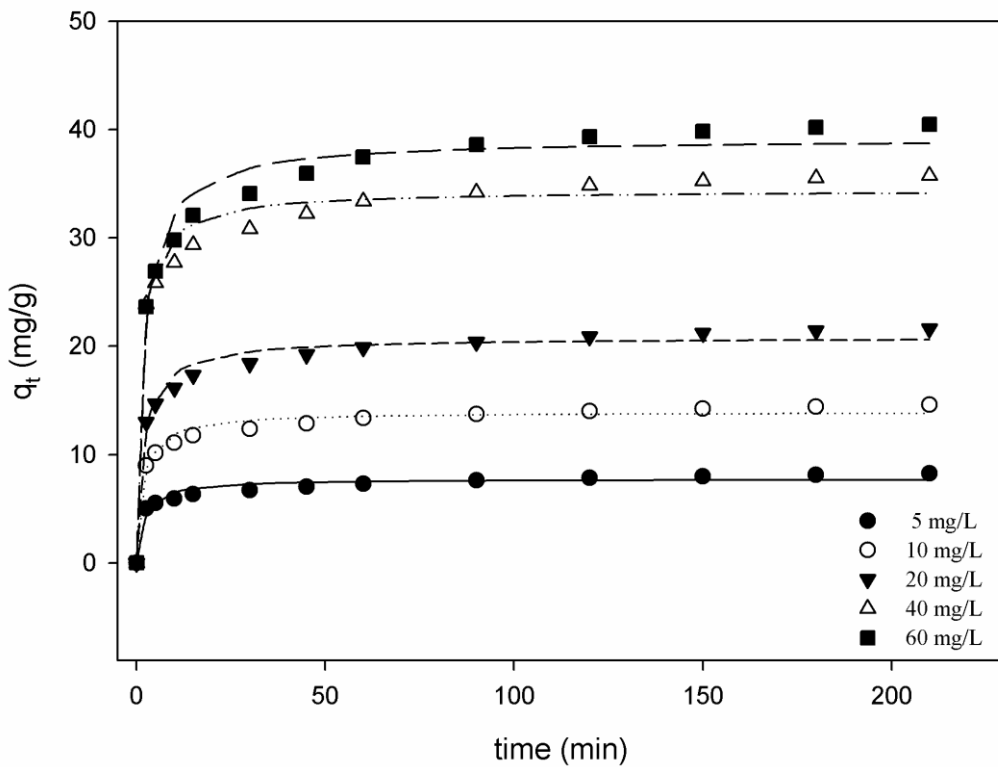


Figure 3.10 Nonlinear Pseudo second order kinetic model for Cu^{+2} ion sorption onto activated hydrochar at 308 K: symbols indicate experimental and lines indicate predicted values

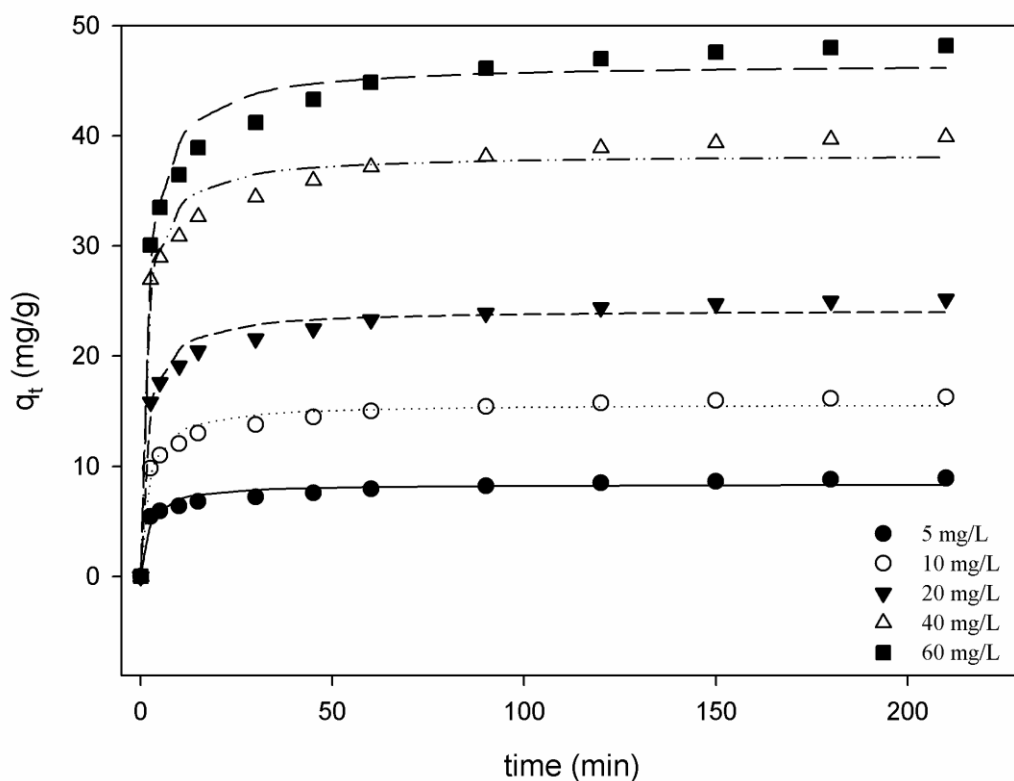


Figure 3.11 Nonlinear Pseudo second order kinetic model for Cu^{+2} ion sorption onto activated hydrochar at 318 K: symbols indicate experimental and lines indicate predicted values

Graphs of that model at three different temperatures showed that, there was a fast sorption process in the first twenty min ($p < 0.05$). As time progresses, the number of active sites of activated hydrochar decreased and the non-adsorbed Cu^{+2} ions in solution were assembled on the surface, thus limiting adsorption capacity. In the study of Cu^{+2} removal by activated carbon from olive stone, equilibrium was reached after 200 min process time same as in present study and they found R^2 as 0.999 which were 0.96-0.98 in the present study. This might have been related to raw material (olive stone) and carbonization procedure (Bohli, et al., 2015). On the other hand, according to the ANOVA results of whole adsorption rate values, k , there were nonsignificant relationship with temperature increment.

In addition, results of Pseudo second order kinetic model implementation to experimental data showed that, while increasing initial Cu^{+2} concentrations, rate constant, k , of whole system was decreased ($p < 0.05$). This situation suggested that the adsorption equilibrium capacity was established slower at higher Cu^{+2} concentrations due to the limited quantity of binding sites of sorbent surface. In literature, it was interpreted as; this situation related with the available surface sites

for the adsorption during initial stages and enhanced difficulty to occupy them after a lapse of time so; total rate is going to be decreased (Bansal and Goyal, 2001).

3.3.2. Logistic kinetic model

Recently, using of this method in the adsorption systems is a new description way, because, this method has been commonly used for microbial systems. This model is a sigmoidal model (S-shape) and general nonlinear adsorption kinetic curves have similar behavior (upper part of S- shape). Therefore, it has been tried to be used by several researches to describe the adsorption process (Çelekli et al., 2009; Çelekli et al. 2012). In literature, general behavior of Cu^{+2} ion adsorption process has been described with an initial exponential increase and final stabilization at maximum level. In the light of this information, logistic model implementation was found to be suitable in the present study.

To investigate better relationship between q_{exp} and q_{pred} as a function of contact time and initial Cu^{+2} concentration Logistic model was implemented to Cu^{+2} adsorption process by activated hydrochar. Graphics of that relationship were given at Figures 3.12, 3.14. Additionally, maximum sorption values at equilibrium, A (mg/g), sorption rate constant, μ (1/min) values, which were observed from that model and R^2 and SSE values (Eq. 2.3.) of fitting of this model are given at Table 3.3.

According to R^2 and SSE values of fitting of experimental sorption capacity data to calculated sorption capacity data; Logistic model explained that sorption mechanism better than of Pseudo second order model. Analogous with Pseudo-second order kinetic, it could be seen from graphics; 200 min was enough to observe the equilibrium. In literature, Çelekli et al. (2009) used Logistic kinetic model for Cu^{+2} ion sorption on biosorbent and they obtained the best fitting with that model.

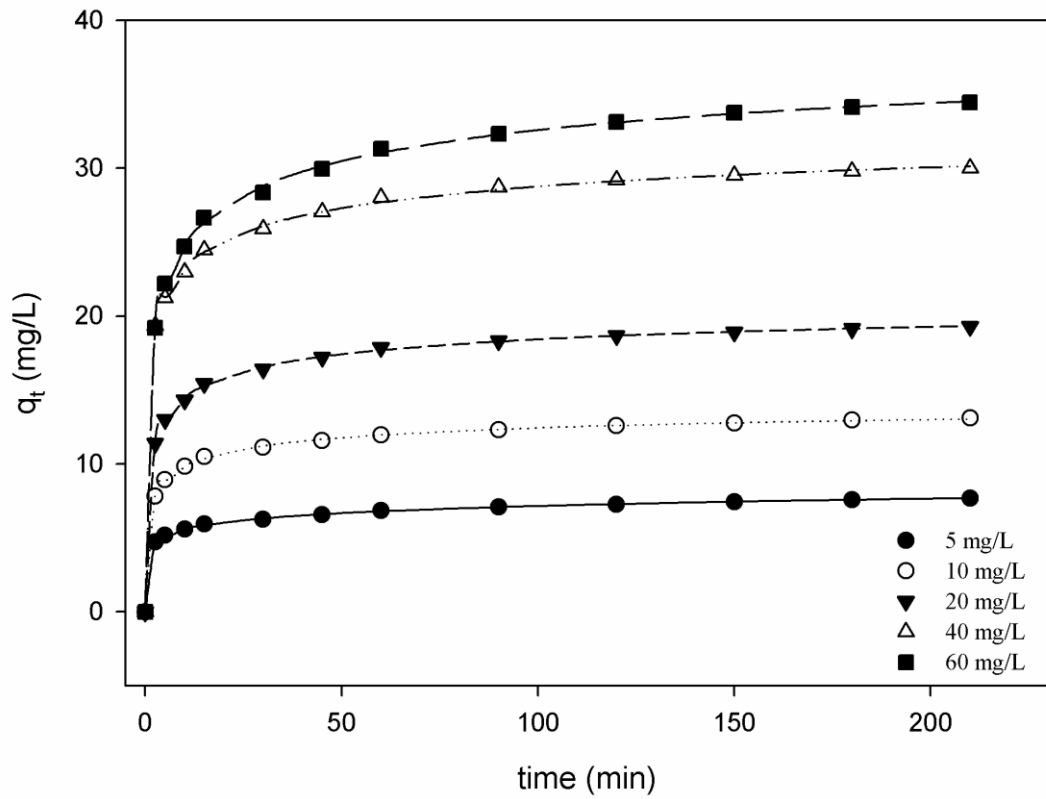


Figure 3.12 Logistic kinetic model for Cu^{+2} ion sorption onto activated hydrochar at 298 K: symbols indicate experimental and lines indicate predicted values

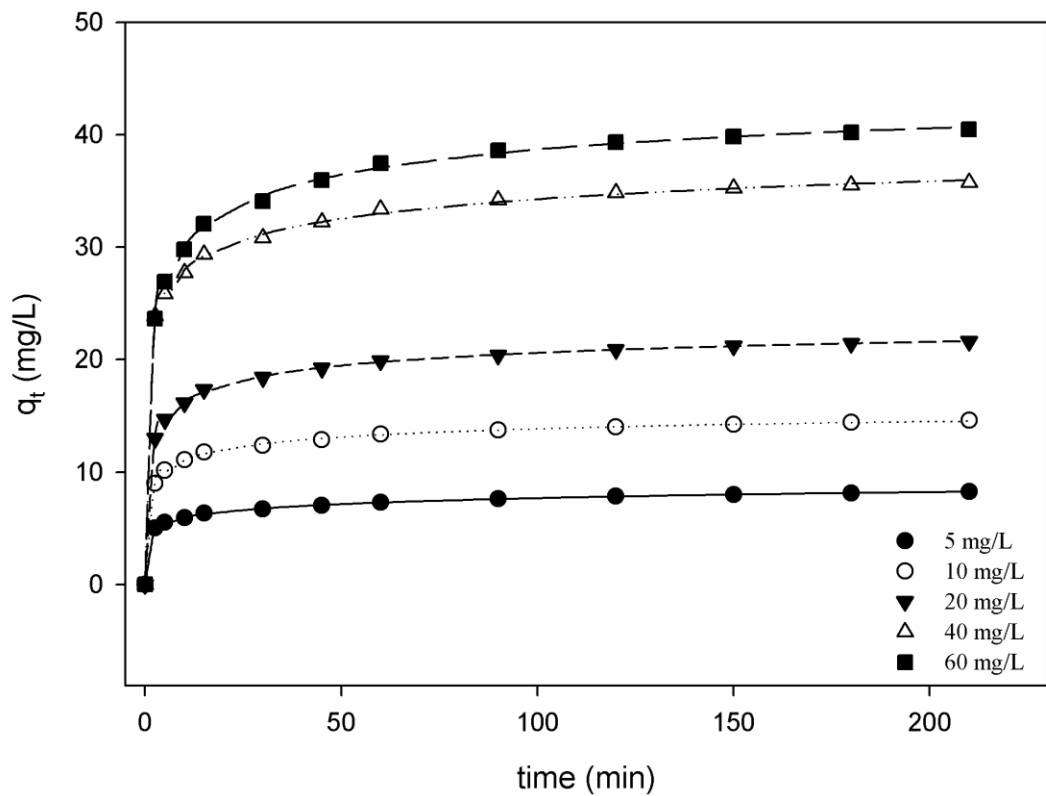


Figure 3.13 Logistic kinetic model for Cu^{+2} ion sorption onto activated hydrochar at 308 K: symbols indicate experimental and lines indicate predicted values

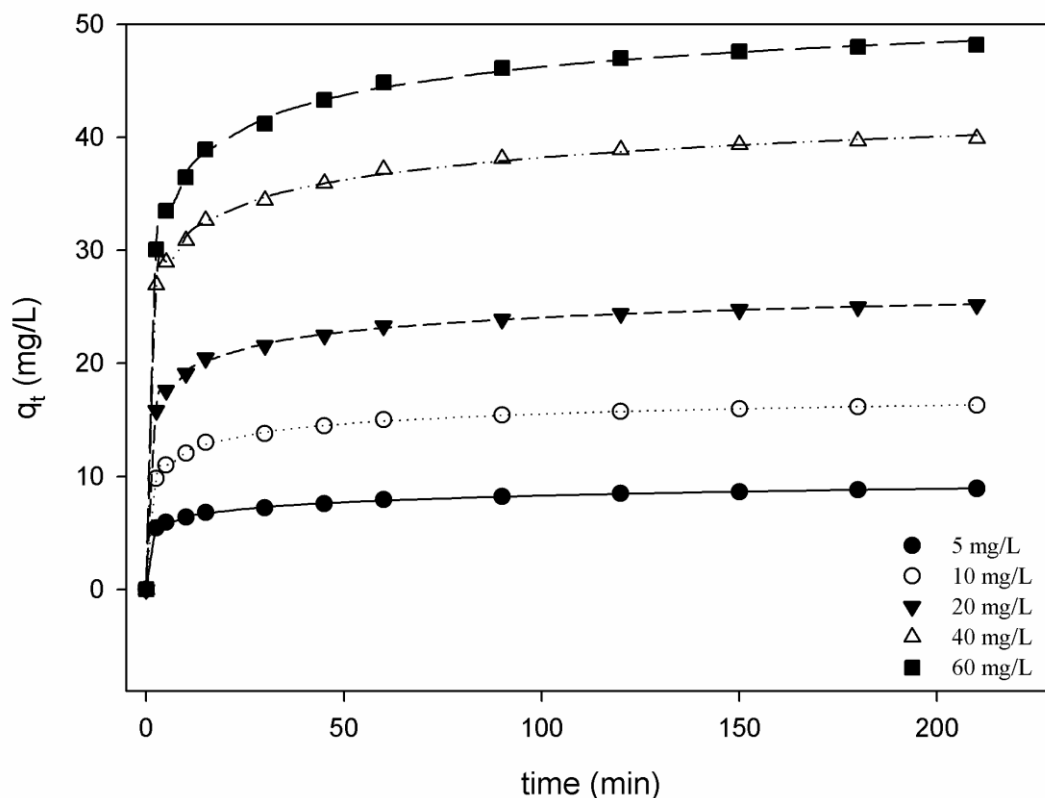


Figure 3.14 Logistic kinetic model for Cu^{+2} ion sorption onto activated hydrochar at 318 K: symbols indicate experimental and lines indicate predicted values

When looking to calculated maximum sorption values at equilibrium, A , (mg/g), they were directly proportional to initial Cu^{+2} concentrations ($p < 0.05$). Increment in the initial concentration caused the increment in maximum sorption at equilibrium. The reason of that might be having more than enough sorption side on hydrochar, therefore; these sides could meet Cu^{+2} concentration exceedingly. On the other hand, at 5, 10, and 20 mg/L initial Cu^{+2} concentrations there was a similar kinetic behavior for 40 and 60 mg/L initial Cu^{+2} concentrations again; there was a similar behavior. Between 20 and 40 mg/L curves, there was a huge difference. Probable reason of that would be effective increment in driving force because of increment in Cu^{+2} concentration. Temperature increment caused increment in calculated maximum sorption values at equilibrium, A , ($p < 0.05$). This result might have related with increment in diffusivity with temperature increment.

Sorption rate constant value, μ , from that model referred the rate of sorption until stabilized part, because this value was obtained from slope of graph. So, at that sloping area; rate was increased with increased temperature. This might be related

with temperature dependency of diffusion in solids. As a general knowledge, temperature increment causes the increment in diffusion.

3.3.3. Elovich kinetic model

Elovich model has been commonly applied to adsorption study because of serving the purpose of describing exponential increment in sorption (Juang and Chen, 1997; Ho et al., 2002; Han et al., 2006; Idris et al., 2011). Fitting of predicted adsorption equilibrium values, $q_{e,pred}$, by nonlinear Elovich Eq. and experimental adsorption equilibrium values, $q_{e,exp}$, was examined with three different graph for each temperature (Figure 3.15, 3.17). R^2 and SSE values of fitting of this model are given at Table 3.3. Initial adsorbate sorption rate (mmol/(g*min), α , and desorption constant (g/mmol), β , values from slope and intercept of given graphic were calculated, but; only desorption constant, β , is given at Table 3.3. Because, there was nonsignificant relationship neither with temperature - α value nor initial Cu^{+2} concentration - α value ($p > 0.05$).

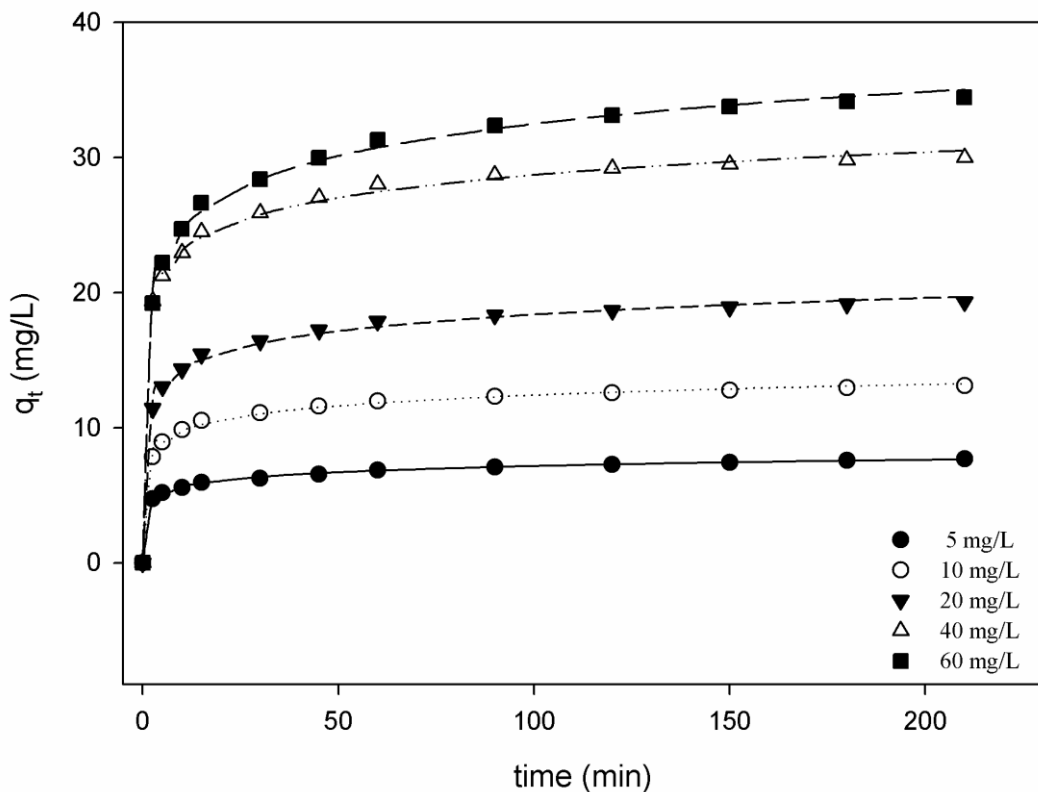


Figure 3.15 Elovich kinetic model for Cu^{+2} ion sorption onto activated hydrochar at 298 K: symbols indicate experimental and lines indicate predicted values

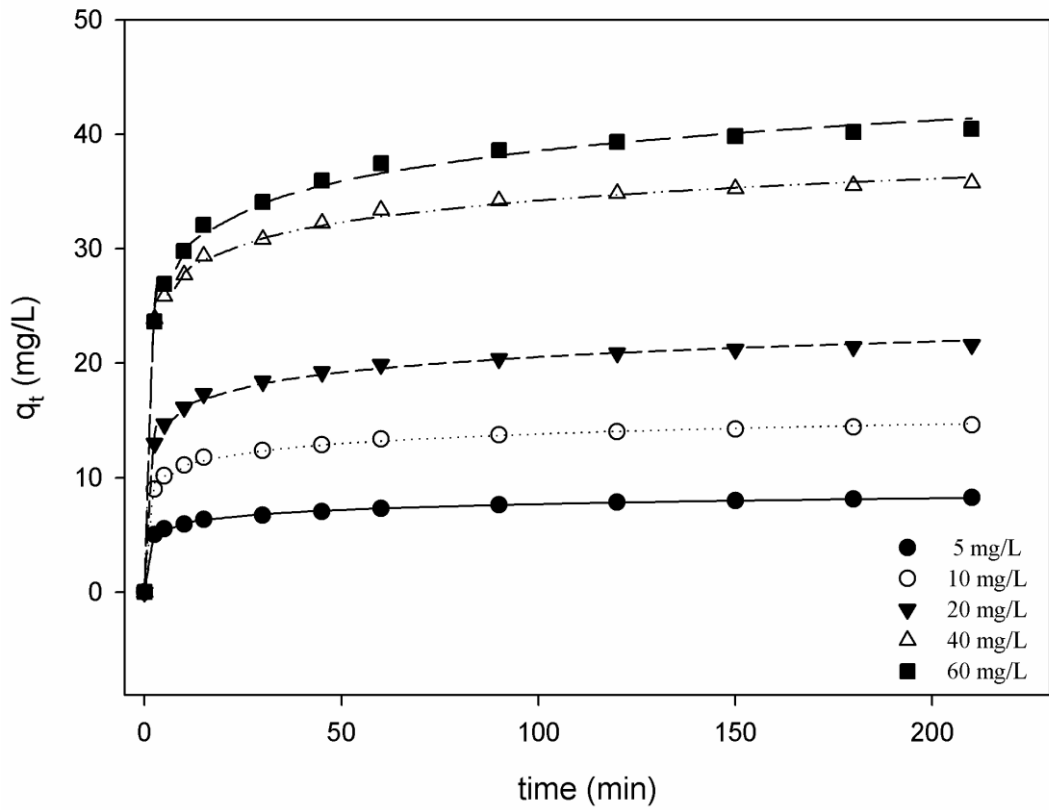


Figure 3.16 Elovich kinetic model for Cu^{+2} ion sorption onto activated hydrochar at 308 K: symbols indicate experimental and lines indicate predicted values

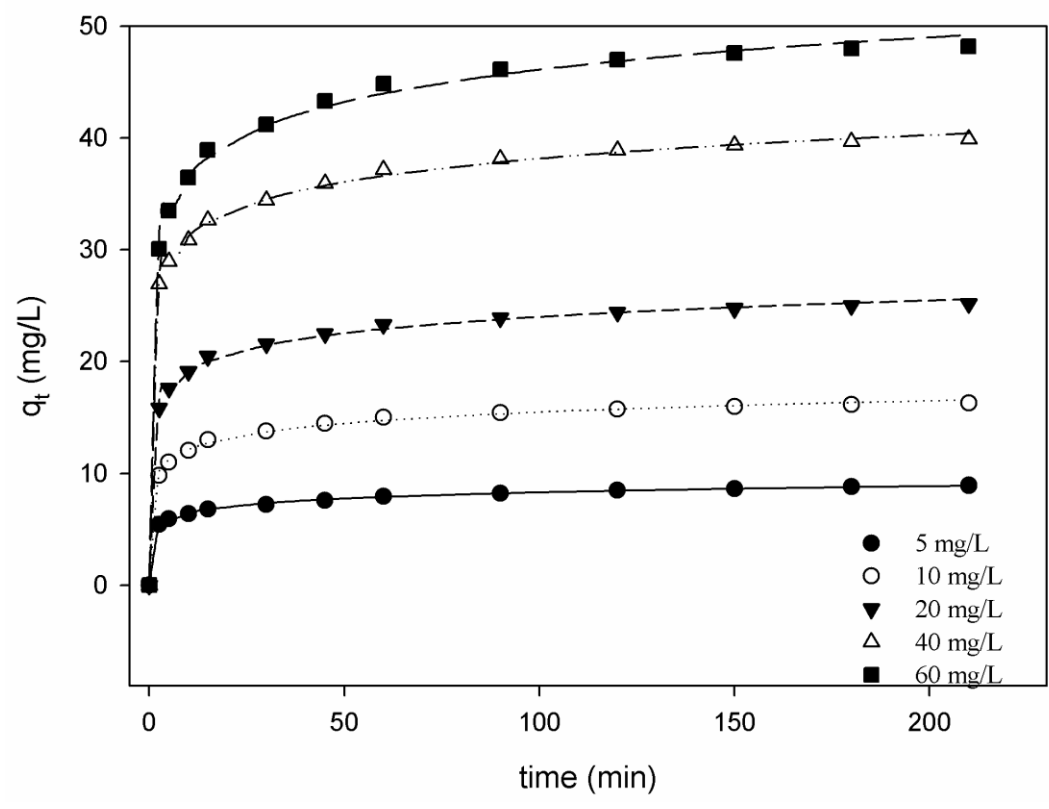


Figure 3.17 Elovich kinetic model for Cu^{+2} ion sorption onto activated hydrochar at 318 K: symbols indicate experimental and lines indicate predicted values

According to the graphics, same behavior for each temperature and each concentration was obtained with other kinetic models but with higher R^2 than Pseudo second order and lower than logistic, averagely (0.997-0.999). In the light of R^2 and SSE values of plotted graphs, this model well described the Cu^{+2} adsorption by activated hydrochar.

Data of β constant gave theoretical idea about desorption rate of Cu^{+2} ions after adsorption. While temperature increasing, this value decreased ($p < 0.05$). In the study of Cu^{+2} adsorption by sand, same kinetic model was used and same behavior was observed for β constant for three different temperatures (Han et al., 2006). It could have related with being endothermic mechanism. Besides, initial adsorbate concentration inversely proportional to that desorption constant value ($p < 0.05$). This means that with the increment in Cu^{+2} ion concentration, while desorption was decreasing; adsorption increased. In the study of Cu^{+2} ion adsorption by peat, there was not same result observed. Ho and McKay (2002) obtained directly proportional relationship between two parameters. It would have related with the sorbent material surface chemistry and process environment.

In conclusion, when looking to the three kinetic model results, the highest correlation coefficient, R^2 , and lowest sum of square error value, SSE , were obtained from Logistic kinetic model. Also, Elovich kinetic model described that adsorption system well. From three models, it was seen that, 200 min contact time was enough than more for reaching equilibrium and exponential rate was observed in first twenty min.

3.4. Adsorption Equilibrium Isotherms

Adsorption equilibrium isotherms describe the distribution of adsorbed material between liquid phase, *adsorbate*, and solid phase, *adsorbent*, when the equilibrium state has reached (Nwabanne and Igbokwe, 2008). Isotherms give idea about adsorbent-adsorbate interaction type at constant temperature and pH conditions. Even, assumptions about the adsorbent material character can be made with the mathematical results of isotherm models. They are the key point in the model or system designing. In the present study, Langmuir, Freundlich and Dubinin-Radushkevich isotherms were performed to understand the adsorption mechanism of

hydrochar. Correlation coefficient, R^2 , and SSE values (Eq. 2.3.) and parameters of three isotherms are given in Table 3.4.

Table 3.4 R^2 , and SSE values and parameters of three isotherms

Temp (K)	Freundlich				Langmuir					Dubinin-Radushkevich			
	R^2	SSE	K_f^*	n	R^2	SSE	K_L^{**}	q_L^{***}	R_L	R^2	SSE	q_m^{****}	E^{*****}
298	0.995	0.997	7.472	2.400	0.983	0.991	0.136	39.480	0.310	0.742	0.861	24.420	0.989
308	0.99	0.995	9.020	2.380	0.978	0.989	0.153	46.300	0.290	0.741	0.861	28.240	1.206
318	0.995	0.997	11.88	2.520	0.976	0.988	0.198	53,054	0.245	0.747	0.864	32.400	1.684

* : Freundlich constant as adsorption capacity [(mg/g) (L/g)^{1/n}]

** : Langmuir constant (L/mg)

*** : Monolayer sorption capacity (mg/g) from Langmuir isotherm

**** : Maximum sorption capacity (mg/g) from Freundlich isotherm

***** : Free energy (kJ/mol) from Dubinin–Radushkevich isotherm

3.4.1. Langmuir isotherm

The Langmuir isotherm assumes that maximum adsorption corresponds to a saturated monolayer of adsorbate molecules on the adsorbent surface and homogeneous adsorption with constant energy and no transmigration of adsorbate in the plane of the surface (Krishna et al., 2012). This type of adsorption is known as monolayer, in which all the adsorbed molecules are in contact with the surface layer of the adsorbent. From this isotherm, theoretical monolayer adsorption capacity, q_L (mg/g), and Langmuir constant, K_L (L/mg) related to the energy of adsorption can be found by Eq. (1.4).

In order to understand whether presence of this behavior or not, Langmuir isotherm was applied to experimental data. R^2 and SSE values and K_L (L/mg) and q_L (mg/g) parameters of model are given at Table 3.4. Results of model are given in Figure 3.18. According to correlation coefficient, R^2 , and SSE values, this isotherm gave good fitting.

From theoretical data, temperature effect on monolayer adsorption capacity (mg/g), q_L , could be seen obviously. This value increased with increased temperature. This indicated that adsorption process was endothermic.

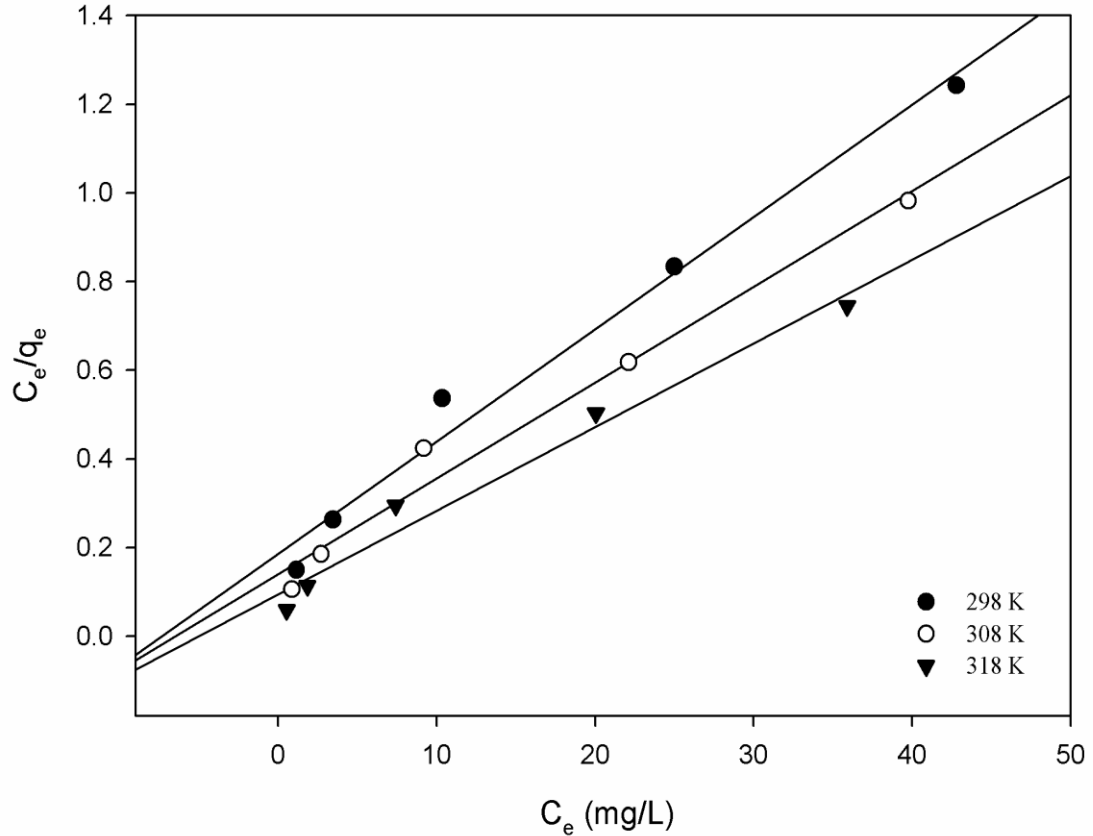


Figure 3.18 Langmuir Isotherm for adsorption of Cu^{+2} on activated hydrochar at different temperature

Langmuir constant, K_L , was used in calculation of equilibrium parameter R_L , which is a dimensionless constant referred to as separation factor or equilibrium parameter (Webber and Chakravarti, 1974). Value of R_L indicates that adsorption process is irreversible ($R_L = 0$); favorable ($0 < R_L < 1$); linear ($R_L = 1$); and unfavorable ($R_L > 1$). These values were calculated (Eq. 1.6) and they are given at Table 3.4. Whole R_L values were obtained in range of $0 < R_L < 1$ which means adsorption of Cu^{+2} by activated hydrochar was favorable according to Langmuir isotherm definition.

3.4.2. Freundlich isotherm

The Freundlich isotherm, one of the most widely used mathematical descriptions, is an empirical model which can be applied to multilayer adsorption system on heterogeneous surface. In literature, it has been used to describe Cu^{+2} adsorption by dried peanut husk (Salam et al., 2011), by activated carbon from olive stone (Bohli et al., 2014), by dried orange peel and banana peel (Annadurai et al., 2002), by activated carbon from hazelnut shell (Demirbas et al., 2009). There were different Freundlich isotherm results for Cu^{+2} adsorption onto different sorbent. Some of them

had good fitting and some of them had weak fitting with that model. Because, type of adsorption mechanism depends sorbent chemistry and physiology, correspondingly; sorbent-sorbate interaction. So, this isotherm gives theoretical idea about mechanism for current sorbent-sorbate couple specifically. According to that model, Freundlich constant, K_F , is approximate indicator of adsorption capacity and n indicates the favorability of adsorption (Eq. 1.6). R^2 and SSE values of fitting of this isotherm to present study and predictive parameters of that model are given on Table 3.4 and plotted model is given in Figure 3.19.

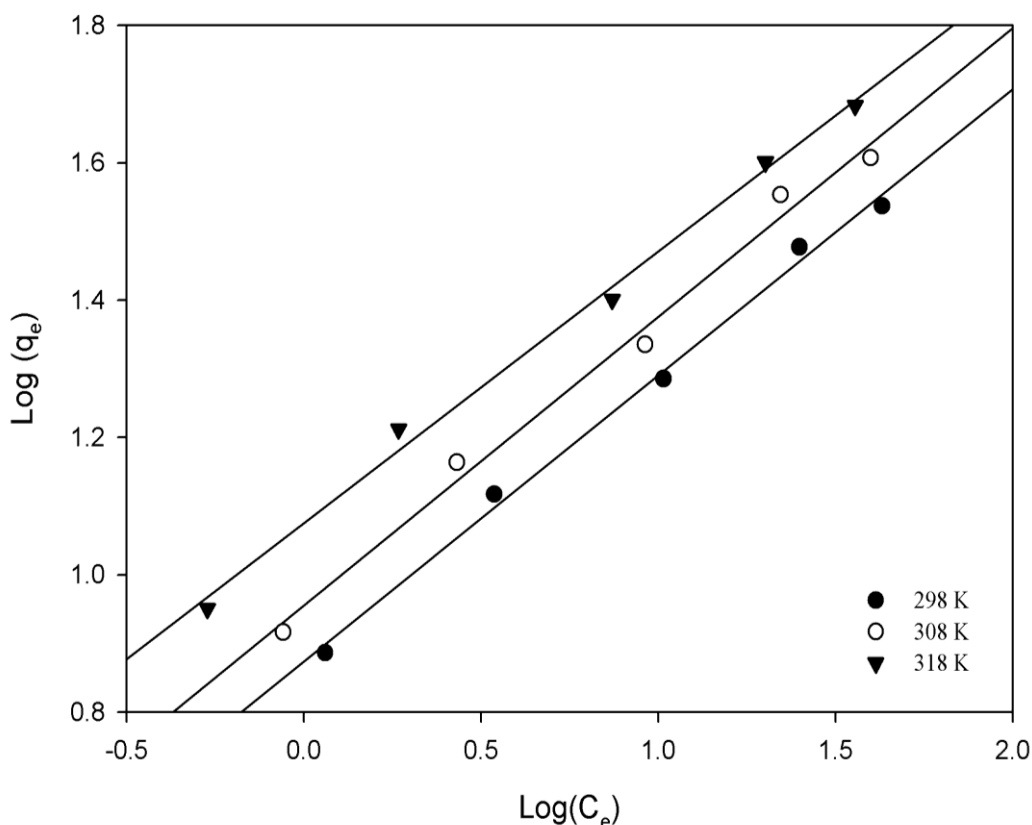


Figure 3.19 Freundlich isotherm for adsorption of Cu^{+2} on activated hydrochar at different temperature

When looking to the R^2 and SSE values, Freundlich isotherm model was found to be the best fitting model which means there was multilayer adsorption mechanism and heterogenic surface character dominantly. In multilayer adsorption, sorbent surface has more than one layer of molecules and not all adsorbed molecules are in contact with the surface layer of the sorbent. Fitting results of both Freundlich and Langmuir isotherms gave idea that there were multiple disciplines in adsorption mechanism;

monolayer adsorption took place and at the same time multilayer adsorption had started between adsorbed molecules.

According to calculated adsorption capacity values, K_F , there was directly proportional relationship with temperature ($p < 0.05$). Temperature increment might have caused the favoring of diffusion. Additionally there would be another possibility; while temperature was increasing, porosity of sorbent might have increased because of expansion with temperature. So, capacity would be increased by this way.

In order to understand favorability of adsorption, $1/n$ values were found from slope of Freundlich graph and n values were calculated. If $n < 1$, it refers poor; $1 < n < 2$ it refers moderately difficult; ranging from 2 to 10 refers good favorability (Chen et al., 2011). In the present study all values were in the range of 2-10 which indicates good favorability. On the other hand, there was no directly relationship ($p > 0.05$) with temperature.

3.4.3. Dubinin-Radushkevich isotherm

This model describes the adsorption system with regard to Gaussian energy distribution onto heterogeneous surface and generally, it has been used for adsorption in microporous materials (Nguyen and Do, 2001). In literature, this model has been used to distinguish the physisorption and chemisorption behavior of metal ions by means of mean free energy of adsorption, E , per molecule of adsorbate, in other words; energy for removing a molecule from its location in the adsorption space to the infinity (Dubinin and Radushkevich 1947; Hobson, 1969). If value of E is between 8 kJ/mol and 16 kJ/mol, it can be said that adsorption process is chemical in nature, while lower than 8 kJ/mol indicates that the adsorption is physical in nature (Zheng, 2008).

Correlation coefficient, R^2 , and SSE values of plotted graphs of isotherm and maximum adsorption capacity, q_m , (mg/g), and calculated free energy values, E , (Eq. 1.9.) are given at Table 3.4.

R^2 values (0.741-0.747) of this model did not correlate with experimental data of the Cu^{+2} ion adsorption onto activated hydrochar quite well, it might have deduced that adsorbent had not a microporous structure, although; parameters of isotherm could

be used to theoretical examination of experiment. There were directly proportional relationship between temperature and maximum adsorption capacity, q_m , (mg/g) which refers the probable endothermic mechanism. Another parameter of that isotherm is β which is a constant related to the adsorption energy. This parameter was used in Eq. 1.9. and free energy values, E were calculated. As it can be seen from Table 3.4, calculated free energy values of per adsorbent molecule were between 0.99-1.68 kJ/mol. This referred the Cu^{+2} ion adsorption mechanism of activated hydrochar was physisorption in nature.

Eventually, if kinetic and equilibrium isotherm models are thought together, there would be physisorption as dominant mechanism and partially effective chemisorption in adsorption system of Cu^{+2} by activated hydrochar and adsorption process was favorable at experiments' conditions.

3.5. Thermodynamic Studies

Thermodynamic studies of an adsorption system can give idea about type of adsorption mechanism as physisorption or chemisorption, spontaneity of process in nature, temperature dependency as exothermic or endothermic, disorderedness and activation energy which must be overcome by the adsorbate to interact with the functional groups on the surface of the adsorbent.

In order to make an approach to adsorption mechanism by the means of thermodynamic, activation energy, E_a , was calculated from Eq. 1.10. It was found 12.46 kJ/ mol which meant the presence of physisorption. Because, in physical adsorption energy is required, ranging from 5 to 40 kJ/ mol. On the other hand, chemical adsorption involves stronger forces than the physical adsorption and thus high activation energy is required (40–800 kJ/ mol) (Çelekli et al., 2012).

Spontaneity of Cu^{+2} ion adsorption by activated hydrochar was determined by using of the Gibbs free energy change. Langmuir constant, K_L , was used in determination of that value by Eq.1.11.

Gibbs free energy change is the driving force and the fundamental criterion of spontaneity. Reactions occur spontaneously at a given temperature if ΔG^o is a negative. Moreover, ΔG^o up to -20 kJ/mol are consistent with electrostatic interaction between adsorption sites and the metal ion (physical adsorption) while

ΔG^o values more negative than -40 kJ/mol involve charge sharing or transfer from the biomass surface to the metal ion to form a coordinate bond (chemical adsorption) (Horsfall and Spiff, 2004).

Table 3.5 Gibbs free energy, enthalpy and entropy change values of adsorption process

Temp (K)	ΔG^o (kJ)	ΔH^o (kJ/mol)	ΔS^o (kJ/mol*K)
298	-22.4632		
308	-23.518	14.814	0.124
318	-24.9607		

In the present study, this value was calculated for each temperature; 298, 308, and 318 K by using Eq. 1.11 and they were -22.46 , -23.52 , and -24.96 kJ/mol, respectively (Table 3.5). So it could have concluded that there was spontaneous adsorption process of Cu^{+2} ions by activated hydrochar and it was controlled by physico-chemical adsorption mechanism rather than a pure physical or chemical adsorption mechanism.

Moreover, as it can be seen from the ΔG^o values, there was a decrement in free energy changing with temperature increment. In literature this situation was interpreted as; the adsorption process is more favourable at higher temperatures. This might have been possible because the mobility of adsorbate ions in the solution increase with increase in temperature, so; the affinity of adsorbate on the adsorbent might be higher at high temperatures. In other words, final free energy was lower than initial free energy and this caused the negative change and this means, after process; free energy decreased because of using of that energy by particles. According to results, more free energy at the environment was used in adsorption process with the temperature increment. On the other hand, diffusivity in solutes is a temperature dependent parameter and increasing temperature increased diffusivity coefficient. Additionally; if there is chemisorption mechanism; temperature has a positive effect on adsorption. From all these information, reason of decrement in free energy change with temperature was meaningful for the present study. In the studies of Pb^{+2} adsorption onto the peat (Ho, 2006), Cu^{+2} ion adsorption onto mimosa tannin

resin (Şengil and Özaçar, 2008) and dye adsorption onto orange peel (Mafra et al. 2013) same behavior with temperature increment was observed for ΔG^o values.

The values of enthalpy change, ΔH^o , and entropy change, ΔS^o were obtained from the slope and intercept of plots of ΔG^o vs. temperature (K) (Eq. 1.12). Negative value of enthalpy change, ΔH^o , indicates that the adsorption phenomenon is exothermic while a positive value implies that the adsorption process is endothermic. In the present study, it was calculated as 14.81 kJ/mol (Table 3.5). This meant there was endothermic mechanism in adsorption of Cu^{+2} onto activated hydrochar and this coincided with isothermal results. Value of entropy change, ΔS^o , gives idea about measure of disorder; positive value of ΔS^o indicates increasement of randomness at the solid/solution interface; a negative value of entropy change, ΔS^o , indicates a decreased disorderliness at the solid/liquid interface during the adsorption process (Horsfall and Spiff, 2004). In present study this value was calculated as 124 J/K*mol, which referred increased disorder at the solid–liquid interface during the Cu^{+2} adsorption onto activated hydrochar.

CHAPTER IV

CONCLUSION

In this research, waste grapefruit peel was transformed into hydrochar by Microwave Assisted-Low Temperature Hydrothermal Carbonization (HTC) technique followed by cold activation process. Obtained activated hydrochar was performed as adsorbent in Cu^{+2} ion removal process. Copper (II) metal is the mainly found in wastewater since its intensive using in industries. Therefore, it was selected as adsorbate. Effects of pH, adsorbent dose, adsorbate dose, temperature and time on the adsorption capacity were investigated by Atomic Absorption Spectroscopy measurements; mathematical models were used to describe kinetic, isotherm and thermodynamic data. Findings of this study were summarized as;

- ❖ Newly opened sides and increased surface area was observed in developed material; additionally, this material had slightly acidic surface character,
- ❖ During carbonization, new aromatic surface sides or increased intensity observation in carbon-rich sides occurred and lots of them took part in adsorption process,
- ❖ Cold activation step improved the adsorption capacity of Cu^{+2} ion almost two times,
- ❖ Higher pH values effected the Cu^{+2} ion adsorption capacity positively,
- ❖ Highest adsorption capacity was observed at lowest adsorbent dose,
- ❖ Adsorbed Cu^{+2} ion amount increased with increment in initial Cu^{+2} ion concentration,
- ❖ Temperature increment promoted the Cu^{+2} ion adsorption capacity, especially at higher initial Cu^{+2} ion concentration,

- ❖ Adsorption of Cu^{+2} ion was faster during the first twenty min and equilibrium was reached after 50 min,
- ❖ According to R^2 and SSE values; each three kinetic model, Nonlinear Pseudo-second Order, Logistic and Elovich, had good fitting but the best one was Logistic model,
- ❖ Freundlich equilibrium isotherm model gave highest fitting which means there were multilayer physisorption mechanism dominantly, on the other hand; Langmuir equilibrium isotherm model had considerable R^2 and SSE values which means there was also monolayer chemisorption mechanism also. Briefly, there was multisystem discipline, and
- ❖ According to thermodynamic calculations, adsorption of Cu^{+2} ions by sorbent was spontaneous and it was controlled by physico-chemical adsorption mechanism same as the observation from equilibrium isotherms, moreover; process was endothermic.

In a conclusion, activated hydrochar from grapefruit peel gave good performance in the Cu^{+2} ion adsorption as *green adsorbent* and its character can be improved with modified HTC conditions.

REFERENCES

- Alchin, D. (2008). XIII-Water-D-Ion Exchange Resins Article <http://nzic.org.nz/ChemProcesses/water/13D.pdf>
- Al-Enezi, G., Hamoda M.F., Fawzi, N. (2004). Ion exchange extraction of heavy metals from wastewater sludges. *Journal of Environment Science Health Part A Toxic/Hazardous Substances and Environmental Engineering*. **39**, 455-64.
- Annadurai, G., Juang, R.S., Lee, D.J. (2002). Adsorption of heavy metals from water using banana and orange peels, *Water Science and Technology*. **47**, 185–190.
- Aydıncak, K. (2012). Hidrotermal karbonizasyon yöntemiyle gerçek ve model biyokütlelerden karbon nanoküre sentezi ve karakterizasyonu. Ankara University, Institute of Science, M.Sc. Thesis.
- Balu, A.M., Budarin, V., Shuttleworth, P.S., Pfaltzgraff, L.A., Waldron, K., Luque, R., Clark, J.H. (2012). Valorisation of orange peel residues: Waste to biochemicals and nanoporous materials, *ChemSusChem*, **5**, 1694 – 1697.
- Bampidis, V. A., Robinson, P. H. (2006). Citrus by-products as ruminant feeds: A review. *Animal Feed Science and Technology*. **128**, 175 –217.
- Bansal, R.C., Goyal, M. (2001). Removal of copper from aqueous solutions by adsorption on activated carbons. *Colloids and Surfaces A: Physicochemical and Engineering Aspects*. **190**, 229–238.
- Bansal, R.C., Goyal, M. (2005). Activated carbon adsorption. USA: Taylor and Francis.
- Bayram, N.Z. (2014). *Cladophora glomerata* ile bakır arıtımının adsorpsiyon kinetiği, MSc Thesis, Biology Department, Gaziantep University.
- Behrendt, F., Neubauer, Y., Oevermann, M., Wilmes, B., Zobel, N. (2008). Direct liquefaction of biomass. *Chemical Engineering Technology*. **31**, 667–677.
- Bobleter, O. (1994). Hydrothermal degradation of polymers derived from plants. *Progress in Polymer Science*. **19**, 797–841.
- Bohli, T., Ouederni A., Fiol, N., Villaescusa, I. (2015). Evaluation of an activated carbon from olive stones used as an adsorbent for heavy metal removal from aqueous phases, *Comptes Rendus Chimie*. **18** 88–99.
- Brunauer, S., Emmett, P. H., Teller, E. (1938). Adsorption of gases in multimolecular layers. *Journal of the American Chemical Society*. **60**, 309–319.
- Carrington, S., Fraser, H., Gilmore, J., Forde, A. (2003). A-Z of Barbados Heritage. UK: Macmillan.
- Çelekli, A., Yavuzatmaca, M., Bozkurt, H. (2009). An eco-friendly process: Predictive modelling of copper adsorption from aqueous solution on *Spirulina platensis*, *Journal of Hazardous Materials*. **173**, 123–129.

- Çelekli, A., İlgün, G., Bozkurt, H. (2012). Sorption equilibrium, kinetic, thermodynamic, and desorption studies of Reactive Red 120 on *Chara contraria*. *Chemical Engineering Journal*. **191**, 228–235.
- Chang, Q., Wang, G. (2007). Study on the macromolecular coagulant PEX which traps heavy metals. *Chemical Engineering Science*. **62**, 4636–4643
- Chen, H., Zhao, J., Wu, J., Dai, G. (2011). Isotherm, thermodynamic, kinetics and adsorption mechanism studies of methyl orange by surfactant modified silkworm exuviae. *Journal of Hazardous Materials*. **192** 246–254.
- Cheung, C.W., Porter, J.F., McKay, G. (2001). Sorption kinetic analysis for the removal of cadmium ions from effluents using bone char. *Water Research*. **35**, 605-612.
- Clarck, E., Sutton, W. H. (1996). Microwave processing of materials. *Annual Reviews of Material Science*, **26**, 299-331.
- Cséfalvay, E., Pauer, V., Mizsey, P. (2009). Recovery of copper from process waters by nanofiltration and reverse osmosis. *Desalination*. **240**, 132-142.
- Dabrowski, A. (2001). Adsorption: from theory to practice. *Advances in Colloid Interface Science*. **93**, 135–224
- Dada, A.O., Olalekan, A. P., Olatunya, A. M., Dada, O. (2012). Langmuir, Freundlich, Temkin and Dubinin–Radushkevich Isotherms Studies of Equilibrium Sorption of Zn^{2+} Unto Phosphoric Acid Modified Rice Husk. *IOSR Journal of Applied Chemistry*. **3**, 38-45.
- Dalgıç, A.C. (1998). Biogas production from olive residue. Ph.D. Thesis. Department of Food Engineering, Gaziantep University.
- Demirbaş, E., Dizge, N., Sulak, M.T., Kobya, M. (2009). Adsorption kinetics and equilibrium of copper from aqueous solutions using hazelnut shell activated carbon. *Chemical Engineering Journal*. **148**. 480–487.
- Deng, H., Yang, L., Tao, G., Dai, J. (2009). Preparation and characterization of activated carbon from cotton stalk by microwave assisted chemical activation - Application in methylene blue adsorption from aqueous solution. *Journal of Hazardous Materials*. **166**, 1514–1521.
- Dubinin, M.M., Radushkevich, L.V. (1947). The equation of the characteristic curve of the activated charcoal. *Proceedings of USSR Academy of Sciences*. **55**, 331.
- Duruibe, J. O., Ogwuegbu, M. O. C, and Egwurugwu, J. N. (2007). Heavy metal pollution and human biotoxic effects. *International Journal of Physical Sciences*. **2**, 112-118.
- El Samrani1, A.G., Lartiges, B.S., Villiéras, F. (2008). Chemical coagulation of combined sewer overflow: Heavy metal removal and treatment optimization. *Water Research*. **42**, 951–960.
- Faust, S.D., Aly, O.M. (1998). *Chemistry of Water Treatment*, 2nd edition, USA: Lewis Publishers.
- Fitzer, E., Kochling, K., Boehm, H.P., Marsh, H. (1995). Recommended terminology for the description of carbon as a solid. *Pure and Applied Chemistry*. **67**, 473–506.

- Foo, K.Y., Hameed, B.H. (2010). Insights into the modeling of adsorption isotherm systems, *Review Chemical Engineering Journal*. **156**, 2–10.
- Foo, K.Y., Hameed, B.H. (2011). Utilization of rice husks as a feedstock for preparation of activated carbon by microwave induced KOH and K₂CO₃ activation, *Bioresource Technology*. **102**, 9814-9817.
- Foo, K.Y., Hameed, B. H. (2012a). Porous structure and adsorptive properties of pineapple peel based activated carbons prepared via microwave assisted KOH and K₂CO₃ activation. *Microporous and Mesoporous Materials*. **148**, 191-195.
- Foo, K.Y., Hameed, B.H. (2012b). Factors affecting the carbon yield and adsorption capability of the mangosteen peel activated carbon prepared by microwave assisted K₂CO₃ activation, *Chemical Engineering Journal*. **180**, 66–74.
- Foo, K.Y., Hameed, B.H. (2012c). Preparation, characterization and evaluation of adsorptive properties of orange peel based activated carbon via microwave induced K₂CO₃ activation, *Bioresource Technology*. **104**, 679-86.
- Freundlich, H.M.F., (1906). Uber die adsorption in losungen. *Z. Phys. Chem.*, **57** (A), 385-470.
- Fu, F., Wang, Q. (2011). Removal of heavy metal ions from wastewaters: A review. *Journal of Environmental Management*. **92**, 407-418.
- Fuertes, A. B., Arbestain, M.C., Sevilla, M., Maciá-Agulló, J. A., Fiol, S., López, R., Smernik, R. J., Aitkenhead, W. P., Arce, F., Macias, F. (2010). Chemical and structural properties of carbonaceous products obtained by pyrolysis and hydrothermal carbonisation of corn stover, *Australian Journal of Soil Research*. **48**, 618–626.
- Funke, A., Ziegler, F. (2010). *Biofuels, Bioproducts and Biorefining*. UK: John Wiley & Sons.
- Goldman, S.J., Jackson, K., Bursztynsky, T.A. (1986). *Erosion & Sediment Control Handbook*. New York: McGraw-Hill Book Company.
- González-Muñoz, M.J. Rodríguez, M.A., Luque, S., Álvarez, J.R. (2006). Recovery of heavy metals from metal industry waste waters by chemical precipitation and nanofiltration. *Desalination*. **200**, 742–744.
- Grénman, H., Eränen, K., Krogell, J., Willför, S., Salmi, T., Murzin, D.Y. (2011). The kinetics of aqueous extraction of hemicelluloses from spruce in an intensified reactor system. *Industrial and Engineering Chemistry Research*. **50**, 3818–3828.
- Groenli, M.G., Varhegyi, G., Di, B. C. (2002). Thermogravimetric analysis and devolatilization kinetics of wood. *Industrial and Engineering Chemistry Research*. **41**, 4201–4208.
- Guiotoku, M., Maia, C.M.B.F., Rambo, C.R., Hotza, D. (2011). *Microwave Heating, Croatia (EU): InTech*.
- Günay, A., Arslankaya, E., Tosun, I. (2007). Lead removal from aqueous solution by natural and pretreated clinoptilolite: adsorption equilibrium and kinetics. *Journal of Hazardous Materials*. **146**, 362–371.
- Gupta, V.K, Pathania, D., Sharma, S. (In press). Adsorptive remediation of Cu(II) and Ni(II) by microwave assisted H₃PO₄ activated carbon, *Arabian Journal of Chemistry*. In press.

- Gustan, P., Darmawan, S., Prihandoko, B. (2014). Porous Carbon Spheres from Hydrothermal Carbonization and KOH Activation on Cassava and Tapioca Flour Raw Material. *Procedia Environmental Sciences*. **20**, 342 – 351.
- Hackskaylo, J.J., Levan, M.D. (1985). Correlation of adsorption equilibrium data using a modified Antonie equation: a new approach for pore-filling models. *Langmuir*. **1**, 97-100.
- Hameed B.H., El-Khaiary, M.I. (2008). Batch removal of malachite green from aqueous solutions by adsorption on oil palm trunk fibre: Equilibrium isotherms and kinetic studies. *Journal of Hazardous Materials*. **154**, 237–244.
- Hammer, M. J. (1975). *Water and Waste-Water Technology*. New York: John Wiley & Sons.
- Hammud, H.H., Fayoumi, L., Holail, H., Mostafa, S.M.E. (2011). Biosorption Studies of Methylene Blue by Mediterranean Algae *Carolina* and Its Chemically Modified Forms. Linear and Nonlinear Models' Prediction Based on Statistical Error Calculation. *International Journal of Chemistry*. **3**, 147-163.
- Han, R., Zou, W., Zhang, Z., Shi, J., Yang, J. (2006). Removal of copper(II) and lead(II) from aqueous solution by manganese oxide coated sand: I. Characterization and kinetic study. *Journal of Hazardous Materials*. **137**, 384–395.
- Han, R., Han, P., Cai, Z., Zhao, Z., Tang, M. (2008). Kinetics and isotherms of Neutral Red adsorption on peanut husk. *Journal of Environmental Sciences*. **20**, 1035–1041.
- Hawkes, J.S. (1997). Heavy Metals. *Journal of Chemical Education*. **74**, 1374.
- Heidmann, I., Calmano, W. (2008). Removal of Cr(VI) from model wastewaters by electrocoagulation with Fe electrodes. *Separation and Purification Technology*. **61**, 15–21.
- Hesas, R.H., Niya, A., Daud, W.M.A.W., Sahu, J.N. (2013). Activated carbon sorbent. *BioResources*. **8**, 2950-2966
- Ho, Y.S., McKay, G. (1999). Pseudo second-order model for sorption processes, *Process. Biochem.* **34** 451-465.
- Ho, Y. S., McKay, G. (2002). Application of kinetic models to the sorption of copper(ii) on to peat. *Adsorption Science and Technology*. **20**, 797-815.
- Ho, Y.S. (2006). Isotherms for the sorption of lead onto peat: comparison of linear and non-linear methods. *Polish Journal of Environmental Studies*. **15**, 81-86.
- Hobson, J.P. (1969). Physical adsorption isotherms extending from ultra-high vacuum to vapor pressure. *Journal of Physical Chemistry*. **73**, 2720– 2727.
- Horsfall, M., Spiff, A. I. (2004). Studies on the effect of pH on the sorption of Pb²⁺ and Cd²⁺ ions from aqueous solutions by *caladium bicolor* (wild cocoyam) biomass. *Electronic Journal of Biotechnology*. **7**, 1-7.
- Hutson, N. D., and Yang, R. T. (2000). Theoretical Basis for the Dubinin-Radushkevich (D-R) Adsorption Isotherm Equation. *Adsorption*. **3**, 189–195.
- İdris, S., Iyaka, Y.A., Ndamitso, M.M., Mohammed, E.B., Umar, M.T. (2011). Evaluation of kinetic models of copper and lead uptake from dye wastewater by activated pride of barbados shell. *American Journal of Chemistry*. **1**, 47-51.

- Inglezakis, V.J., Pouloupoulos, S.G. (2006). Adsorption, Ion Exchange, and Catalysis: Design of Operations and Environmental Applications. Amsterdam: Elsevier.
- IUPAC, International Union of Pure and Applied Chemistry. (1997). Compendium of Chemical Terminology. 2nd Edition. Blackwell Science, Oxford, UK.
- Juang, R.S., Chen, M.L. (1997). Application of the Elovich Equation to the Kinetics of Metal Sorption with Solvent-Impregnated Resins, *Industrial and Engineering Chemistry Research*. **36**, 813–820.
- Koch, A., Krzton, A., Fingueneisel, G., Heintz, O., Weber, J.V., Zimny, T. (1998). A study of carbonaceous char oxidation in air by semi-quantitative FTIR spectroscopy. *Fuel*. **77**, 563–569
- Krishna, R. H., Swamy, A.V.V.S., (2011). Studies on the Removal of Ni (II) from Aqueous Solutions Using Powder of Mosambi Fruit Peelings as a Low Cost Sorbent. *Chemical Sciences Journal*. **31**, 1-13.
- Kruse, A., Dahmen, N. (2015). Water – A magic solvent for biomass conversion. *The Journal of Supercritical Fluids*. **96**, 36–45.
- Kumar, K.V., Porkodi, K. (2007). Mass transfer, kinetics and equilibrium studies for the biosorption of methylene blue using *Paspalum notatum*. *Journal of Hazardous Materials*. **146**, 214–226.
- Langmuir, I. (1916). The constitution and fundamental properties of solids and liquids. Part I. Solids. *Journal of American Chemical Society*. **38**, 2221–2295.
- Langmuir, I. (1918). The adsorption of gases on plane surfaces of glass, mica, and platinum. *Journal of American Chemical Society*. **40**, 1361–1403.
- Lehmann, J., Joseph, S. (2009). Biochar for Environmental Management: Science and Technology. 1st edition. London, UK: Earthscan, 1–12.
- Li, W., Zhang, L., Peng, J., Li, N., Zhu, X., (2008). Preparation of high surface area activated carbons from tobacco stems with K₂CO₃ activation using microwave radiation. *Industrial Crops and Products*. **27**, 341–347.
- Libra, J.A., Ro, K.S., Kammann, C., Funke, A., Berge, N.D., Neubauer, Y., Titirici, M.M., Fühner, C., Bens, O., Kern, J., Emmerich K.H. (2011). Hydrothermal carbonization of biomass residuals: a comparative review of the chemistry, processes and applications of wet and dry pyrolysis. *Biofuels*. **2**, 89–124.
- Mafra, M. R., Igarashi, L., Zuim, D. R., Vasques, E. C., Ferreira, M.A. (2013). Adsorption of remazol brilliant blue on an orange peel adsorbent, *Brazilian Journal of Chemical Engineering*. **30**, 657-665.
- Marin, F. R., Rivas, C., Garcia, O., Castillo, J., Alvarez, J.A. (2007). By-products from different citrus processes as a source of customized functional fibres. *Food Chemistry*. **100**, 736–741
- Mok, W.S.L., Antal, M.J., Szabo, P., Varhegyi, G. Zelei, B. (1992). Formation of charcoal from biomass in a sealed reactor. *Industrial and Engineering Chemistry Research*. **31**, 1162–1166.
- Nguyen, C., Do, D.D. (2001). The Dubinin–Radushkevich equation and the underlying microscopic adsorption description. *Carbon*. **39**, 1327–1336.

- Nwabanne, J.T., Igbokwe, P.K. (2008). Kinetics and equilibrium modeling of nickel adsorption by cassava peel. *Journal of Engineering and Applied Sciences*. **3**, 829-834.
- Oghbaei, M., Mirzaee, O. (2010). Microwave versus conventional sintering: A review of fundamentals, advantages and applications. *Journal of Alloys and Compounds*. **494**, 175-189.
- Omelia, C. (1998). Coagulation and sedimentation in lakes, reservoirs and water treatment plants. *Water Science and Technology*. **37**, 129.
- Önal, Y., Başar, C., Özdemir, Ç., Depci, T. (2010). Karbonize edilmiş kayısı çekirdeğinden kimyasal aktivasyon yöntemi ile aktif karbon eldesi. 24. Ulusal Kimya Kongresi, 29 June- 2 July, 2010, Zonguldak Karaelmas Üniversitesi.
- Ozmaç, M., Gürten, I., Yağmur, E., Aktaş, Z. (2010). Çay atıklarından aktif karbon üretimi ve adsorpsiyon proseslerinde kullanımı, 9.Ulusal Kimya Mühendisliği Kongresi, 22-25 June, 2010, Ankara,
- Pala, M., Kantarlı, I.C., Büyüksık, H. B., Yanık, J. (2014). Hydrothermal carbonization and torrefaction of grape pomace: A comparative evaluation. *Bioresource Technology*. **161**, 255–262.
- Plazinski, W., Rudzinski, W., Plazinska, A. (2009). Theoretical models of sorption kinetics including a surface reaction mechanism: A review. *Advances in Colloid and Interface Science*. **152**, 2–13.
- Plazinski, W., Dziuba, J., Rudzinski, W. (2013). Modeling of sorption kinetics: the Pseudo-second order equation and the sorbate intraparticle diffusivity. *Adsorption*. **19**, 1055–1064.
- Pradhan, B.K., Sandle, N.K. (1998). Effect of different oxidizing agent treatments on the surface properties of activated carbons. *Carbon*. **37**, 1323–1332.
- Prakash, N., Karunanithi, T. (2008). Kinetic modeling in biomass pyrolysis – A Review. *Journal of Applied Sciences Research*. **4**, 1627-1636.
- Rao, K.S., Anand, S., Venkateswarlu, P. (2010). Adsorption of Cd²⁺ ions from aqueous solution by *Tectona Grandis* L.F. (Teak Leave Powder). *BioResources*. **5**, 438-454.
- Regmi, P., Moscoso, J.L.G., Kumar, S., Cao, X., Mao, J., Schafran, G. (2012). Removal of copper and cadmium from aqueous solution using switchgrass biochar produced via hydrothermal carbonization process. *Journal of Environmental Management*. **109**, 61-69.
- Reza, M.T., Uddin, M.H., Lynam, J.G., Coronella, C.J. (2013). Hydrothermal carbonization: fate of inorganics. *Biomass Bioenergy*. **49**, 86–94.
- Reza M.T., Uddin M.H., Lynam J.G., Hoekman K., Coronella C.J. (2014a) Hydrothermal carbonization of loblolly pine: Reaction chemistry and water balance. *Biomass Conversion and Biorefinery*. **4**, 311-321.
- Reza, M.T., Andert, J., Wirth, B., Busch, D., Pielert, J., Lynam, J.G., Mumme, J. (2014b). Hydrothermal Carbonization of Biomass for Energy and Crop Production. *Applied Bioenergy*. **1**, 11–29.

- Reza, M.T., Wirth, B., Lüder, U., Werner, M. (2014c). Behavior of selected hydrolyzed and dehydrated products during hydrothermal carbonization of biomass. *Bioresource Technology*. **169**, 352–361.
- Robati, D. (2013). Pseudo-second-order kinetic equations for modeling adsorption systems for removal of lead ions using multi-walled carbon nanotube. *Journal of Nanostructure in Chemistry*. **3**, 55.
- Roman, S., Nabais, J.M., Ledesma, B., Gonzalez, J.F., Laginhas, C., Titirici, M.M. (2013). Production of low-cost adsorbents with tunable surface chemistry by conjunction of hydrothermal carbonization and activation processes. *Microporous and Mesoporous Materials*. **165**, 127–133.
- Rubio, J., Tessele, F. (1997). Removal of heavy metal ions by adsorptive particulate flotation. *Minerals Engineering*. **10**, 671–679.
- Rubio, J., Souza, M.L., Smith, R.W. (2002). Overview of flotation as a wastewater treatment technique. *Mineral Engineering*. **15**, 139-155.
- Sağ, Y., Aktay, Y. (2002). Kinetic studies on sorption of Cr(VI) and Cu(II) ions by chitin, chitosan and *Rhizopus arrhizus*. *Biochemical Engineering Journal*. **12**, 143–153.
- Saha, P., Chowdhury, S. (2011). Thermodynamics. Croatia (EU): InTech, 349-364p.
- Salam, O.E.A., Reiad, N.A., ElShafei, M.M. (2011). A study of the removal characteristics of heavy metals from wastewater by low-cost adsorbents. *Journal of Advanced Research*. **2**, 297–303.
- Salkind, N. J. (2010). Encyclopedia of Research Design, London, UK: Sage Publications
- Şengil, I. A., Özaçar, M. (2008). Biosorption of Cu(II) from aqueous solutions by mimosa tannin gel. *Journal of Hazardous Materials*. **157**, 277–285.
- Sevilla, M., Fuertes, A.B. (2009a). The production of carbon materials by hydrothermal carbonization of cellulose. *Carbon*. **47**, 2281 –2289.
- Sevilla, M., Fuertes, A.B. (2009b). Chemical and structural properties of carbonaceous products obtained by hydrothermal carbonization of saccharides. *Chemistry: A European Journal*. **15**, 4195–4203.
- Temkin, M. I. (1940). The Arrhenius equation and the active complex method. *Acta Physicochimica URSS*. **13**, 733.
- Thakur, S.K., Kong, T.S., Gupta, M. (2007). Microwave synthesis and characterization of metastable (Al/Ti) and hybrid (Al/Ti+SiC) composites. *Materials Science and Engineering A*. **452-453**, 61-69.
- Thostenson, E.T., Chou, T.W. (1999). Microwave processing: Fundamentals and applications, Composites Part A. *Applied Science and Manufacturing*. **30**, 1055-1071.
- Titirici, M. M. (2012). Hydrothermal Carbonisation: A Sustainable Alternative to Versatile Carbon Materials. Habilitation Thesis, Universität Potsdam, Potsdam.
- Turan, N.G., Mesci, B. (2011). Use of pistachio shells as an adsorbent for the removal of Zn(II) ion. *Clean – Soil, Air, Water*. **39 (5)**, 475–481

- USDA, United States Department of Agriculture. (2013-2014). Foreign Agricultural Service Database. <http://apps.fas.usda.gov/psdonline/psdQuery.aspx>
- Vermeulan, T.H., Vermeulan, K.R., Hall, L.C. (1966). Fundamental. *Industrial and Engineering Chemistry*. **5**, 212–223.
- Wang, X., Qin, Y. (2005). Equilibrium sorption isotherms for of Cu^{+2} on rice bran. *Process Biochemistry*. **40**, 677–680.
- Webber, T.N., Chakravarti, R.K. (1974). Pore and solid diffusion models for fixed bed adsorbers. *Journal of American Institute Chemical Engineers*. **20**, 228- 238.
- WHO (World Health Organization). (2011). WHO Guidelines for Drinking-water Quality. 4th edition, Drinking-water Quality Committee members. Switzerland: WHO Publications.
- Xie, Z., Yang, J., Huang, Y. (1999). Microwave processing and properties of ceramics with different dielectric loss. *Journal of European Ceramic Society*. **19**, 381-387.
- Yadoji, P., Peelamedu, R., Agrawal, D., Roy, R. (2003). Microwave sintering of Ni-Zn ferrites: Comparison with conventional sinterin. *Materials Science and Engineering*. **98**, 269-278.
- Yan, W., Acharjee, T. C., Coronella, C. J., Vasquez, V. R. (2009). Thermal Pretreatment of Lignocellulosic Biomass. *Environmental Progress and Sustainable Energy*. **28**, 435-440.
- Yang, R. T. (2003). Adsorbents: Fundamentals and Applications. New Jersey and Canada: John Wiley & Sons.
- Zhang, B., Huang, H.J., Ramaswamy, S. (2008). Reaction kinetics of the hydrothermal treatment of lignin. *Applied Biochemistry and Biotechnology*. **147**, 119-131.
- Zheng, H., Wang, Y., Zheng, Y., Zhang, H., Liang, S., Long, M. (2008). Equilibrium, kinetic and thermodynamic studies on the sorption of 4-hydroxyphenol on Cr-bentonite. *Chemical Engineering Journal*. **143**, 117–123.
- Zwietering, M.H., Jongenburger, I., Rombouts, F.M., Van't Riet K. (1990). Modeling of bacterial growth curve. *Applied and Environmental Microbiology*. **56**, 1875–1881.

APPENDIX

Table A.1 q_t values of experiments at 298 K

Time (min)	Initial Cu⁺² Con. (mg/L)				
	5	10	20	40	60
0	0	0	0	0	0
2.5	4,74	7,82	11,41	19,36	19,22
5	5,18	8,94	13,01	21,24	22,20
10	5,58	9,86	14,33	22,96	24,69
15	5,94	10,52	15,43	24,49	26,65
30	6,26	11,11	16,41	25,89	28,37
45	6,56	11,58	17,21	27,05	29,97
60	6,84	11,98	17,87	28,03	31,31
90	7,08	12,31	18,33	28,71	32,34
120	7,28	12,57	18,67	29,18	33,14
150	7,44	12,78	18,91	29,50	33,76
180	7,58	12,96	19,14	29,79	34,15
210	7,70	13,10	19,30	30,00	34,44

Table A.2 q_t values of experiments at 308 K

Time (min)	Initial Cu⁺² Con. (mg/L)				
	5	10	20	40	60
0	0	0	0	0	0
2.5	5,04	9,00	12,99	23,89	23,62
5	5,51	10,16	14,66	25,85	26,93
10	5,95	11,10	16,14	27,70	29,83
15	6,34	11,78	17,34	29,36	32,11
30	6,70	12,38	18,40	30,83	34,11
45	7,03	12,89	19,22	32,23	35,95
60	7,33	13,36	19,89	33,40	37,46
90	7,61	13,72	20,40	34,21	38,60
120	7,84	14,02	20,89	34,83	39,35
150	8,00	14,24	21,21	35,24	39,87
180	8,13	14,42	21,45	35,53	40,23
210	8,25	14,59	21,64	35,76	40,48

Table A.3 q_t values of experiments at 318 K

Time (min)	Initial Cu ⁺² Con. (mg/L)				
	5	10	20	40	60
0	0	0	0	0	0
2.5	5,44	9,81	15,84	26,95	30,07
5	5,94	10,99	17,62	28,95	33,49
10	6,41	12,07	19,12	30,85	36,47
15	6,81	13,01	20,44	32,66	38,91
30	7,19	13,79	21,58	34,44	41,20
45	7,57	14,45	22,50	35,94	43,30
60	7,92	15,02	23,30	37,18	44,87
90	8,22	15,42	23,91	38,13	46,14
120	8,48	15,75	24,40	38,88	47,02
150	8,65	15,98	24,75	39,35	47,62
180	8,80	16,16	24,99	39,67	48,00
210	8,93	16,30	25,18	39,90	48,22

Table A.4 q_t predicted values of experiments at 298 K from Pseudo second order kinetic model

	Time (min)	Initial Cu ⁺² Con. (mg/L)				
		5	10	20	40	60
298 K	0	0	0	0	0	0
	2.5	4.11	7.02	10.10	17.30	16.64
	5	5.24	9.00	13.10	21.65	22.14
	10	6.07	10.48	15.38	24.76	26.52
	15	6.41	11.09	16.33	26.01	28.39
	30	6.79	11.78	17.40	27.38	30.55
	45	6.92	12.02	17.79	27.88	31.34
	60	6.99	12.15	17.99	28.13	31.76
	90	7.06	12.28	18.20	28.39	32.18
	120	7.10	12.35	18.30	28.52	32.40
	150	7.12	12.39	18.36	28.60	32.53
	180	7.14	12.41	18.41	28.65	32.61
	210	7.15	12.43	18.44	28.69	32.68

Table A.5 q_t predicted values of experiments at 308 K from Pseudo second order kinetic model

	Time (min)	Initial Cu⁺² Con. (mg/L)				
		5	10	20	40	60
308 K	0	0	0	0	0	0
	2.5	4.34	8.10	11.52	21.44	20.72
	5	5.56	10.25	14.82	26.41	27.10
	10	6.48	11.82	17.31	29.88	32.02
	15	6.85	12.45	18.34	31.24	34.09
	30	7.27	13.15	19.49	32.74	36.44
	45	7.42	13.41	19.91	33.27	37.30
	60	7.50	13.54	20.12	33.54	37.75
	90	7.58	13.67	20.34	33.82	38.20
	120	7.62	13.74	20.46	33.96	38.43
	150	7.65	13.78	20.52	34.04	38.57
	180	7.66	13.81	20.57	34.10	38.67
	210	7.67	13.82	20.60	34.14	38.74

Table A.6 q_t predicted values of experiments at 318 K from Pseudo second order kinetic model

	Time (min)	Initial Cu⁺² Con. (mg/L)				
		5	10	20	40	60
318 K	0	0	0	0	0	0
	2.5	4.67	8.62	14.15	24.13	26.68
	5	5.99	11.12	17.86	29.61	33.93
	10	6.98	13.01	20.56	33.41	39.26
	15	7.39	13.79	21.65	34.90	41.43
	30	7.85	14.67	22.86	36.53	43.85
	45	8.01	14.99	23.29	37.10	44.72
	60	8.10	15.15	23.52	37.40	45.17
	90	8.19	15.32	23.74	37.70	45.63
	120	8.23	15.41	23.86	37.85	45.86
	150	8.26	15.46	23.93	37.94	46.01
	180	8.28	15.49	23.97	38.01	46.10
	210	8.29	15.52	24.01	38.05	46.17

Table A.7 q_t predicted values of experiments at 298 K from Logistic kinetic model

	Time (min)	Initial Cu⁺² Con. (mg/L)				
		5	10	20	40	60
298 K	0	0	0	0	0	0
	2.5	4.76	7.89	11.41	19.23	19.33
	5	5.17	8.89	12.97	21.28	22.06
	10	5.60	9.84	14.46	23.24	24.77
	15	5.86	10.37	15.28	24.34	26.30
	30	6.32	11.21	16.57	26.11	28.80
	45	6.60	11.66	17.25	27.06	30.16
	60	6.80	11.96	17.70	27.70	31.07
	90	7.08	12.35	18.29	28.56	32.29
	120	7.29	12.60	18.67	29.12	33.09
	150	7.45	12.78	18.94	29.54	33.69
	180	7.58	12.93	19.15	29.87	34.15
	210	7.69	13.05	19.32	30.14	34.53

Table A.8 q_t predicted values of experiments at 308 K from Logistic kinetic model

	Time (min)	Initial Cu⁺² Con. (mg/L)				
		5	10	20	40	60
308 K	0	0	0	0	0	0
	2.5	5.05	9.08	13.00	23.74	23.60
	5	5.50	10.09	14.65	25.89	26.87
	10	5.98	11.08	16.24	28.00	30.04
	15	6.26	11.63	17.12	29.20	31.81
	30	6.77	12.51	18.53	31.16	34.60
	45	7.07	12.99	19.28	32.26	36.10
	60	7.29	13.32	19.79	33.01	37.08
	90	7.60	13.74	20.45	34.02	38.38
	120	7.82	14.03	20.88	34.71	39.22
	150	8.00	14.24	21.20	35.23	39.84
	180	8.14	14.41	21.44	35.64	40.31
	210	8.26	14.54	21.64	35.98	40.70

Table A.9 q_t predicted values of experiments at 318 K from Logistic kinetic model

	Time (min)	Initial Cu⁺² Con. (mg/L)				
		5	10	20	40	60
318 K	0	0	0	0	0	0
	2.5	5.44	9.78	15.83	26.73	29.96
	5	5.92	11.00	17.59	29.01	33.44
	10	6.43	12.19	19.28	31.26	36.80
	15	6.74	12.85	20.23	32.56	38.68
	30	7.29	13.92	21.75	34.71	41.70
	45	7.62	14.50	22.58	35.93	43.33
	60	7.86	14.89	23.14	36.77	44.43
	90	8.20	15.40	23.87	37.92	45.88
	120	8.45	15.73	24.37	38.72	46.84
	150	8.65	15.98	24.73	39.32	47.55
	180	8.81	16.18	25.01	39.79	48.10
	210	8.94	16.34	25.24	40.19	48.56

Table A.10 q_t predicted values of experiments at 298 K from Elovich kinetic model

	Time (min)	Initial Cu⁺² Con. (mg/L)				
		5	10	20	40	60
298 K	0	0	0	0	0	0
	2.5	4.70	8.16	11.87	19.72	19.88
	5	5.16	8.96	13.09	21.41	22.25
	10	5.62	9.76	14.31	23.09	24.62
	15	5.89	10.22	15.02	24.08	26.00
	30	6.36	11.02	16.25	25.77	28.37
	45	6.63	11.49	16.96	26.76	29.76
	60	6.82	11.82	17.47	27.46	30.74
	90	7.09	12.28	18.18	28.44	32.13
	120	7.28	12.61	18.69	29.14	33.11
	150	7.43	12.87	19.08	29.69	33.87
	180	7.55	13.08	19.41	30.13	34.50
	210	7.66	13.26	19.68	30.51	35.02

Table A.11 q_t predicted values of experiments at 308 K from Elovich kinetic model

	Time (min)	Initial Cu⁺² Con. (mg/L)				
		5	10	20	40	60
308 K	0	0	0	0	0	0
	2.5	4.99	9.31	13.43	24.09	24.48
	5	5.49	10.15	14.77	25.99	27.13
	10	6.00	11.00	16.10	27.90	29.77
	15	6.30	11.50	16.89	29.01	31.32
	30	6.80	12.35	18.23	30.91	33.97
	45	7.10	12.84	19.01	32.03	35.52
	60	7.31	13.19	19.56	32.82	36.61
	90	7.61	13.69	20.35	33.93	38.16
	120	7.82	14.04	20.90	34.72	39.26
	150	7.98	14.31	21.33	35.33	40.11
	180	8.11	14.54	21.68	35.83	40.81
	210	8.23	14.73	21.98	36.26	41.40

Table A.12 q_t predicted values of experiments at 318 K from Elovich kinetic model

	Time (min)	Initial Cu⁺² Con. (mg/L)				
		5	10	20	40	60
318 K	0	0	0	0	0	0
	2.5	5.36	10.07	16.24	26.99	30.79
	5	5.91	11.08	17.70	29.09	33.67
	10	6.46	12.10	19.15	31.19	36.55
	15	6.79	12.70	20.01	32.42	38.24
	30	7.34	13.71	21.47	34.52	41.12
	45	7.66	14.31	22.32	35.75	42.80
	60	7.89	14.73	22.93	36.62	44.00
	90	8.22	15.33	23.78	37.85	45.68
	120	8.45	15.75	24.38	38.72	46.88
	150	8.62	16.07	24.85	39.40	47.81
	180	8.77	16.34	25.24	39.95	48.56
	210	8.89	16.57	25.56	40.41	49.20

Table A.13 ANOVA results of q_t values of experiments for each initial Cu^{+2} concentration at 298K

5mg/L	Sum of Squares	df	Mean Square	F	Sig.
Between Groups	99,581	12	8,298	41,495	0,000
Within Groups	2,600	13	0,200		
Total	102,180	25			

10 mg/L	Sum of Squares	df	Mean Square	F	Sig.
Between Groups	299,022	12	24,918	41,467	0,000
Within Groups	7,812	13	0,601		
Total	306,834	25			

20 mg/L	Sum of Squares	df	Mean Square	F	Sig.
Between Groups	662,262	12	55,189	42,100	0,000
Within Groups	17,042	13	1,311		
Total	679,304	25			

40 mg/L	Sum of Squares	df	Mean Square	F	Sig.
Between Groups	1565,997	12	130,500	40,041	0,000
Within Groups	42,369	13	3,259		
Total	1608,365	25			

60 mg/L	Sum of Squares	df	Mean Square	F	Sig.
Between Groups	2131,262	12	177,605	43,971	0,000
Within Groups	52,509	13	4,039		
Total	2183,771	25			

Table A.14 ANOVA results of q_t values of experiments for each initial Cu^{+2} concentration at 308K

5 mg/L	Sum of Squares	df	Mean Square	F	Sig.
Between Groups	115,324	12	9,610	41,862	0,000
Within Groups	2,984	13	0,230		
Total	118,309	25			

10 mg/L	Sum of Squares	df	Mean Square	F	Sig.
Between Groups	366,443	12	30,537	40,667	0,000
Within Groups	9,762	13	0,751		
Total	376,205	25			

20 mg/L	Sum of Squares	df	Mean Square	F	Sig.
Between Groups	823,150	12	68,596	41,679	0,000
Within Groups	21,396	13	1,646		
Total	844,546	25			

40 mg/L	Sum of Squares	df	Mean Square	F	Sig.
Between Groups	2200,287	12	183,357	39,271	0,000
Within Groups	60,697	13	4,669		
Total	2260,984	25			

60 mg/L	Sum of Squares	df	Mean Square	F	Sig.
Between Groups	2946,175	12	245,515	42,703	0,000
Within Groups	74,742	13	5,749		
Total	3020,917	25			

Table A.15 ANOVA results of q_t values of experiments for each initial Cu^{+2} concentration at 318K

5 mg/L	Sum of Squares	df	Mean Square	F	Sig.
Between Groups	134,979	12	11,248	42,048	0,000
Within Groups	3,478	13	0,268		
Total	138,456	25			

10 mg/L	Sum of Squares	df	Mean Square	F	Sig.
Between Groups	468,207	12	39,017	41,837	0,000
Within Groups	12,124	13	0,933		
Total	480,331	25			

20 mg/L	Sum of Squares	df	Mean Square	F	Sig.
Between Groups	1102,981	12	91,915	40,522	0,000
Within Groups	29,488	13	2,268		
Total	1132,468	25			

40 mg/L	Sum of Squares	df	Mean Square	F	Sig.
Between Groups	2730,862	12	227,572	39,122	0,000
Within Groups	75,620	13	5,817		
Total	2806,483	25			

60 mg/L	Sum of Squares	df	Mean Square	F	Sig.
Between Groups	4101,022	12	341,752	40,965	0,000
Within Groups	108,454	13	8,343		
Total	4209,476	25			

Table A.16 ANOVA results of q_t - initial Cu^{+2} concentration relationship for each time at 298 K

210 min.	Sum of Squares	df	Mean Square	F	Sig.
Between Groups	1007,557	4	251,889	93,656	0,000
Within Groups	13,448	5	2,690		
Total	1021,005	9			

180 min	Sum of Squares	df	Mean Square	F	Sig.
Between Groups	996,002	4	249,000	94,125	0,000
Within Groups	13,227	5	2,645		
Total	1009,229	9			

150 min	Sum of Squares	df	Mean Square	F	Sig.
Between Groups	979,026	4	244,756	94,637	0,000
Within Groups	12,931	5	2,586		
Total	991,957	9			

120 min	Sum of Squares	df	Mean Square	F	Sig.
Between Groups	951,129	4	237,782	94,755	0,000
Within Groups	12,547	5	2,509		
Total	963,676	9			

90 min	Sum of Squares	df	Mean Square	F	Sig.
Between Groups	913,389	4	228,347	94,835	0,000
Within Groups	12,039	5	2,408		
Total	925,429	9			

60 min	Sum of Squares	df	Mean Square	F	Sig.
Between Groups	862,580	4	215,645	94,765	0,000
Within Groups	11,378	5	2,276		
Total	873,958	9			

45 min	Sum of Squares	df	Mean Square	F	Sig.
Between Groups	793,544	4	198,386	94,325	0,000
Within Groups	10,516	5	2,103		
Total	804,060	9			

30 min	Sum of Squares	df	Mean Square	F	Sig.
Between Groups	713,369	4	178,342	93,748	0,000
Within Groups	9,512	5	1,902		
Total	722,881	9			

15 min	Sum of Squares	df	Mean Square	F	Sig.
Between Groups	630,274	4	157,568	92,872	0,000
Within Groups	8,483	5	1,697		
Total	638,757	9			

10 min	Sum of Squares	df	Mean Square	F	Sig.
Between Groups	543,221	4	135,805	92,329	0,000
Within Groups	7,354	5	1,471		
Total	550,575	9			

5 min	Sum of Squares	df	Mean Square	F	Sig.
Between Groups	447,967	4	111,992	91,800	0,000
Within Groups	6,100	5	1,220		
Total	454,067	9			

2.5 min	Sum of Squares	df	Mean Square	F	Sig.
Between Groups	351,086	4	87,771	91,620	0,000
Within Groups	4,790	5	0,958		
Total	355,876	9			

Table A.17 ANOVA results of q_t - initial Cu^{+2} concentration relationship for each time at 308K

210 min	Sum of Squares	df	Mean Square	F	Sig.
Between Groups	1504,101	4	376,025	102,557	0,000
Within Groups	18,332	5	3,666		
Total	1522,434	9			

180 min	Sum of Squares	df	Mean Square	F	Sig.
Between Groups	1492,869	4	373,217	103,240	0,000
Within Groups	18,075	5	3,615		
Total	1510,944	9			

150 min	Sum of Squares	df	Mean Square	F	Sig.
Between Groups	1473,643	4	368,411	103,828	0,000
Within Groups	17,741	5	3,548		
Total	1491,384	9			

120 min	Sum of Squares	df	Mean Square	F	Sig.
Between Groups	1442,903	4	360,726	104,379	0,000
Within Groups	17,280	5	3,456		
Total	1460,183	9			

90 min	Sum of Squares	df	Mean Square	F	Sig.
Between Groups	1397,524	4	349,381	105,148	0,000
Within Groups	16,614	5	3,323		
Total	1414,138	9			

60 min	Sum of Squares	df	Mean Square	F	Sig.
Between Groups	1325,405	4	331,351	105,316	0,000
Within Groups	15,731	5	3,146		
Total	1341,136	9			

45 min	Sum of Squares	df	Mean Square	F	Sig.
Between Groups	1225,297	4	306,324	105,044	0,000
Within Groups	14,581	5	2,916		
Total	1239,878	9			

30 min	Sum of Squares	df	Mean Square	F	Sig.
Between Groups	1105,411	4	276,353	104,261	0,000
Within Groups	13,253	5	2,651		
Total	1118,664	9			

15 min	Sum of Squares	df	Mean Square	F	Sig.
Between Groups	987,287	4	246,822	104,026	0,000
Within Groups	11,863	5	2,373		
Total	999,151	9			

10 min	Sum of Squares	df	Mean Square	F	Sig.
Between Groups	860,638	4	215,159	103,632	0,000
Within Groups	10,381	5	2,076		
Total	871,019	9			

5 min	Sum of Squares	df	Mean Square	F	Sig.
Between Groups	720,995	4	180,249	103,477	0,000
Within Groups	8,710	5	1,742		
Total	729,705	9			

2.5 min	Sum of Squares	df	Mean Square	F	Sig.
Between Groups	585,421	4	146,355	104,246	0,000
Within Groups	7,020	5	1,404		
Total	592,441	9			

Table A.18 ANOVA results of q_t - initial Cu^{+2} concentration relationship for each time at 318 K

210 min	Sum of Squares	df	Mean Square	F	Sig.
Between Groups	2116,869	4	529,217	108,082	0,000
Within Groups	24,482	5	4,896		
Total	2141,352	9			

180 min	Sum of Squares	df	Mean Square	F	Sig.
Between Groups	2106,000	4	526,500	108,759	0,000
Within Groups	24,205	5	4,841		
Total	2130,205	9			

150 min	Sum of Squares	df	Mean Square	F	Sig.
Between Groups	2081,088	4	520,272	109,327	0,000
Within Groups	23,794	5	4,759		
Total	2104,882	9			

120 min	Sum of Squares	df	Mean Square	F	Sig.
Between Groups	2036,407	4	509,102	109,771	0,000
Within Groups	23,189	5	4,638		
Total	2059,596	9			

90 min	Sum of Squares	df	Mean Square	F	Sig.
Between Groups	1968,692	4	492,173	110,359	0,000
Within Groups	22,299	5	4,460		
Total	1990,991	9			

60 min	Sum of Squares	df	Mean Square	F	Sig.
Between Groups	1870,037	4	467,509	110,614	0,000
Within Groups	21,132	5	4,226		
Total	1891,170	9			

45 min	Sum of Squares	df	Mean Square	F	Sig.
Between Groups	1751,352	4	437,838	111,157	0,000
Within Groups	19,695	5	3,939		
Total	1771,047	9			

30 min	Sum of Squares	df	Mean Square	F	Sig.
Between Groups	1593,645	4	398,411	110,945	0,000
Within Groups	17,955	5	3,591		
Total	1611,600	9			

15 min	Sum of Squares	df	Mean Square	F	Sig.
Between Groups	1425,935	4	356,484	110,908	0,000
Within Groups	16,071	5	3,214		
Total	1442,006	9			

10 min	Sum of Squares	df	Mean Square	F	Sig.
Between Groups	1264,935	4	316,234	111,568	0,000
Within Groups	14,172	5	2,834		
Total	1279,107	9			

5 min	Sum of Squares	df	Mean Square	F	Sig.
Between Groups	1089,882	4	272,470	112,297	0,000
Within Groups	12,132	5	2,426		
Total	1102,014	9			

2.5 min	Sum of Squares	df	Mean Square	F	Sig.
Between Groups	909,337	4	227,334	113,255	0,000
Within Groups	10,036	5	2,007		
Total	919,374	9			

Table A.19 ANOVA results of q_t - initial Cu^{+2} concentration relationship for each time at 318 K

Dependent Variable:qt

Source	Type III Sum of Squares	df	Mean Square	F	Sig.
Model	208337,006 ^a	99	2104,414	996,807	0,000
time	15414,349	12	1284,529	608,448	0,000
conc	38350,423	4	9587,606	4541,402	0,000
temp	2116,785	2	1058,392	501,333	0,000
time * conc	4041,883	48	84,206	39,886	0,000
time * temp	198,051	24	8,252	3,909	0,000
conc * temp	1039,881	8	129,985	61,571	0,000
Error	614,346	291	2,111		
Total	208951,352	390			

a. R Squared = ,997 (Adjusted R Squared = ,996)

Figure A.1 pH_{zpc} of activated hydrochar

